

IMPROVING SPATIAL REUSE AND THROUGHPUT VIA OBSS/PD IN IEEE
802.11AX

by

Ali Karakoç

B.S., Electrical and Electronics Engineering, Middle East Technical University, 2015

Submitted to the Institute for Graduate Studies in
Science and Engineering in partial fulfillment of
the requirements for the degree of
Master of Science

Graduate Program in Software Engineering
Boğaziçi University

2021

ACKNOWLEDGEMENTS

I would like to express my deepest gratitude to a number of people for their great support during this thesis study.

I am extremely thankful to my thesis co-supervisors Assist. Prof. H. Birkan Yilmaz and Assist. Prof. Mehmet Şükrü Kuran for their constant guidance and assistance during the thesis. This thesis would not be finished without their patience and endless supports.

I greatly appreciate Prof. Cem Ersoy, Assist. Prof. Ece Gelal Soyak and Prof. Tuna Tuğcu for participation in my thesis committee and their precious comments on this thesis.

Many thanks to Boğaziçi University TETAM Lab for providing me the infrastructure I used in the simulations.

Lastly, I am extremely grateful to my parents and my brother. Their unconditional support and love kept me motivated throughout the entire thesis process.

ABSTRACT

IMPROVING SPATIAL REUSE AND THROUGHPUT VIA OBSS/PD IN IEEE 802.11AX

The aim of this thesis is to improve spatial reuse by using special mechanisms in IEEE 802.11ax wireless local area networks. If there are numbers of basic service sets (BSSs) in the same vicinity, overlapping BSSs may create interference. In this situation, BSSs cannot transmit simultaneously, because of the collisions. Moreover, there may be spectral efficiency problems like “Hidden Node Problem” or “Exposed Node Problem”, that may cause significant performance degradation to the system. In IEEE 802.11ax amendment, to address these spectral efficiency problems, a couple of mechanisms are introduced. One of the spectral efficiency mechanisms that address these problems is the overlapping BSS preamble detection (OBSS/PD) mechanism. OBSS/PD is a color-based mechanism that is used to detect and prevent overlapping BSS interference efficiently. In this thesis, we propose a rate-adaptive dynamic OBSS/PD threshold algorithm that dynamically adjusts the OBSS/PD threshold with respect to the changes in the channel conditions and selected data rates. Additionally, hidden and exposed node problems due to overlapping BSS are reduced. The proposed mechanism is designed to work along with the rate selection algorithms. In this study, the scenarios are performed with Minstrel and Thompson rate selection algorithms. The performance of the proposed mechanism has been compared with the legacy carrier sensitivity threshold algorithms (DSC and RTOT). Our algorithm has shown more stable performance than the reference algorithms in the Minstrel scenario, and none of the threshold algorithms have shown a significant performance enhancement relative to the others. When the Thompson rate selection algorithm is used, our proposed algorithm has shown a better performance and stability than the legacy carrier sensitivity threshold algorithms.

ÖZET

IEEE 802.11AX KABLOSUZ AĞLARINDA OBSS/PD MEKANİZMASINI KULLANARAK UZAMSAL YENİDEN KULLANIM VE VERİ HACMİ İYİLEŞTİRME

Tezin amacı, IEEE 802.11ax kablosuz ağlarında, OBSS/PD mekanizmasını kullanarak uzamsal yeniden kullanma ve verimliliği artırmaktır. Kablosuz ağ ortamı sınırlı sayıda kanal kullandığından, ortamda bulunan BSS'ler, birbirlerinin menziline girebilir ve iletim esnasında çarpışmalar yaşanabilir. Kablosuz ağlarda sıklıkla karşılaşılan iki spektral verimlilik problemi, “Gizli Düğüm Sorunu” ve “Açık Düğüm Sorunu”’dur. Bu iki problem, kablosuz ağlarda ciddi performans düşüşüne sebep olabilmektedir. IEEE 802.11ax standardı, beraberinde verimlilik artırmaya yönelik bir çok yenilik getirmiştir. Bu yeniliklerden birisi de OBSS/PD mekanizmasıdır. OBSS/PD mekanizmasının temel amacı, BSS'ler arası çarpışmaları ve performans problemlerini en aza indirmektir. Bu tezde geliştirdiğimiz algoritma, OBSS/PD eşiğini, veri hızı ve çarpışma sayısını baz alarak dinamik bir biçimde ayarlamaktadır. Maksimum kullanılabilir veri hızı da baz alınarak, diğer BSS'ler duyulmayacak şekilde bir OBSS/PD eşigi seçilir. Bu sayede hız seçim algoritmaları, elverişli iletim gücü dolayısıyla daha yüksek hızları seçebilir. Bunun yanında, algoritma açık ve gizli düğüm sorunlarını da azaltmaktadır. Yapılan simülasyonlarda, geliştirdiğimiz algoritma Minstrel ve Thompson hız seçim algoritmaları ile birlikte ele alınıp, DSC ve RTOT eşik algoritmaları ile karşılaştırma yapılmıştır. Minstrel algoritması ile elde edilen sonuçlarda, geliştirmiş olduğumuz algoritma performans düşüşüne yol açmayıp referans algoritmalara göre stabil sonuçlar vermiştir. Tüm algoritmaların gözle görülür bir iyileştirme sağlamadığı da gözlemlenmiştir. Thompson algoritması ile elde edilen sonuçlarda ise referans algoritmalara nazaran belirgin iyileştirme gözlemlenmiş, toplam verimlilik ve stabilite artmıştır.

TABLE OF CONTENTS

ACKNOWLEDGEMENTS	iii
ABSTRACT	iv
ÖZET	v
LIST OF FIGURES	viii
LIST OF TABLES	xii
LIST OF SYMBOLS	xiii
LIST OF ACRONYMS/ABBREVIATIONS	xvi
1. INTRODUCTION	1
1.1. Key Contributions	2
1.2. Thesis Outline	3
2. IEEE 802.11 STANDARD AND WIFI6	4
2.1. IEEE 802.11 Protocol and CSMA/CA Basics	4
2.2. IEEE 802.11ax Protocol	10
2.2.1. Main Features of IEEE 802.11ax Protocol	11
2.2.2. OFDMA As a Digital Modulation Scheme	16
2.2.3. OBSS/PD Mechanism	18
2.2.4. Microsleep and TWT	26
3. SPATIAL REUSE TECHNIQUES AND RATE SELECTION ALGORITHMS IN WIFI NETWORKS	28
3.1. Spatial Reuse Techniques in IEEE 802.11 Protocols	28
3.1.1. Channel Access Mechanisms	28
3.1.2. Spectral Efficiency Problems	29
3.1.2.1. Hidden Node Problem	29
3.1.2.2. Exposed Terminal Problem	30
3.1.3. Pre 802.11ax Solutions	32
3.1.3.1. Solutions To the Hidden Node Problem	32
3.1.3.2. Solutions To the Exposed Terminal Problem	40
3.1.4. Proprietary Solutions	43

3.1.5.	Carrier Sensitivity Thresholds and OBSS/PD	44
3.1.6.	Spectral Efficiency in Other Wireless Protocols	53
3.2.	Rate Selection Algorithms	54
4.	RACEBOT ALGORITHM	61
5.	EXPERIMENTAL SETUP AND SIMULATION RESULTS	69
5.1.	NS-3 Simulation Framework	69
5.2.	System Parameters and Performance Metrics	70
5.3.	Simulation Topology	72
5.4.	Simulation Results	77
5.4.1.	Box5 Scenario	77
5.4.2.	Minstrel Scenarios	79
5.4.3.	Thompson custom Box5 Scenario 1	79
5.4.4.	Thompson custom Box5 Scenario 2	81
5.4.5.	Thompson custom Box5 Scenario 3	83
5.4.6.	Thompson custom Box5 Scenario 4	84
5.4.7.	Thompson custom Box5 Scenario 5	86
5.4.8.	Thompson custom Box5 Scenario 6	87
5.4.9.	Overall Comparison of Scenarios	88
6.	CONTRIBUTIONS AND FUTURE DIRECTIONS	92
6.1.	Contributions of RACEBOT Algorithm	92
6.2.	Future Directions	93
	REFERENCES	94

LIST OF FIGURES

Figure 2.1.	MAC frame of 802.11 protocol.	7
Figure 2.2.	DCF mechanism flowchart.	8
Figure 2.3.	DCF mechanism for an example scenario.	9
Figure 2.4.	PCF-DCF coexistence mechanism illustration.	11
Figure 2.5.	802.11ax color header in HE operation element.	14
Figure 2.6.	802.11ax HE-PPDU structures.	15
Figure 2.7.	An example of spectral efficiency problem.	19
Figure 2.8.	OBSS/PD mechanism on top of legacy preamble detection.	20
Figure 2.9.	OBSS/PD-Transmission power relationship.	21
Figure 2.10.	A simple scenario for OBSS/PD mechanism.	23
Figure 2.11.	An example implementation of color assignment for the BSSs.	24
Figure 2.12.	SRG HE operation element.	25
Figure 2.13.	A simple scenario for SRG based OBSS/PD mechanism.	26
Figure 3.1.	An example scenario for hidden node problem: STA-2 cannot detect that there is an active transmission between STA-1 and AP-1.	30

Figure 3.2.	An example scenario for exposed node problem: STA-1 has transmission with AP-1. STA-2 hears STA-1 and does not transmit even if it is able to do it.	31
Figure 3.3.	RTS/CTS Mechanism.	34
Figure 3.4.	Four Way Handshake RTS/CTS mechanism.	35
Figure 3.5.	RI-BTMA mechanism.	36
Figure 3.6.	PAMAS Mechanism.	37
Figure 3.7.	A scenario for directional hidden node problem.	38
Figure 3.8.	Dynamic sensitivity algorithm flowchart.	46
Figure 3.9.	RTOT algorithm.	49
Figure 3.10.	COST algorithm	50
Figure 3.11.	Opportunity based OBSS/PD algorithm.	52
Figure 3.12.	Modified Thompson sampling (MTS) algorithm.	59
Figure 4.1.	OBSS/PD threshold and TxPower adjustment scenario.	62
Figure 4.2.	A histogram for OBSS frame counts for each RSSI.	64
Figure 4.3.	Another histogram for OBSS frame counts for each RSSI.	65
Figure 4.4.	RACEBOT algorithm.	66

Figure 4.5.	RACEBOT flowchart.	68
Figure 5.1.	TGax Box5 outdoor topology.	73
Figure 5.2.	Custom Box5 topology generator algorithm.	74
Figure 5.3.	Custom Box topology with 3 STA and <i>Seed</i> =1.	75
Figure 5.4.	Custom Box topology with 6 STA and <i>Seed</i> =1.	75
Figure 5.5.	Custom Box topology with 6 STA and <i>Seed</i> =2.	76
Figure 5.6.	Custom Box topology with 45 STA and <i>Seed</i> =2.	76
Figure 5.7.	Scenario Box5 - Minstrel.	78
Figure 5.8.	Scenario Box5 - Thompson.	79
Figure 5.9.	Minstrel performance diagram.	80
Figure 5.10.	Scenario 1 - Topology for <i>Seed</i> = 1.	80
Figure 5.11.	Scenario 1: 3 STA 3 AP Custom Box5 Thompson rate algorithm.	81
Figure 5.12.	Scenario 2 - Topology for <i>Seed</i> = 1.	82
Figure 5.13.	Scenario 2: 6 STA 3 AP Custom Box5 Thompson rate algorithm.	82
Figure 5.14.	Scenario 3 - Topology for <i>Seed</i> = 1.	83
Figure 5.15.	Scenario 3: 9 STA 3 AP Custom Box5 Thompson rate algorithm.	84

Figure 5.16. Scenario 4 - Topology for <i>Seed</i> = 1.	85
Figure 5.17. Scenario 4: 15 STA 3 AP Custom Box5 Thompson rate algorithm aggregated throughput.	85
Figure 5.18. Scenario 4: 15 STA 3 AP Custom Box5 Thompson rate algorithm.	86
Figure 5.19. Scenario 5 - Topology for <i>Seed</i> = 1.	86
Figure 5.20. Scenario 5: 21 STA 3 AP Custom Box5 Thompson rate algorithm.	87
Figure 5.21. Scenario 6: 27 STA 3 AP Custom Box5 Thompson rate algorithm.	88
Figure 5.22. Scenario 6: 27 STA 3 AP Custom Box5 Thompson rate algorithm aggregated throughput.	89
Figure 5.23. Scenario 6: 27 STA 3 AP Custom Box5 Thompson rate algorithm.	89
Figure 5.24. Sparse node density performance comparison.	90
Figure 5.25. Medium node density performance comparison.	91
Figure 5.26. High node density performance comparison.	91

LIST OF TABLES

Table 2.1.	Main substandards of the IEEE 802.11 standard family.	5
Table 2.2.	802.11ax OFDM rates (20 and 40 MHz) for single spatial stream [1].	12
Table 2.3.	802.11ax OFDM rates (80 and 160 MHz) for single spatial stream [1].	12
Table 2.4.	802.11ax comparison with legacy 802.11ac.	13
Table 2.5.	OBSS/PD ranges at different channel bandwidths.	22
Table 3.1.	Minstrel retry chain	58
Table 4.1.	802.11ax receiver minimum Input level sensitivity [1].	61
Table 5.1.	System parameters.	71

LIST OF SYMBOLS

a	Coefficient of ETX that is used to tune ETP algorithm
$alpha$	A variable that is used to set M_{New} value
$AP_{(x,y)}$	A list of AP coordinates
b	Variable that is used to tune ETP algorithm
$B(.,.)$	Beta function
CCA^{Thr}	Clear channel assessment threshold
CCA_{Max}^{Thr}	Maximum value that CCA^{Thr} can take
CCA_{Min}^{Thr}	Minimum value that CCA^{Thr} can take
$Color$	Color value of an HE frame
$decay$	Decay parameter of Thompson algorithm
$Diff$	Absolute value of the difference between \overline{RSSI}^{OBSS} and \overline{RSSI}^{BSS}
$Diff_{Max}$	Maximum value that $Diff$ can take
$Diff_{Min}$	Minimum value that $Diff$ can take
$DIFS$	DFS inter frame space
ETX	Expected transmission count
$f(.)$	Probability density function success probabilities of each rate
F_i	Number of failed transmission at i 'th rate
K	Retry count
M	A value that is used as a guard interval for $RSSI$
M_{New}	A tuned version of M parameter
MCS	Modulation coding scheme
\overline{MCS}	Average of modulation coding scheme
$Node_i$	i 'th node
$nSTA_{AP}$	Number of stations per AP
N_{Step}	Number steps
$OBSS/PD$	Overlapped basic service set/preamble detection
$OBSS/PD^G$	Aimed OBSS/PD threshold value

$OBSS/PD_{Curr}$	Current OBSS/PD level
$OBSS/PD_i^G$	Aimed OBSS/PD threshold value of i 'th node
$OBSS/PD_{Max}$	Maximum value of OBSS/PD threshold
$OBSS/PD_{Min}$	Minimum value of OBSS/PD threshold
$OBSS/PD_{Tmp}$	Temporary value of OBSS/PD threshold
OFC	Total number of OBSS frames arrived at nodes in a specific time interval
$\overline{OFC}_{i,j}(T)$	Number of OBSS frames arrived at node i during time T with RSSI level of j
OFC_{Thr}	A threshold for the count of $OFCs$
$PIFS$	Point coordination function inter frame space
PST	Probability of successful transmission
R^{Max}	Maximum range that a node can be located away from AP
R^{Min}	Topology parameter for minimum range that a node can be located away from AP to be considered as a far field while forming the topology
$R_{AP_j}^{Max}$	Maximum range that a node can be located away from j 'th AP while forming the topology
$R_{AP_j}^{Min}$	Minimum range that a node can be located away from j 'th AP
r_i	Data rate for the i 'th modulation index
$rBytes_i$	Total received bytes at i 'th node
$RSSI$	Received signal strength indicator
$RSSI^{Beacon}$	RSSI of beacon frames
$RSSI^{BSS}$	RSSI value of the BSS beacon frames
\overline{RSSI}^{BSS}	Average value of $RSSI^{BSS}$
$RSSI^{OBSS}$	RSSI value of the Inter-BSS nodes
\overline{RSSI}^{OBSS}	Average value of $RSSI^{OBSS}$
$RSSI_{Avg}^{Beacon}$	EWMA RSSI of beacon frames
\overline{RSSI}_i^{BSS}	Average value of $RSSI^{BSS}$ at i 'th node
$RSSI_{i,j}^{OBSS}$	Value of the j 'th $RSSI^{OBSS}$ at i 'th node

$RSSI_{Max}^{OBSS_AP}$	Maximum RSSI value of Inter-BSS APs
$RSSI_{Min}^{INBSS_STA}$	Minimum RSSI of Intra-BSS STAs
S_i	Number of successful transmission at i 'th rate
$Seed$	Seed parameter for topology
$SIFS$	Short inter frame space
T	Time
T_{Slot}	Slot time
T_{Step}	Time period that <i>Throughput</i> is measured
T_{Tot}	Total transmission time
T_U	A time period that algorithm updates threshold parameters
<i>Throughput</i>	Throughput value of a node
<i>Throughput</i> ^{Agg}	Aggregated throughput
<i>Throughput</i> _{i}	Throughput value of the i 'th node
TM	Total transferred data in Mbits in each T_{Step}
TM_{Tot}	Total transferred data in Mbits in T_{Tot}
$TxPower$	Transmission power
$TxPower_{Min}$	Minimum value of transmission power
$TxPower_{Ref}$	Maximum value of transmission power
W	Size of the moving average window
α	Weight of EWMA function
γ	A criteria that is used to estimate the change of \overline{MCS}
$\Gamma(.)$	Gamma function
θ_i	Success probability of i 'th rate

LIST OF ACRONYMS/ABBREVIATIONS

AARF	Adaptive ARF
ACK	Acknowledgement
AIFS	Arbitration inter frame space
AODV	Ad hoc on-demand distance vector
AP	Access point
API	Application programming interface
ARF	Automated rate fallback
ASK	Amplitude shift key
BER	Bit error rate
BI	BUSY/IDLE
BOF	Backoff
BPSK	Binary phase shift key
BSS	Basic service set
BSSID	Basic service set identifier
BTMA	Busy tone multiple access
BUSY	Busy
BusySiMOn	Busy signal-based mechanism turned on
CCA	Clear channel assessment
CCA_BUSY	Clear channel assessment busy
CCA/CS	Clear channel assessment / carrier sensing
CCA/ED	Clear channel assessment / energy detection
CCI	Co-channel interference
CCM-MAC	Cooperative CDMA-based multi-channel MAC
CDMA	Code division multiple access
CDMAC	Cooperative diversity MAC
CDR-MAC	Circular directional RTS MAC
CFP	Contention free period
COST	Control OBSS/PD sensitivity threshold

CP	Contention period
CSMA	Carrier sense multiple access
CSMA/CA	Carrier sense multiple access with collision avoidance
CSMA/CD	Carrier sense multiple access with collision detection
CTS	Clear-to-send
CTSS	Clear-to-send-simultaneously
D-CTS	Directional-CTS
D-RTS	Directional-RTS
DBTMA	Dual busy tone multiple access
DCF	Distributed coordination function
DIFS	Distributed coordination function inter frame space
DL	Downlink
DMAC	Directional MAC
DMAC-PCDR	DMAC with power control and directional receiving
DSC	Dynamic sensitivity control
DTDMA	Distributed time division multiple access
DUCHA	Dual channel MAC protocol for multihop ad-hoc
ECHOS	Enhanced capacity 802.11 hotspots
ETP	ETX-to-power
ETX	Expected transmission count
EWMA	Exponential weighted moving average
FAMA	Floor acquisition multiple access)
FDMA	Frequency division multiple access
FSK	Frequency shift key
HE	High efficiency
HT	High throughput
HEW SG	High efficiency WLAN study group
ICI	Inter carrier interference
ICSMA	Interleaved carrier sense multiple access
IDLE	Idle
IEEE	Institute of Electrical and Electronics Engineers

IFS	Inter frame space
JMAC	Jamming based MAC protocol
LAN	Local area network
M-VRMA	Multi channel variable radius multiple access
MAC	Medium access control
MAC-SCC	MAC with a separate control channel
MACA	Multiple access with collision avoidance
MACA-BI	MACA-by-invitation
MACA-P	Medium access via collision avoidance with enhanced parallelism
MACAW	MACA for wireless
MCS	Modulation coding scheme
MIMO	Multiple input multiple output
MMAC	Multichannel medium access control
MU	Multi user
MU-MIMO	Multi user-multiple input multiple output
NAV	Network allocation vector
NIC	Network interface card
OBO	OFDMA backoff
OBSS	Overlapping basic service set
OBSS/PD	Overlapping basic service set/preamble detection
OFC	OBSS frame count
OFDM	Orthogonal frequency division multiplexing
OFDMA	Orthogonal frequency division multiple access
OPS	Opportunistic power save
PAMAS	Power aware multi access protocol with signalling
PCF	Point coordination function
PCMA	Power controlled multiple access
PER	Packet error rate
PHY	Physical layer
PIFS	Point coordination function inter frame space

PNC	Piconet controller
PRC	Power rate control
PSK	Phase shift key
PUMA	Priority unavoidable multiple access
QAM	Quadrature amplitude modulation
QPSK	Quadrature phase shift keying
QTP	Quiet time period
RACEBOT	Rate adaptive inter-BSS carrier elimination-based OBSS/PD threshold
RBAR	Receiver based auto rate protocol
RDMAC	Reservation-based directional MAC
RI-BTMA	Receiver initiated busy tone multiple access
RSSI	Received signal strength indicator
RTOT	RSSI-to-OBSS threshold
RTS	Request-to-send
RTSS	Request-to-send-simultaneously
Rx-Sensitivity	Received signal sensitivity
RU	Resource unit
SAM-MAC	Self adjustable multi channel MAC
SDMA	Space division multiple access
SDN	Selective disregard NAV
SIFS	Short inter frame space
SINR	Signal to interference plus noise ratio
SR-DIV	Diversity scheduler
SRG	Spatial reuse group
SRP	Spatial reuse parameter
SRP_CCA	Spatial reuse parameter clear channel assessment
SSID	Service set identifier
STA	Station
STDMA	Self organized time division multiple access
TCMA	Tiered contention multiple access

TDMA	Time division multiple access
TGax	Task group-ax
TXOP	Transmission opportunity
TxPower	Transmission power
TW	Target wake
Two-NAV	Two network allocation vectors
TWT	Target wake time
UL	Uplink
UL-MU	Uplink multiple user
UORA	Uplink OFDMA random access
WBAN	Wireless body area network
WiMAX	World-wide interoperability for microwave access
WLAN	Wireless local area network
WPAN	Wireless personal area network

1. INTRODUCTION

Managing the access mechanisms in wireless networks is a challenging problem. Since multiple nodes try to transmit at the same time, the limited number of channels and interference complicate the simultaneous transmission. To address this problem, in IEEE 802.11 standard, access of the nodes to the medium is managed by the carrier sense multiple access with collision avoidance (CSMA/CA) mechanism. CSMA/CA manages the node access with respect to the carrier sensing and time-based transmission opportunities. Even if CSMA/CA manages the access of each node in the medium, there may still be access problems and inefficiencies. Most common inefficiency problems in wireless networks are “Hidden Node Problem” and “Exposed Node Problem”. Please note that spectral efficiency problems are directly related to carrier sensing and random access mechanisms. Before transmission, each node checks the channel availability and even if there is no ongoing transmission, there may be collisions at the time of transmission.

IEEE 802.11ax (WiFi6) standard was introduced to address these efficiency problems and to increase the spectral efficiency in wireless local area networks (WLANs). One of the major mechanisms introduced in WiFi6 is OFDMA. OFDMA increases the number of non-overlapping sub-channels and enables multiuser communication over orthogonal frequencies. By that way, multiple users can communicate simultaneously with enhanced spectral efficiency. Besides this, TWT and microsleep mechanisms are introduced in WiFi6 standard to enable power management and efficiency. And lastly, to enhance the spatial reuse, WiFi6 proposed the OBSS/PD mechanism. OBSS/PD is a carrier sensing threshold that is used to reduce the interference of overlapping BSSs. The OBSS/PD threshold and transmission power is dependent on each other. Therefore, increasing the OBSS/PD threshold necessitates to decrease the transmission power at the same time for reducing the interference. Since the transmission power is directly related to the data rate, there is a trade off between increasing OBSS/PD threshold and transmission power.

WiFi6 has 12 modulation coding scheme (MCS) levels that can be used by the nodes with respect to the minimum signal-to-interference-plus-noise-ratio (SINR) and packet error rate (PER) requirements of each corresponding MCS level. Rate selection algorithms evaluate the transmission or channel conditions to select an appropriate data rate. Therefore, to use the maximum potential of the situation, rate selection algorithms try to find the highest possible MCS levels as much as possible.

In this thesis, we propose a rate adaptive inter-BSS carrier elimination-based OBSS/PD threshold (RACEBOT) algorithm. Mainly, RACEBOT algorithm is a received signal strength indicator (RSSI) based carrier sensing threshold algorithm and it is designed to be used with common rate selection algorithms. Since changing OBSS/PD threshold also affects the transmission power, this operation is also related to rate selection algorithms. If the transmission power is not enough to transmit for a corresponding MCS level, the transmission fails. RACEBOT algorithm also considers the transmission power and increases the OBSS/PD threshold with the necessary amount of value. However, changing the transmission power degrades the rate selection algorithm stability and performance. Because of this, the rate selection algorithm does not set OBSS/PD threshold directly. It changes the OBSS/PD threshold with small steps. Besides, RACEBOT algorithm looks at the count of each OBSS RSSI level and if any of these are below the count threshold, these RSSI levels are ignored. Therefore, OBSS/PD threshold can be chosen at lower levels and due to the higher transmission power, higher MCS levels may be selected.

1.1. Key Contributions

The main contributions of RACEBOT algorithm are:

- (i) RACEBOT algorithm is a rate adaptive OBSS/PD threshold algorithm that enables higher MCS levels by reducing the interference,
- (ii) RACEBOT algorithm applies an appropriate OBSS/PD threshold to decrease the number of exposed nodes,

- (iii) The algorithm reduces the number of hidden nodes,
- (iv) It can work with other rate selection algorithms,
- (v) RACEBOT algorithm can be tuned with respect to node density.

1.2. Thesis Outline

In chapter 2, firstly IEEE 802.11 standard and channel access mechanisms are discussed. The second part of the section focuses on IEEE 802.11ax standard and its features like OFDMA, OBSS/PD, and power management mechanisms.

Chapter 3 focuses on spatial reuse techniques in the first part, and the second part is mostly focused on rate selection algorithms. Spatial reuse techniques begin with the description of spectral efficiency problems in wireless networks. Then the solutions that were proposed before WiFi6 standard are discussed. Then some of the proprietary solutions are outlined. The most significant part of this section is the recent studies on the carrier sensitivity threshold and OBSS/PD mechanisms. Then the spectral efficiency in other wireless networks is mentioned. In the second part of the section focuses on the recent studies on rate selection algorithms.

In chapter 4, our proposed algorithm is introduced. The working principle of the algorithm and theoretical background are given. The algorithm and the details of the mechanism are illustrated clearly with use cases.

Chapter 5 is about the experimental setup and evaluation of the simulation results. In this section, the simulation infrastructure and a set of scenarios were described. Then, the simulation and topology parameters are defined. The simulation results are illustrated, and each result is evaluated.

In the final chapter, the contributions of our algorithm and the future directions are discussed.

2. IEEE 802.11 STANDARD AND WIFI6

In this section, an introductory level of information on wireless network technologies and channel access mechanisms will be given. Then, the topic will be elaborated by focusing on IEEE 802.11ax (WiFi6) Protocol and its main features. These main features will be discussed under three subsections: orthogonal frequency division multiple access (OFDMA), OBSS/PD, and target wake time (TWT).

2.1. IEEE 802.11 Protocol and CSMA/CA Basics

The early footsteps of wireless communication were taken by Alexander Graham Bell by the invention of photophone, which was working via visible light [2]. At late 1890's, several scientists including Heinrich Hertz, Guglielmo Marconi, and Karl Ferdinand Braun started considering long-distance wireless communication via radio waves [3]. Although there have been small-scale implementations in the following decades, wireless communication via radio waves has seen first widespread practical usage during the Second World War. As such, in the early 1940s both the Allied and Axis military command deployed wireless communication systems for a variety of scenarios. However, one cannot argue that the main revolution of wireless communication occurred during the 1980's and 1990s where it started to be used for non-military cases. From then on, a plethora of mechanisms, communication protocols, and standards have been developed and deployed under the broad wireless communication umbrella. As the portable devices are getting smaller and the computational power increasing, importance of wireless communication will become a ubiquitous and indispensable part of the overall human technology.

A standardization effort for a wireless local area network (WLAN) system took place between the 1990 and 1997 by the Institute of Electrical and Electronics engineers (IEEE). The resulting standard, named IEEE 802.11, has been published in 1997. In the veins of the wired local area network (LAN) standard, the Ethernet; IEEE

802.11 also consists of mechanisms governing both the physical and data link layers of the Internet protocol stack. Then in 1999, to facilitate the interoperability between devices of different companies using this IEEE 802.11 standard and develop the best user experience, a non-profit organization called WiFi Alliance has been formed. One year later, in 2000, the WiFi Alliance created the “WiFi” trademark for solutions based on the IEEE 802.11 standard family [4].

From the day of the initial release of the standard to today, many 802.11 protocols have been released. As seen in the Table 2.1, data rates have been significantly improved with each subsequent WiFi protocol. Since this thesis study is built on top of the IEEE 802.11ax (WiFi 6) protocol. In the next sections, IEEE 802.11ax and WiFi 6 WiFi 6 will be used interchangeably.

Table 2.1. Main substandards of the IEEE 802.11 standard family.

Standard	Frequency (GHz)	Maximum Data Rate	Release
IEEE 802.11	2.4	2 Mbps	1997
IEEE 802.11a (WiFi 1)	3.7/5	54 Mbps	1999
IEEE 802.11b (WiFi 2)	2.4	11 Mbps	1999
IEEE 802.11g (WiFi 3)	2.4	54 Mbps	2003
IEEE 802.11n (WiFi 4)	2.4/5	600 Mbps	2009
IEEE 802.11ac (WiFi 5)	2.4/5	450-1300 Mbps	2013
IEEE 802.11ax (WiFi 6)	2.4/5-(6 for WiFi 6E)	450 Mbps-10.53 Gbps	2021

The default topology of a WiFi network is a star topology consisting of a single wireless access point (AP) and a multitude of user stations (STA). Alternatively each WiFi device in a WiFi network, either a STA or an AP, can also be called a node. In a BSS, all STAs need to be within the range of the AP to have a communication link. However, they may or may not be in the range of other STAs. Since there is no central authority controlling WiFi networks, there can be multiple WiFi networks in the same area. To distinguish different WiFi networks in close proximity, a special identifier called service set identifier (SSID) is used. As such, all devices belonging to

the same BSS use the same SSID in their packets to distinguish their traffic from other WiFi networks in the same area.

WiFi networks operate in some dedicated frequency intervals named WiFi channels. Since all nodes in a given WiFi network use the same channel, they cannot transmit data simultaneously because of a possible collision. Therefore, each node should check whether the medium is busy or not, before transmitting data. Following the footsteps of the Ethernet protocol, IEEE 802.11 is also designed as a distributed protocol where each node in a network works on its own without any central network entity. In such a distributed network, a mechanism is required for the coordination between nodes in their transmissions to avoid or eliminate collisions. Due to the inherent differences between a wired communication system and a wireless communication system, 802.11 protocols use CSMA/CA mechanism instead of the carrier sense multiple access with collision detection (CSMA/CD) mechanism of the Ethernet protocol. Here, the main goal is to avoid collisions.

The first part of CSMA/CA is carrier sensing and it can be performed via two mechanisms: physical carrier sensing and virtual carrier sensing. As the word “physical” implies, physical carrier sensing uses the physical layer and detects whether there is a signal in the medium or not. If any signal is detected, the channel is considered as BUSY otherwise it is considered as IDLE. The second mechanism, the virtual carrier sensing, does not use any physical attributes, instead it uses a duration field called the network allocation vector (NAV). When a communication starts between a STA and the AP, the duration field in the medium access control (MAC) header (Figure 2.1) is set and other STAs in the same BSS use this information to set their NAV values to determine how long will the ongoing transmission take. For a given STA, when the NAV is set, the STA waits until the NAV period before using its physical carrier sensing again.

IEEE 802.11 protocol defines two corresponding multiple access mechanisms: distributed coordination function (DCF) and point coordination function (PCF).

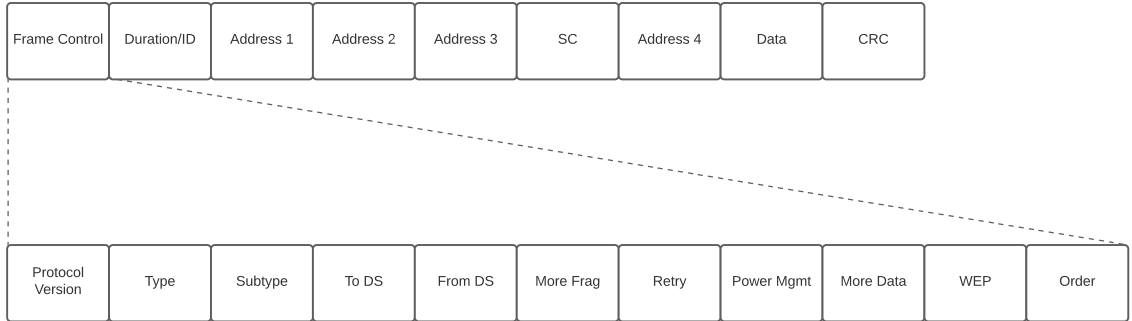


Figure 2.1. MAC frame of 802.11 protocol.

While DCF is supported by all WiFi nodes and can work on its own, PCF can only be used in conjunction with DCF [5]. Both PCF and DCF use a common concept called inter frame space (IFS), that are used for controlling the time interval between frames [5]. Different types of IFS duration enable priority among different types of frames, e.g., if a waiting time interval is shorter for a specific frame then that frame has a priority compared to longer waiting-time intervals. There are three main types of IFS intervals [6]:

- (i) DCF-IFS (DIFS) is the main interval used to check if the medium is IDLE state or not. DIFS is also used prior to RTS frames, and its value is calculated as

$$DIFS = SIFS + (2 \times T_{Slot}). \quad (2.1)$$

- (ii) Short IFS (SIFS) is a shorter (i.e., 10 μ s) interval and therefore have the highest priority among all IFS types. It is used prior to acknowledgement (ACK) frames, Block ACK frames or CTS frames. where T_{Slot} represents slot time.
- (iii) PCF-IFS (PIFS) is similar to DIFS, but it is used by PCF within contention-free operations. The priority of PIFS is greater than DIFS. PIFS calculation is formulated as:

$$PIFS = SIFS + T_{Slot}. \quad (2.2)$$

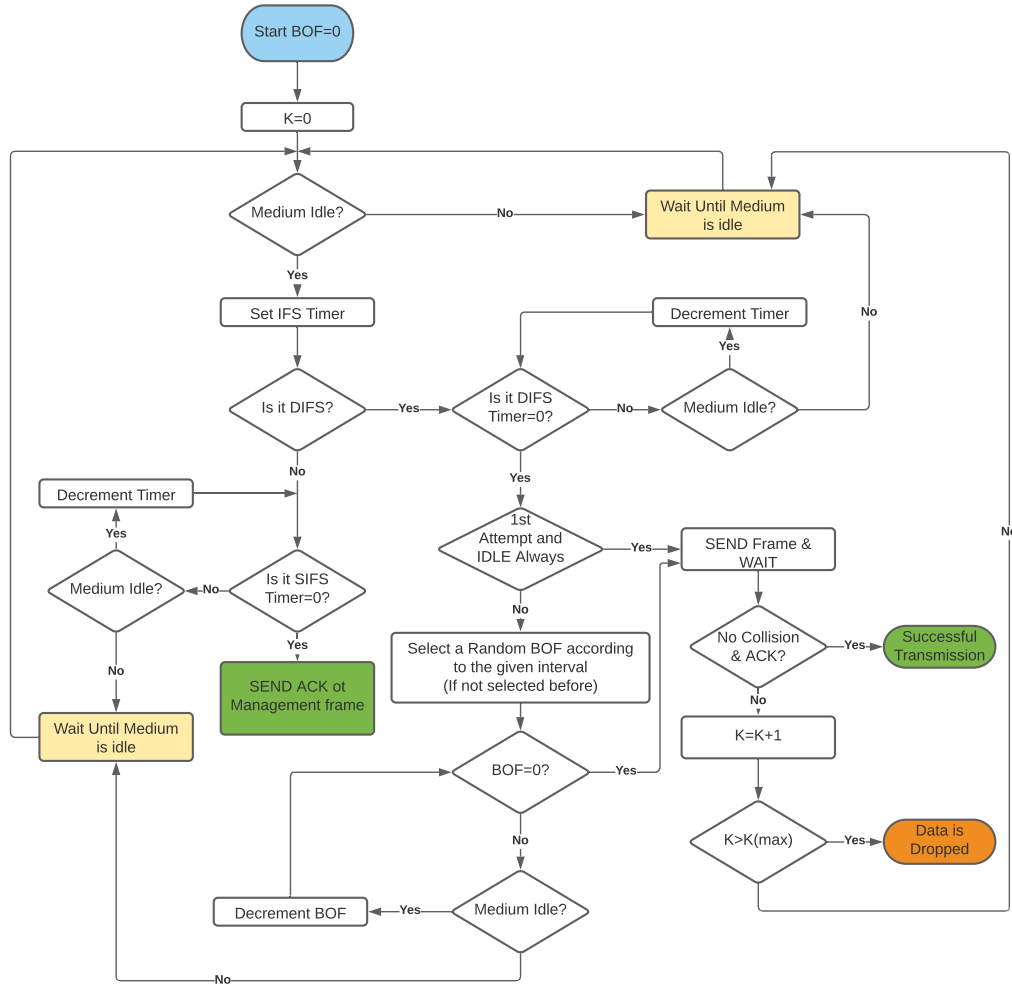


Figure 2.2. DCF mechanism flowchart.

In Figure 2.2, a flowchart of DCF mechanism is illustrated [6]. When checking the status of the channel, first the node determines which IFS to use based on the type of the frame. Using the applicable IFS value, the node checks if the medium is idle for this period. If so, it sends the frame at the end of this period. If an ACK frame is received, the transmission is considered as successful. If no such ACK frame is received until the end of a timeout value, the transmission is assumed to be lost and has to be retried. Each frame shall be retried up to a maximum value (K_{max}). In case the retry count, K , exceeds K_{max} , then the transmission is considered as failed. Before sending a frame, the channel status is evaluated until it is observed as in idle state. Moreover, it is waited for a random back-off duration in case of the medium is idle and it is not

the first attempt (there is an exception for the first attempt that enables skipping the back-off duration). When this waiting duration ends, the frame is sent, waiting for the aforementioned ACK frame until a certain timeout value. For the waiting duration of SIFS, if the timer reaches zero, ACK or Management frame can be sent.

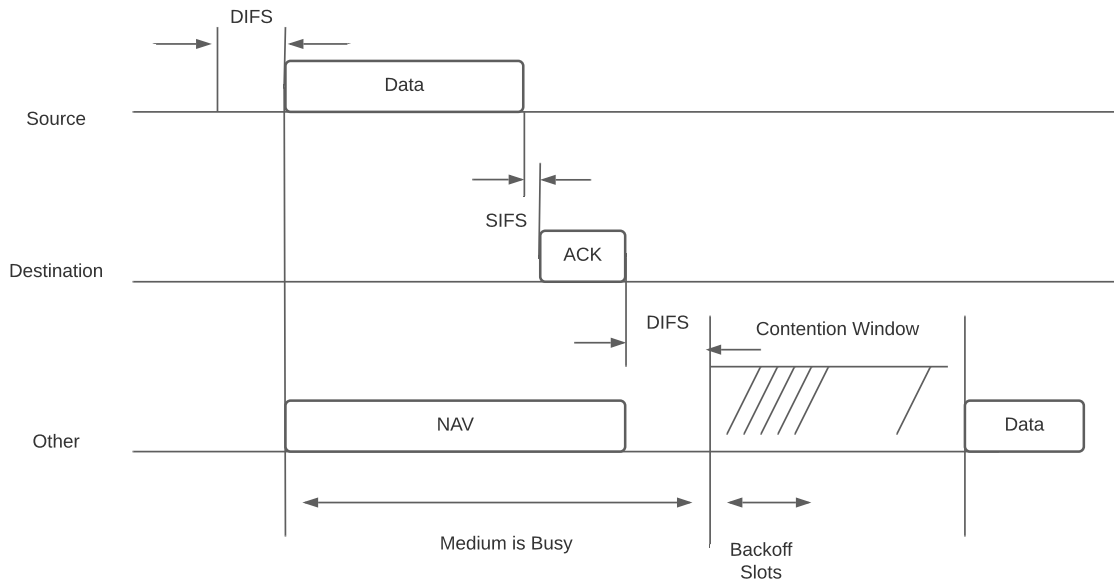


Figure 2.3. DCF mechanism for an example scenario.

In Figure 2.3, an example scenario for DCF is given. In this scenario, the “Source” node waits for a DIFS period of time since it is trying to transmit a data frame and the medium is detected as IDLE. After this verification, the “Source” node sets the duration in the MAC frame header as in Figure 2.1 according to the length of the data frame and sends the data frame to the “Destination” node. The “other” node receives the frame via its physical layer. Since it is not the destination of this frame, it only looks at the duration field. Based on the value of this duration field, it understands that the medium will be BUSY for this duration. Then, it sets its NAV and waits until the ongoing transmission is finished. Meanwhile, after sending the data frame, the “Destination” node waits for the mandatory SIFS time and sends ACK frame to the “Source”. After the communication ends, all the nodes should wait for DIFS interval and the backoff time to send new data. The backoff mechanism is used to prevent the nodes to initiate transmission at the same time. By that way, it reduces the probability

of collision after the DIFS period. If the backoff mechanism did not exist after the ACK frame or at the end of the NAV timer, each node would try to initiate a transmission after DIFS and collision would occur. Therefore, the backoff mechanism is used to select a small random waiting time for each node. This provides a different starting time to each node for the transmission. The backoff mechanism can be summarized as follows: the backoff time is chosen in an interval uniformly between zero and a window size. If the transmission is failed, the value of the window size is doubled until the maximum window size value is reached and it stays at this level unless a successful transmission occurs. A successful transmission resets the window size to its initial value. This backoff time is calculated by the binary exponential backoff algorithm and this interval is called as “Contention Window” [6].

While DCF is mandatory for all STAs, PCF is an optional mechanism and can be used only by APs. However, today PCF is not widely used in actual WiFi networks and is mainly considered as obsolete. In the IEEE 802.11 standard, PCF is located above DCF and must be used together with DCF. Main feature of PCF is the Contention-Free period for AP-Coordinated frame transfer. In Figure 2.4, coexistence structure of PCF and DCF is illustrated. The PCF is repeated every contention-free period (CFP) repetition interval, which has two parts: CFP portion is allocated to PCF duration and contention period (CP) portion is allocated to DCF duration. Since the contention free medium is not always available, beacon and NAV duration are operated by PCF and the rest of the repeating interval is managed by the DCF mechanism.

2.2. IEEE 802.11ax Protocol

In 2013, one of the subgroups of 802.11 group, named high efficiency WLAN study group (HEW SG) began to study on a next generation high efficiency WLAN standard. Finally, in 2014, task group ax (TGax) was formed and first draft of 802.11ax standard has been published [7]. 802.11ax protocol can be considered as the successor of 802.11ac and the main goal is increasing the spatial efficiency and throughput per area in dense networks [8].

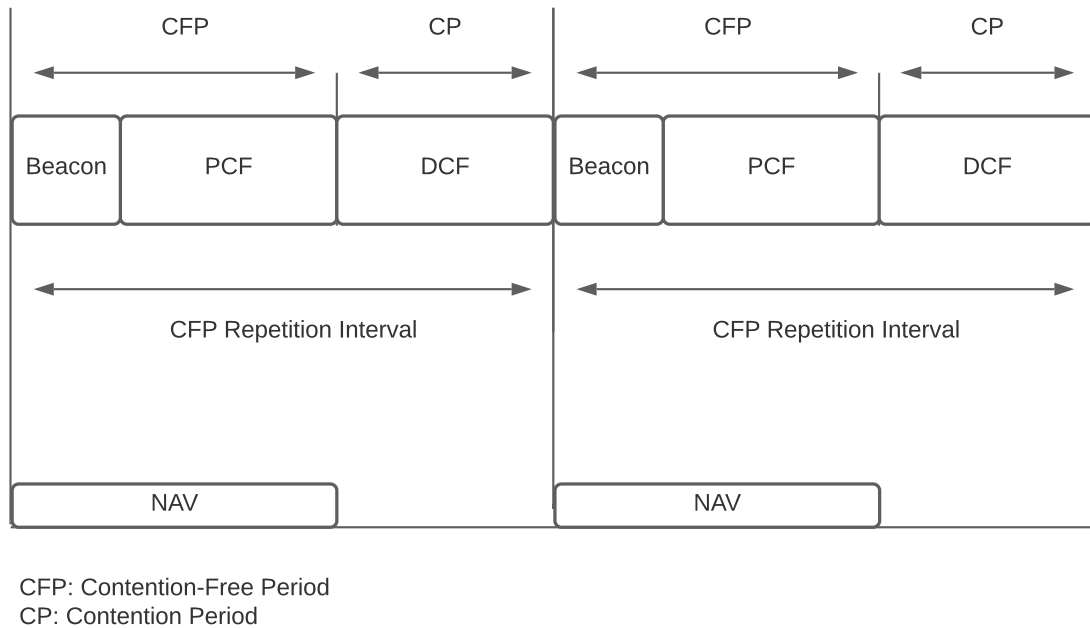


Figure 2.4. PCF-DCF coexistence mechanism illustration.

2.2.1. Main Features of IEEE 802.11ax Protocol

Starting with PHY layer changes and additions, WiFi6 offers a multitude of changes regarding the PHY layer. Although the main goal of the IEEE 802.11ax protocol is spectral efficiency in dense environments, which contains a high number of stations and overlapping BSSs, there are also two new MCS levels added to the standard. Accordingly, the data rate increases up to gigabit level via 1024-QAM with a single antenna. A sample MCS schema of 802.11ax protocol for OFDM is shown in Table 2.2 and Table 2.3. As seen in the tables, 802.11ax protocol has 12 different MCS indexes.

Initially, 802.11ax is planned to work only with classical WiFi channels in 2.4 GHz and 5 GHz frequency bands, but with the extension called WiFi-6E, the new 6 GHz frequency band has been added recently [1]. In addition to the frequency bands, 802.11ax has three guard interval options; 0.8 μ s, 1.6 μ s and 3.2 μ s.

Table 2.2. 802.11ax OFDM rates (20 and 40 MHz) for single spatial stream [1].

802.11ax OFDM Rates (Theoretical)								
MCS	Modulation	Coding	20 MHz			40 MHz		
			0.8 μ s GI	1.6 μ s GI	3.2 μ s GI	0.8 μ s GI	1.6 μ s GI	3.2 μ s GI
0	BPSK	1/2	8.6	8.1	7.3	17.2	16.3	14.6
1	QPSK	1/2	17.2	16.3	14.6	34.4	32.5	29.3
2	QPSK	3/4	25.8	24.4	21.9	51.6	48.8	43.9
3	16-QAM	1/2	34.4	32.5	29.3	68.8	65	58.5
4	16-QAM	3/4	51.6	48.8	43.9	103.2	97.5	87.8
5	64-QAM	2/3	68.8	65	58.5	137.6	130	117
6	64-QAM	3/4	77.4	73.1	65.8	154.9	146.3	131.6
7	64-QAM	5/6	86	81.3	73.1	172.1	162.5	146.3
8	256-QAM	3/4	103.2	97.5	87.8	206.5	195	175.5
9	256-QAM	5/6	114.7	108.3	97.5	229.4	216.7	195
10	1024-QAM	3/4	129	121.9	109.7	258.1	243.8	219.4
11	1024-QAM	5/6	143.4	135.4	121.9	286.8	270.8	243.8

Table 2.3. 802.11ax OFDM rates (80 and 160 MHz) for single spatial stream [1].

802.11ax OFDM Rates (Theoretical)								
MCS	Modulation	Coding	80 MHz			160 MHz		
			0.8 μ s GI	1.6 μ s GI	3.2 μ s GI	0.8 μ s GI	1.6 μ s GI	3.2 μ s GI
0	BPSK	1/2	36	34	30.6	72.1	68.1	61.3
1	QPSK	1/2	72.1	68.1	61.3	144.1	136.1	122.5
2	QPSK	3/4	108.1	102.1	91.9	216.2	204.2	183.8
3	16-QAM	1/2	144.1	136.1	122.5	288.2	272.2	245
4	16-QAM	3/4	216.2	204.2	183.8	432.4	408.3	367.5
5	64-QAM	2/3	288.2	272.2	245	576.5	544.4	490
6	64-QAM	3/4	324.3	306.3	275.6	648.5	612.5	551.3
7	64-QAM	5/6	360.3	340.3	306.3	720.6	680.6	612.5
8	256-QAM	3/4	432.4	408.3	367.5	864.7	816.7	735
9	256-QAM	5/6	480.4	453.7	408.3	960.8	907.4	816.7
10	1024-QAM	3/4	540.4	510.4	459.4	1080.9	1020.8	918.8
11	1024-QAM	5/6	600.5	567.1	510.4	1201	1134.3	1020.8

Finally, IEEE 802.11ax supports Multi User - Multiple Input Multiple Output (MU-MIMO) in both uplink (UL) and downlink (DL) directions unlike 802.11ac, which has MU-MIMO only in DL direction. All of these additions in IEEE 802.11ax and differences with IEEE 802.11ac (i.e., WiFi5) have been given Table 2.4.

Table 2.4. 802.11ax comparison with legacy 802.11ac.

Feature	802.11ac	802.11ax
Frequency (GHz)	2.4/5	2.4/5 and (6 for WiFi-6E)
Bandwidth (MHz) (OFDM)	20/40/80/160	20/40/80/160
Guard Interval (μ s)	0.4/0.8	0.8/1.6/3.2
OFDMA	Not Available	Available
MCS	0-9	0-11
TWT	Not Available	Available
Fragmentation	Static	Dynamic
Symbol Duration (μ s)	3.2	12.8
NAV	Single	Two
OBSS/PD	Not Available	Available

In addition to these PHY layer improvements, WiFi6 also has a quite high number of new MAC layer mechanisms. First and foremost of these mechanisms is the adoption of OFDMA. The main rationale behind adding OFDMA support to WiFi is to allow simultaneous transmission both in the DL and UL direction to reduce delay and increase overall efficiency. In OFDMA, multiple nodes are able to transmit at the same time, reducing the interference by dividing the resource units (RUs) available in the spectrum. OFDMA will be discussed in detail in the following chapters.

Another critical MAC layer addition of WiFi6 is the improved support for spatial reuse by BSS coloring that was introduced in 802.11ac and 802.11ah protocols before. According to the color mechanism of the 802.11ax protocol, each BSS has its own color defined in the management frame with 6 bits information as in the Figure 2.5. Since

the BSS color header is 6 bits long, there are 63 available colors that can be assigned to the each BSS and its nodes. The color information is carried by HE-SIG-A frame as shown in the Figure 2.6 that contains HE-PPDU structure of 802.11ax. If there are overlapping BSSs, the color information of the transmitted frames can be used for increasing the spectral efficiency by increasing the hearing threshold and ignoring the incoming packets from the Inter-BSS nodes. This threshold mechanism is called OBSS/PD and it will be discussed in the following chapters in detail.

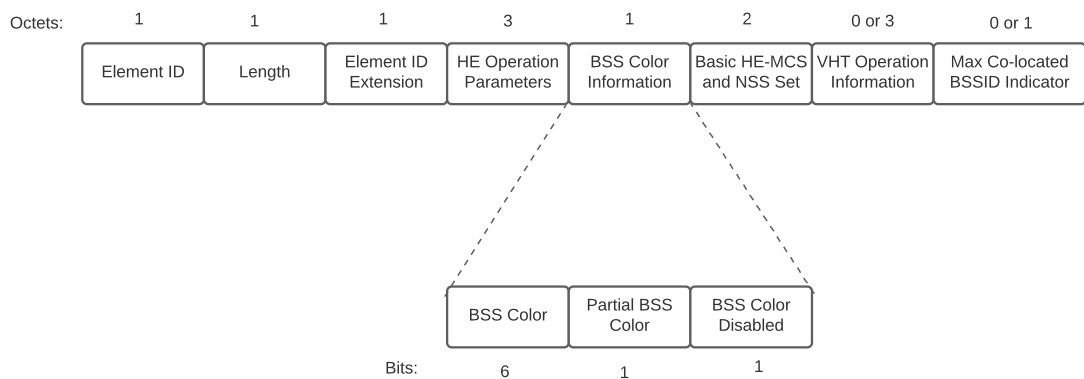


Figure 2.5. 802.11ax color header in HE operation element.

As explained in the Section 2.1, for the legacy WiFi standards, CSMA/CA mechanism has a single NAV as the virtual carrier sensing mechanism. One of the innovations made in 802.11ax is to use two NAVs. In dense environments, due to overlapping BSS's, the NAV value can be reset by another BSS's frame which in turn may cause collisions. In order to overcome this issue, the Two-NAV approach can differentiate the two NAVs as follows; one for Inter-BSS and the second for Intra-BSS. The information of whether the corresponding NAV is an Inter-BSS or an Intra-BSS NAV is distinguished by the color mechanism. If the incoming WiFi frame has the same color with the recipient node, Intra-NAV is set, otherwise Inter-NAV is set. By that way, Inter-BSS frames cannot reset the NAV of the Intra-BSS stations and vice versa [1].

Another MAC layer mechanism introduced with 802.11ax is the quiet time period (QTP) [9]. This mechanism indicates a period that how long a node will be quiet.

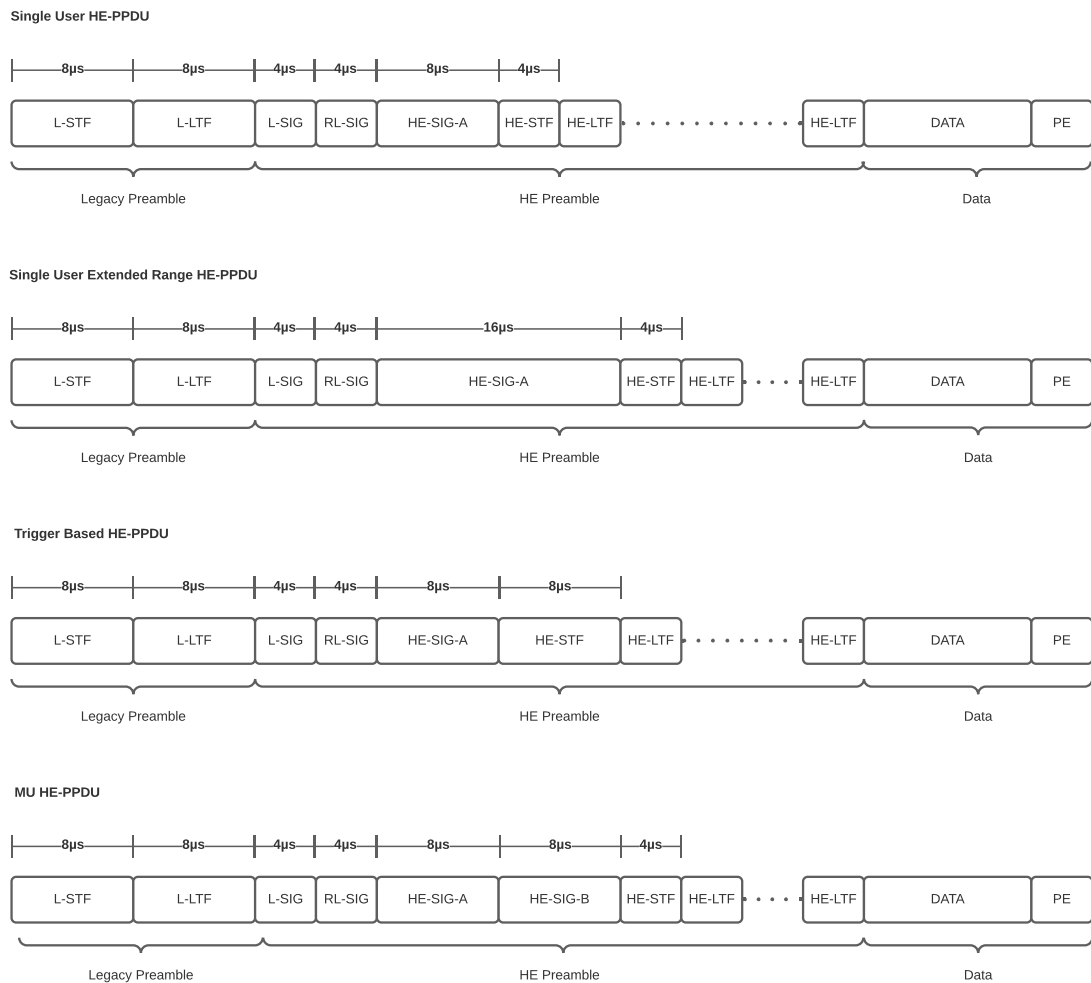


Figure 2.6. 802.11ax HE-PPDU structures.

To set QTP, the STA sends a time allocation information to AP. Then, the AP dedicates the requested time intervals to the corresponding STA and no other STAs can access the channel in these time intervals.

Next is the dynamic fragmentation mechanism. Whereas 802.11ac has static fragmentation (i.e., which means all fragmented data packets have the same size), 802.11ax fragmentation can generate dynamic size data fragments. Using dynamic size data fragments helps to reduce the transmission cost by using the available resource units efficiently.

Another major contribution of IEEE 802.11ax is a much more efficient power saving mechanism called the TWT. Initially introduced in 802.11ah standard, TWT has been adopted to 802.11ax in order to increase efficiency in power consumption. This mechanism is used by AP and it can tell the STAs when to wake and sleep. During the beacon transmission, AP tells the STAs to sleep in a time period and the other time periods the STAs are told to be awake [10]. By that way the STAs know when they should listen to the medium. The main contribution of 802.11ax is STA based TWT handshake. This mechanism increases the flexibility of the TWT mechanism rather than the AP based TWT mechanism.

Finally, a third channel access mechanism called uplink OFDMA random access (UORA) has been introduced. Basically, a mix between the classical random access mechanism of WiFi and the OFDMA mechanism is achieved, it is also called trigger-based random access. In UORA, if STAs are not allocated RUs in UL OFDMA transmission, STAs can use some RUs allocated by the trigger frame for random access. Being a random-access mechanism at its heart, UORA also defines a backoff mechanism. In order to begin transmission without collisions at the same RU, OFDMA back-off (OBO) procedure is applied by STAs. Although this mechanism is still under research; initial works show that the efficiency of UORA is less than the scheduled access of OFDMA in many cases. UORA is expected to be more useful in short packet transmissions [11].

2.2.2. OFDMA As a Digital Modulation Scheme

One of the major innovations of 802.11ax protocol to 802.11 family is to use OFDMA in the PHY layer. OFDMA is a digital modulation scheme like OFDM which has been already used in the legacy standards like 802.11a/g/n/ac. Both OFDM and OFDMA modulation schemes are available in 802.11ax standard. Fundamentally, OFDMA is a multi user version of OFDM and divides the channel into sub frequency intervals called subcarriers. The subcarriers are orthogonal to each other and this prevents the inter carrier interference (ICI) between the neighbour subcarriers. By

using these subcarriers, concurrent transmissions can be made either in DL or UL direction [12].

There are three kinds of subcarriers; pilot subcarriers, data subcarriers, and guard (or null) subcarriers. Pilot subcarriers are used for synchronization between the transmitter and receiver (phase and parameter information), data subcarriers are used for transmitting the modulated data, and guard subcarriers are used for putting guard interval that prevents interference issues between the subcarriers. When describing the subcarriers in 802.11ax OFDMA mechanism, the term “tone” is used instead of the subcarrier. To allow multiple transmissions at the same time, these data tones are aggregated into what is called Resource Units (RUs) one of which can be assigned to a transmission between the AP and a particular STA. Whereas there are 20/40/80/160 Mhz channel bandwidths in OFDM, in OFDMA, 26/52/106/242/484 /996-tone RUs are available. Therefore a given WiFi channel with a certain bandwidth will be composed of several RUs, where each RU can be assigned to a traffic between the AP and a particular STA [11].

One important aspect of OFDMA is the fact that the RU allocation should be done before the actual data transmission. This RU allocation to STAs may be done in two ways: static mapping (scheduling) and dynamic mapping (trigger-based random access). In DL transmission, the RU allocation information and transmission parameters are carried by HE-SIG-B section of the frame for each STA. Since the uplink multiple user (UL-MU) transmission is from STA to AP, before transmitting data, AP sends a trigger frame containing RU allocation and the transmission parameters. The transmission parameters are used for synchronization of STAs with AP. Since the AP requires RSSI values from the STA to synchronize with it, the AP sends RSSI values of the current signal and targets RSSI values to each STA. For UORA, RUs are not allocated for each STA, instead, they are offered to contend for an RU using a random access mechanism. Each RU has the same size and parameters and can be used by each associated and unassociated stations. In order to mitigate collisions on a given RU, the aforementioned OBO is used [1].

2.2.3. OBSS/PD Mechanism

IEEE 802.11ax amendment focuses on spectral efficiency and one of the important features of the standard is the OBSS/PD mechanism. In dense environments, if there are overlapping BSSs that are using the same channels, the traffic belonging to these BSSs must share the channel and contend for access. Before performing the transmission, each STA should check whether the medium is in idle state or not. In some cases, two STAs belonging to different BSSs cannot transmit simultaneously even if their transmissions will not actually cause transmission collisions. Hence, reducing the spectral efficiency.

In Figure 2.7, such a problematic scenario is illustrated when there are two different BSSs in close vicinity. The dotted circles represent the range in which a WiFi can be heard, red dotted circle for STA-1, and blue dotted circle for STA-2. Outside of these ranges, a WiFi transmission can not be heard. In this example, the active UL transmission between STA-1 and AP-1 causes interference to STA-2 and STA-2 cannot start a transmission with AP-2. Such concurrent transmissions will not have affected the reception process, so we are actually reducing the spectral efficiency. It is possible to overcome this problem if we had the option of adjusting the ranges of each STA that affects which frames are received/heard. To continue this example, if the ranges are to be adjusted as the dashed bold circles the STAs cannot hear each other and both STAs can transmit data simultaneously.

At its core, the spatial reuse features of 802.11ax allow the STAs and APs to adjust their ranges in a dynamic fashion to maximize the spectral efficiency. OBSS/PD mechanism is an extension to the legacy CSMA/CA mechanism. In Figure 2.8, the whole OBSS/PD and the legacy clear channel assessment (CCA) mechanism are illustrated. In legacy CSMA/CA, to determine the channel state and perform the signal detection, the first check is done with the received signal sensitivity (Rx-Sensitivity) threshold.

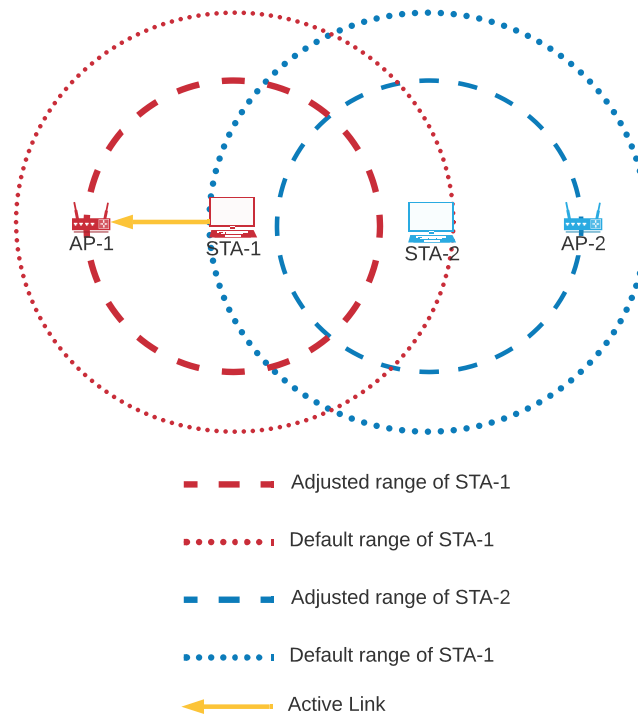


Figure 2.7. An example of spectral efficiency problem.

The Rx-Sensitivity threshold is based on RSSI and if the incoming signal level is below this level, the signal will be dropped and the channel is considered as IDLE. The default value of Rx-Sensitivity is determined by a threshold and a signal which is below this threshold is accepted as a thermal noise. If the RSSI of the incoming signal is greater than the Rx-Sensitivity, as a second assessment, preamble detection is performed. During this step, the channel will be in CCA_BUSY state. If the preamble is not detected, to detect the interference level and perform a clear channel assessment, the signal strength is compared to the clear channel assessment energy detection (CCA/ED) threshold.

In the medium, there may be wireless communications other than WiFi. To prevent the interference with these signals, CCA/ED threshold is set -62 dBm by default and if the received signal is under this value, the channel will be considered in an IDLE state, otherwise it is in a BUSY state.

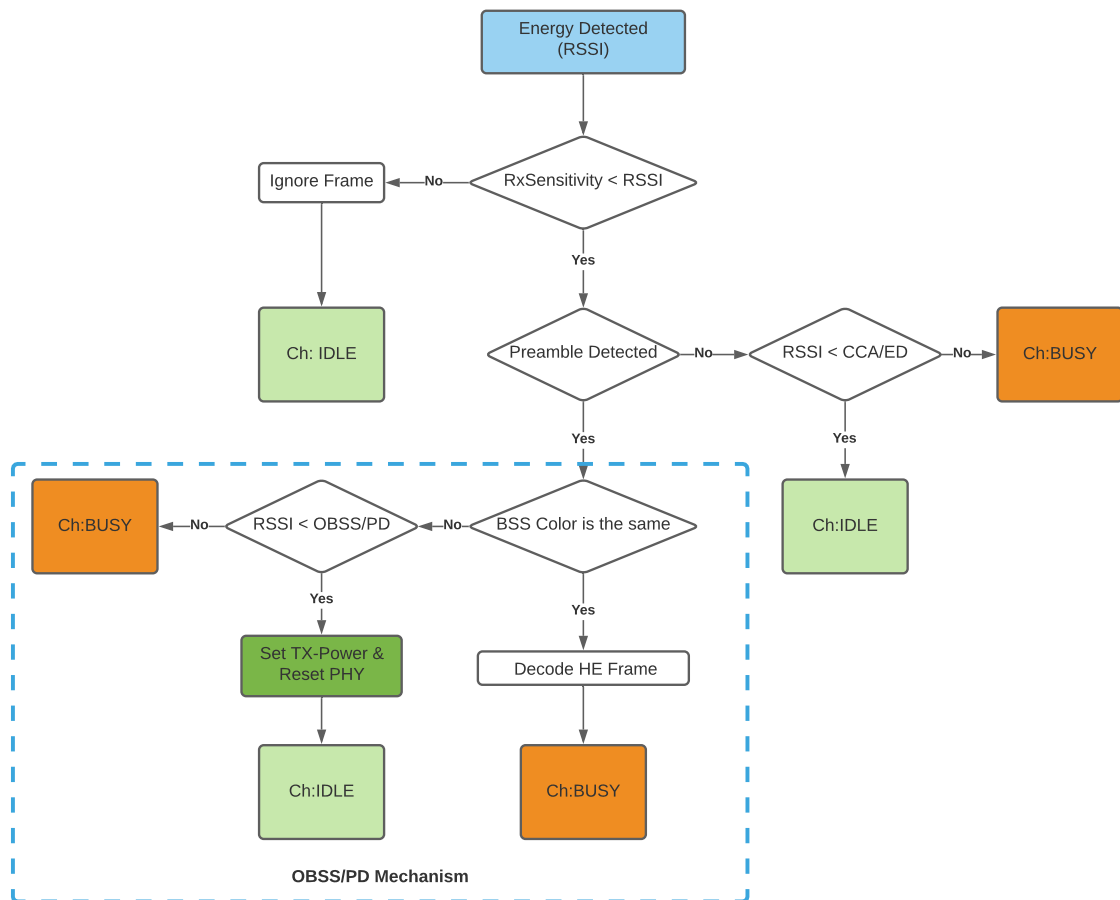


Figure 2.8. OBSS/PD mechanism on top of legacy preamble detection.

If the preamble detection is successful, then OBSS/PD evaluation is performed. OBSS/PD mechanism uses a threshold called the OBSS/PD threshold, when determining the availability of the WiFi channel to eliminate the interference originated from overlapping BSSs. The color mechanism of 802.11ax can be used to distinguish whether the signal is originated from the Inter-BSS or not. First of all, the BSS color is checked via BSS Color Information header. If the color of an incoming signal is the same with the color of the receiver node, the HE-frame of the received signal is decoded and the channel will be considered as BUSY state. If the color is different, the signal is ignored. Then, in order to obtain the channel status, RSSI is compared to the OBSS/PD threshold, and if the RSSI value is greater than the OBSS/PD threshold, the channel is considered as BUSY state. If the RSSI value is below the OBSS/PD

threshold value, Tx-Vector is updated and PHY is reset. Then, the channel state is considered as IDLE state.

The value of the OBSS/PD threshold level is directly related to Tx-Power. In [13], it is shown that when the multiplication of transmission power and carrier sensing threshold is a constant value, the wireless channel utilization/efficiency increases. In Figure 2.9, this relationship is illustrated for OBSS/PD threshold mechanism. If the Inter-BSS based collision signal level is low, the OBSS/PD level should be set to lower levels and at the same time Tx-Power should be set to higher levels.

On the other hand, if the medium has so many Inter-BSS collisions and the signal levels are high, in this case, the OBSS/PD should be set to higher levels to ignore these signals and transmission power should be reduced, i.e., the communications should be carried over in a close vicinity with a lower transmit power and ignoring some of the interference signals.

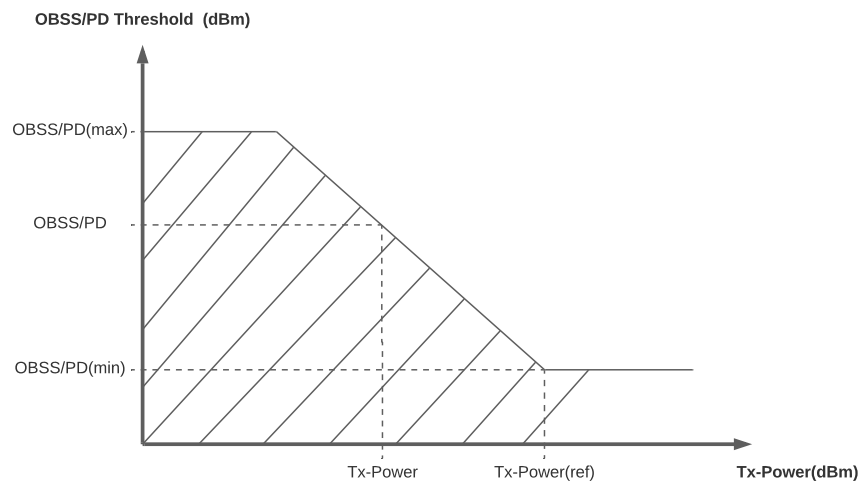


Figure 2.9. OBSS/PD-Transmission power relationship.

From the relationship of OBSS/PD threshold and transmission power, the transmission power is calculated via the given OBSS/PD level according to the Equation (2.3).

Table 2.5. OBSS/PD ranges at different channel bandwidths.

	20 MHz	40 MHz	80 MHz	160 MHz
$OBSS/PD_{Min}$ (dBm)	-82.0	-79.0	-76.0	-73.0
$OBSS/PD_{Max}$ (dBm)	-62.0	-59.0	-56.0	-53.0
$TxPower_{Ref}$ (dBm)	21.0	18.0	15.0	12.0

Since there is a linear relationship between OBSS/PD threshold and transmission power, as the transmission power increases, OBSS/PD should be decreased exactly the same amount of value or vice versa. For each channel bandwidth (i.e., 20 MHz, 40 MHz, 80 MHz, and 160 MHz), there are upper and lower bounds for OBSS/PD threshold and transmission power levels. In Table 2.5, the minimum and maximum limits of OBSS/PD threshold and transmission power ($TxPower$) are given for the corresponding channel bandwidths. These limits determine the region that an algorithm can adjust the OBSS/PD threshold and $TxPower$ accordingly.

$$OBSS/PD = OBSS/PD_{Min} + (TxPower_{Ref} - TxPower) \quad (2.3)$$

where $TxPower_{Ref}$ is the maximum transmission power and $OBSS/PD_{Min}$ is the minimum OBSS/PD threshold that is allowed to be set.

In Figure 2.10, there are two BSSs and each of them has one AP. Each station is associated with an AP and performs an uplink transmission. The default CCA Carrier Sensing thresholds are set to -82 dBm and both transmissions interfere with each other. This issue creates a significant amount of performance degradation in the overall system. In this problematic case, since the interfering signals are originated from Inter-BSS stations, OBSS/PD mechanism can be used to eliminate this interference. If both OBSS/PD thresholds are increased to -72 dBm and -74 dBm, respectively, the incoming Inter-BSS signal under this level will be ignored and each station can initiate transmission with their corresponding APs. According to the conditions and system parameters, while keeping the communication link alive, OBSS/PD level can

be increased and the same amount of transmission power can be decreased to reduce the interference. That means the incoming RSSIs from the Inter-BSS stations will be reduced at the receiver's physical layer and the incoming signals will not collide, because they are under the OBSS/PD threshold.

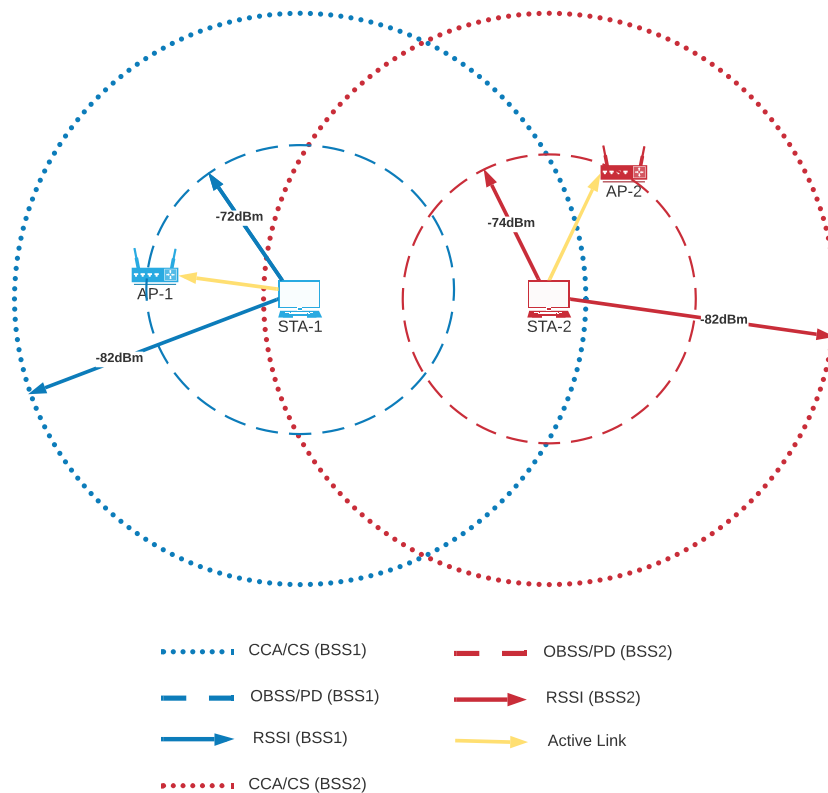


Figure 2.10. A simple scenario for OBSS/PD mechanism.

Please note that the color of an AP is chosen randomly. Therefore, there is always a risk that a neighbour BSS can also have the same color. In such cases, STAs can report this issue to their AP and then the AP picks a new color and sends this information to its STAs during the next beacon frame. In the Figure 2.5, the BSS color information is represented by eight bits (1 octet) of data. Six of these bits represent the BSS color field and there can be at most 63 different colors assigned to different BSSs. In Figure 2.11, an example implementation of the color mechanism is illustrated. BSSs that have the same color use different channels and there is no Inter-BSS interference even if they are close to each other. However, nodes that use

the same channel and different color may increase the probability of collision. These kind of nodes can be distinguished by the color field of HE-SIG-A frames. By that way, the collision probability can be reduced by adjusting the OBSS/PD parameters and the maximum performance gain can be obtained.

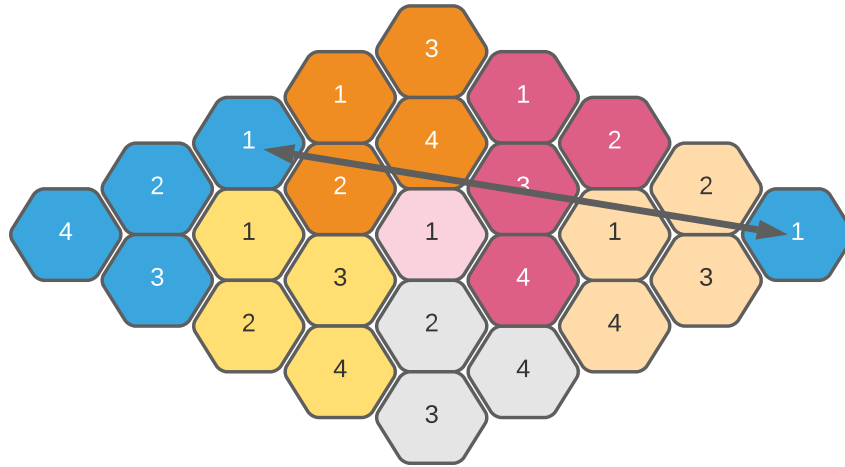


Figure 2.11. An example implementation of color assignment for the BSSs.

In 802.11ax standard, another OBSS/PD mechanism is introduced as the spatial reuse group (SRG) based on OBSS/PD threshold [14]. In the previous example, each station has only one OBSS/PD threshold and, this threshold is applied to each of the sources if there is an incoming HE-Frame. SRG based OBSS/PD mechanism uses two types of OBSS/PD thresholds: Non-SRG OBSS/PD and SRG OBSS/PD. In case of multiple BSS in the medium, applying different OBSS/PD thresholds for different BSSs may be useful. A SRG is a group of BSS and each member is represented within a color-bitmap in HE-frame. The SRG members are set by an AP and this information is forwarded to the corresponding stations.

When an HE-Frame is coming from Inter-BSS station, an SRG and Non-SRG frames can be distinguished by the spatial reuse parameter set [15]. This information is kept in SRG BSS color bitmap section of the spatial reuse parameter set element as in Figure 2.12.

In the case of a mixed topology that contains both SRG and Non-SRG features, If an incoming signal has a color that is a member of the SRG color bitmap, SRG OBSS/PD threshold is applied, otherwise Non-SRG OBSS/PD threshold is applied by the node. Hence, two different OBSS/PD thresholds can be applied to the incoming signals with different values.



Figure 2.12. SRG HE operation element.

An example of SRG based OBSS/PD mechanism is illustrated in Figure 2.13. In the example, even if the AP-2 increases its OBSS/PD level without losing its connection to STA-2, the STA-1 is still in the range and the Inter-BSS communication of BSS-1 has potential to distract the connection of BSS-2. Therefore, increasing the OBSS/PD does not improve the communication between STA-1 and AP-1. Moreover, the ongoing communication between nodes in the same BSS degrades due to the reduced transmission power. Therefore, BSS-2 may use a kind of tolerable OBSS/PD threshold for BSS-1 to preserve the transmission power. However, in this situation AP-3 is still in range and if BSS-2 and BSS-3 are analyzed independently, it can be seen that setting a higher OBSS/PD threshold value prevents the Inter-BSS interference between BSS-2 and BSS-3. In this case, SRG-based OBSS/PD mechanism can be used for setting different OBSS/PD thresholds. BSS-1 and BSS-2 are forming an SRG and whenever a high efficiency (HE) frame comes with a different color that belongs to the SRG group, they apply SRG OBSS/PD threshold. If the incoming frame has a different color and not a member of SRG group, non-SRG based OBSS/PD is applied. This methodology makes the OBSS/PD mechanism flexible and has potential to improve the communication performance.

OBSS/PD mechanism is still under research and there are some dynamic threshold algorithms that have been developed.

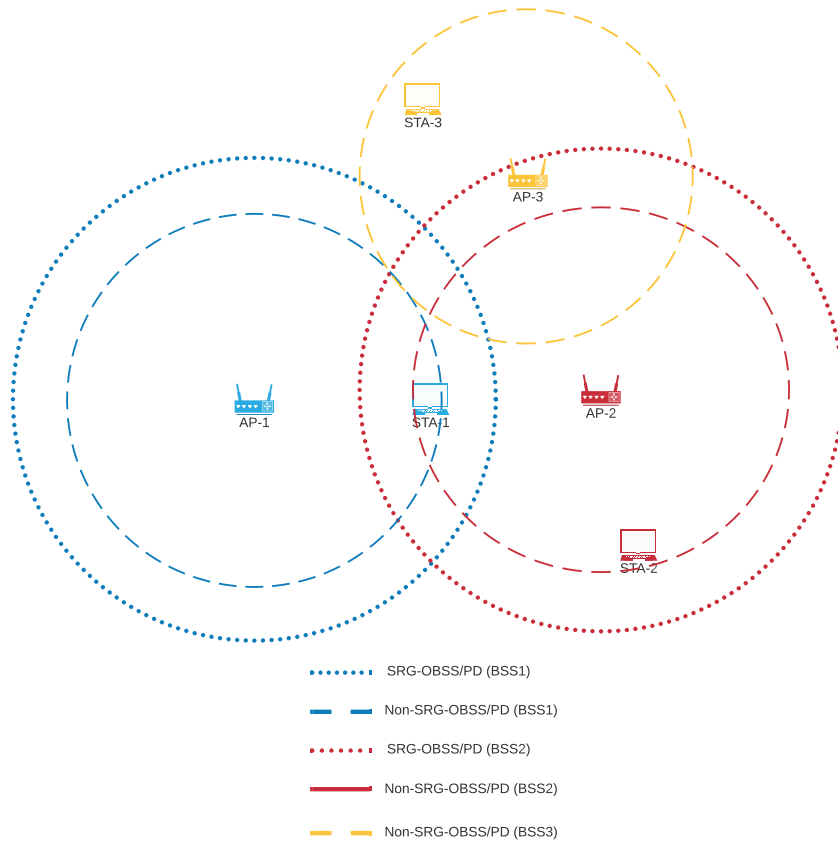


Figure 2.13. A simple scenario for SRG based OBSS/PD mechanism.

The recent works and achievements will be discussed in the next section in detail. This thesis study is also focused on a developing dynamic OBSS/PD threshold control mechanism.

2.2.4. Microsleep and TWT

The third MAC layer mechanisms that are added in IEEE 802.11ax are the microsleep and TWT mechanisms.

The microsleep mechanism is based a simple mode switch to a so-called microsleep state. If there is a signal interference, by using the incoming signal, some information related to the channel can be extracted. In 802.11ax amendment, switching the station

into sleep mode by considering source address, destination address, and frame duration was proposed which is called micro sleep mechanism.

In 802.11ax, even if the mechanism is similar, the information is extracted from HE-SIG-A section that includes information like color, transmission direction, frame duration, and so on. After determining the channel state as BUSY in a specific time interval, the station goes into sleep mode until the ongoing transmission finishes.

TWT on the other hand, is on its own a sophisticated mechanism mainly a more versatile version of the preexisting power saving mode of WiFi protocol. TWT indicates the next time which station will wake up to initiate transmission. After TWT period, the target wake duration (service period) begins and the indicated station should be in wake-up state during that period.

TWT parameters are specified by AP in either the next target beacon or the listen interval inside beacon frames. If there are lots of stations in the medium and they are associated with the same TWT broadcast group, each station does not have to listen each beacon frame. To use this mechanism efficiently, the next target beacon is specified by the AP and the station will get the next TWT broadcast parameters for itself. The listen interval is the similar mechanism, the stations wait for the interval named “listen interval” for the next beacon which includes their TWT parameter until the specified target time, the stations will be in sleep mode [16].

3. SPATIAL REUSE TECHNIQUES AND RATE SELECTION ALGORITHMS IN WIFI NETWORKS

3.1. Spatial Reuse Techniques in IEEE 802.11 Protocols

The term spatial reuse can be defined as an efficiency of using the same channel for transmission at the same time and close vicinity. Since the wireless channel can be accessible physically, there may be lots of associated and unassociated STAs operating in the same medium. Moreover, there may also be STAs associated with other BSSs in the same medium since they are sharing the same physical space. In this section, the spectral efficiency and solutions that were developed to increase spectral efficiency will be discussed. In the first subsection, classical channel access mechanisms in wireless networks will be briefly described. Then, well-known problems regarding channel access will be described and potential solutions to these problems will be discussed. Next, IEEE 802.11ax spatial reuse mechanism will be elaborated and related works will be summarized. Lastly, spectral efficiency of other wireless protocols will be discussed.

3.1.1. Channel Access Mechanisms

Channel access mechanisms can be defined by several spectral parameters like frequency, time, space, power, packet mode, code, etc. These access mechanisms can be used together to increase the efficiency. In essence, the medium access is managed by MAC sublayer and channel access mechanisms can be considered within the MAC sub-layer.

The frequency-based access mechanisms are based on dividing the channel bandwidth into non-overlapping frequency channels for simultaneous multiple data transmission. Frequency division multiple access (FDMA) and OFDMA can be given as examples that work with this principle. Since this method depends on the frequency division, as the bandwidth is divided into sub-channels, the risk of interference between

the neighbouring sub-channels increases (i.e., co-channel interference (CCI)). Physical constraints such as attenuation, quality of the transmitter, quality of the receiver, also limit this operation.

Time-based access mechanisms focus on time domain allocation. Therefore, such mechanisms are based on the management of the time intervals for concurrent transmissions. As a time based random access channel mechanism, as discussed in the Section 2.1, CSMA/CA can be given as an example. Besides, time division multiple access (TDMA), distributed time division multiple access (DTDMA), and self-organized time division multiple access (STDMA) can also be given as examples of time-based multiple channel access mechanism [17–19].

Coding-based access mechanisms are a third option which uses coding schemes to allow simultaneous transmission. code division multiple access (CDMA) can be given as an example of this kind of multiple access mechanism [20]. Finally, there are also space-based channel access mechanisms like space division multiple access (SDMA), which use spatial diversity and directional antennas. In these solutions, each transmission is done according to the physical location of the receiver node and the spectral efficiency is achieved [21].

3.1.2. Spectral Efficiency Problems

In wireless networks, due to their inherent differences from wired networks, there are several unique problems regarding node placements and topology, which in turn affects spectral efficiency. Two well-known such problems are the hidden node problem and the exposed terminal problem.

3.1.2.1. Hidden Node Problem. The carrier sensing procedure explained in Section 2.1 introduces a problem in some topologies that increases the collision probability in such topologies. In a topology consisting of an AP and at least two STAs associated with this AP, in case the two STAs cannot hear each other, a problematic scenario occurs. While

one of the STAs is transmitting, since the other STA is not aware of this transmission, it may also try to transmit at the same time and that may result in collisions. In this case, each STA is considered “hidden” to each other and the whole situation is called the “hidden node problem”. This problem may cause serious performance degradation in the network in terms of throughput and fairness.

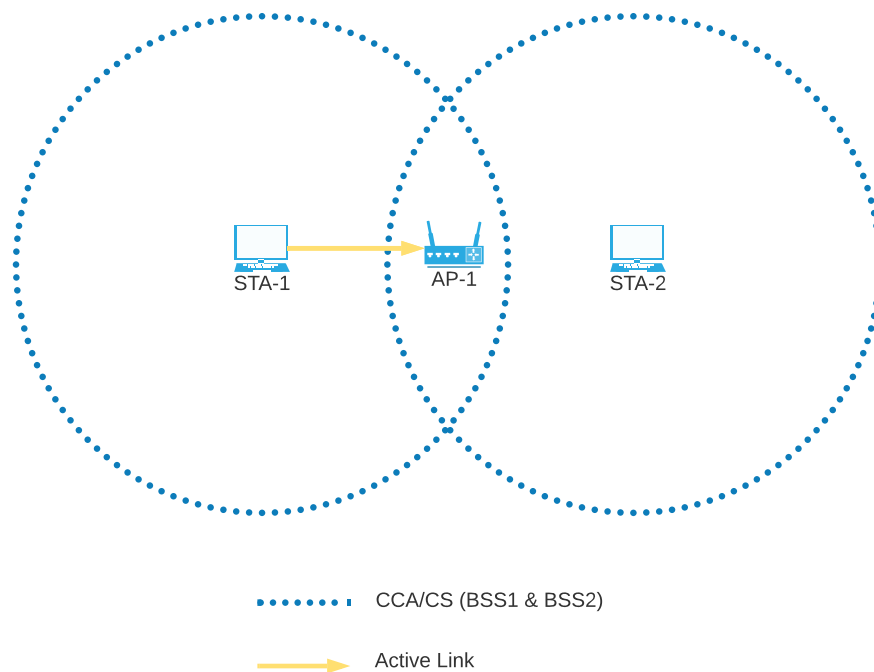


Figure 3.1. An example scenario for hidden node problem: STA-2 cannot detect that there is an active transmission between STA-1 and AP-1.

In Figure 3.1, an example case of a hidden node problem is illustrated. STA-1 and STA-2 belong to same BSS and associated with AP-1. In the case of the uplink transmission, the outgoing transmissions of STAs cannot be detected by each other. For instance, when STA-1 performs an uplink transmission since STA-1 is hidden to STA-2, STA-2 cannot sense the transmission and it considers that the channel is IDLE. Therefore STA-2 may also want to initiate a transmission and that may cause collisions.

3.1.2.2. Exposed Terminal Problem. Another spectral efficiency problem due to the CSMA mechanism is called the 'Exposed Node Problem'. Unlike in the hidden node

problem where STAs cannot hear each other, in this problem, while STAs could have been able to transmit concurrently, they do not transmit, because of the received signals from some inter-BSS STAs in the topology. If the APs could not have heard the inter-BSS STA signals, then the STAs could have transmitted their traffic concurrently. Therefore, this problem prevents the transmission opportunities of the STAs and reduces the overall throughput and fairness of the WiFi networks in the vicinity when we look at the total throughput and average fairness.

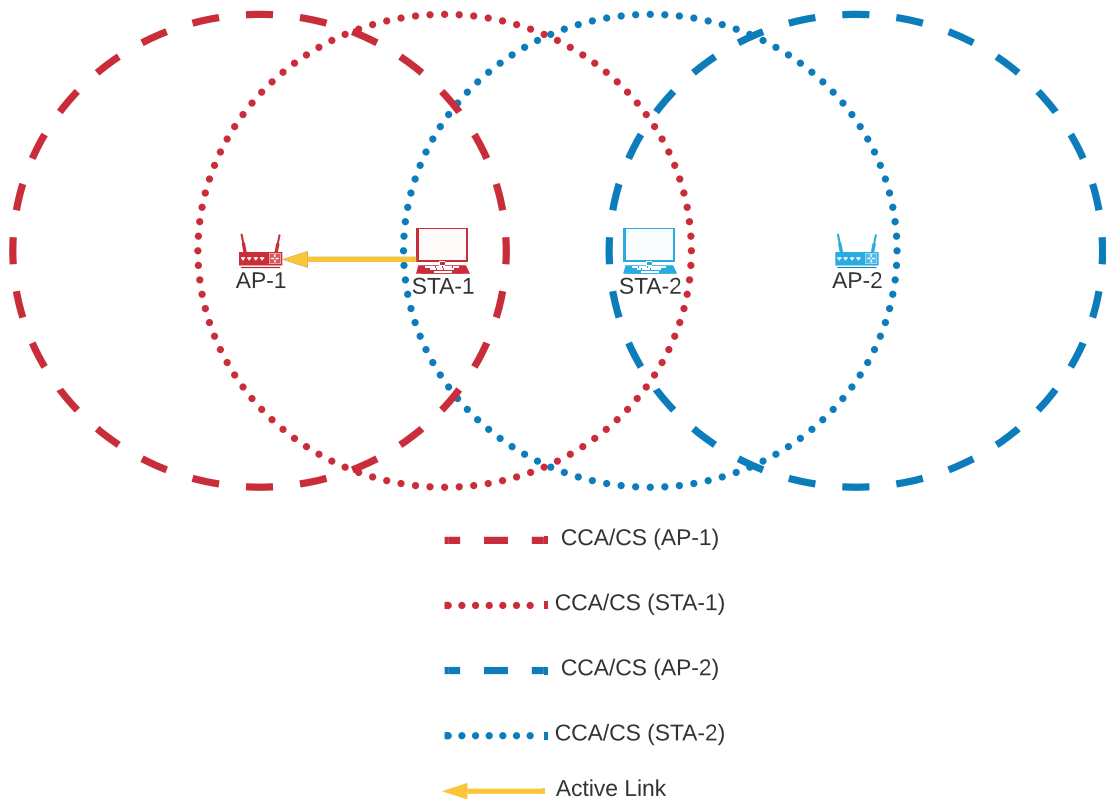


Figure 3.2. An example scenario for exposed node problem: STA-1 has transmission with AP-1. STA-2 hears STA-1 and does not transmit even if it is able to do it.

In Figure 3.2, an example showing a simple scenario for an exposed node problem is illustrated. In the topology, there are two BSSs and the transmission is in the uplink direction. While STA-1 performs transmission with AP-1, since STA-2 can sense the signals of STA-1, it will evaluate that the channel is BUSY and the transmission between STA-2 and AP-2 is not attempted. In this case, STA-2 is an exposed terminal.

Actually, neither AP-1 nor AP-2 can sense the transmission of inter-BSS stations and both stations can transmit concurrently with their associated APs without any collisions, i.e., if STA-2 transmits data to AP-2, AP-1 cannot sense this signal and again if STA-1 transmits data to AP-1, AP-2 cannot hear the signal either. In short, it is safe for STA-1 and STA-2 to transmit data with their associated APs, respectively. However, in this situation they do not transmit simultaneously. Therefore, it creates a performance degradation.

3.1.3. Pre 802.11ax Solutions

In the light of these two critical spectral efficiency problems, several solutions have been developed in the past two decades. In this section, these proposed enhancements that reduce the deteriorating effects of these problems will be discussed.

3.1.3.1. Solutions To the Hidden Node Problem. Since the hidden node problem is caused by the hidden STAs in the same BSS, parameter tuning or basic configurations may help to reduce the effects of the problem. For instance, increasing the transmission power of the STAs, changing the location of the STAs, using omni-directional antennas, or moving the obstacles may help to reduce the effects of hidden node problem [22]. In case of the existence of STAs in the same BSS that cannot hear each other, increasing the transmission power may help to solve this issue. However, increasing the transmission power affects the spatial reuse negatively, because as the range of the STA increases, the possibility of interference also increases. Another issue with this solution is the increased susceptibility to the exposed node problem due to higher transmission power.

In the case of using directional antennas in the network, hidden node problems may arise. To reduce this effect, omni-directional antennas should be used. Since using omni-directional antennas have uniform and 360 degree sensing range, they increase the chance of sensing the Intra-BSS signals and the chance of hidden node problem reduces. If the location of the STAs are far away from each other, reducing the distance

between STAs may also help to reduce the chance of hidden node problem. If there is an obstacle between two STAs, removing the obstacles increases the RSSI of each STA, and this may also help to reduce the effects of hidden node problem.

Although these solutions are good starting points, they require protocol level (i.e., MAC sublayer) tuning depending on the current topology and environment. Such protocol level features to solve the hidden node problem can be classified into five classes [23]:

- Pure contention-based
- Busy-tone-based
- Power-aware
- Directional antenna-based
- Multiple channel-based.

Pure contention-based solutions focus on advanced methods built on top of the core contention-based channel access mechanism. One of the well-known contention-based solutions is the request to send/clear to send (RTS/CTS) mechanism. Since the problem is originated from the hidden STAs, this mechanism works with a coordination of AP. Each STA checks the channel status by asking it to AP. In Figure 3.3 a basic RTS/CTS mechanism is illustrated for the case when STA-1 has a data frame to send to the AP-1. In this example, to ensure that the channel is in IDLE state, before transmitting the actual data frame STA-1 sends an RTS frame to the AP-1 and waits for the response. If the response is CTS, then that means the channel is in IDLE state and STA-1 can initiate the transmission. The same CTS frame is also received by STA-2 and after hearing the CTS frame STA-2 does not initiate transmission. As a result of this, even if there is a hidden node in the topology, STAs can ask the channel status to AP and it can initiate a transmission according to the response.

The RTS/CTS mechanism was first introduced within multiple access with collision avoidance (MACA) mechanism [24].

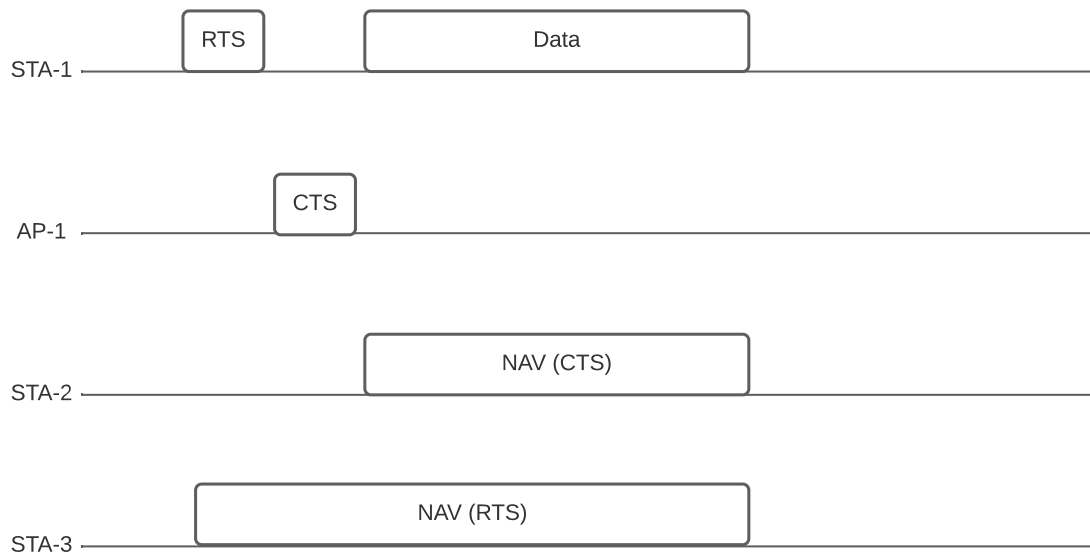


Figure 3.3. RTS/CTS Mechanism.

MACA uses the basic version of RTS/CTS mechanism as in the Figure 3.3. Even if the mechanism reduces the collisions due to the hidden node problem, using RTS frames still may create collisions. However, since the length of RTS frame is generally much shorter than the data frames, the collision probability of RTS frames is at the much lower level.

There are also advanced versions of MACA: MACA for wireless (MACAW), MACA by invitation (MACA-BI), and floor acquisition multiple access (FAMA) that use variations of RTS/CTS mechanism [25–27]. In the IEEE 802.11 standard, another such advanced version of MACA called the “four-way handshake mechanism” is used by default as an RTS/CTS mechanism. This four way handshake mechanism expands upon the three-way handshake mechanism of MACA by adding a fourth ACK frame. In this four way handshake mechanism, four frame types are used: RTS, CTS, DATA and ACK. In Figure 3.4, four way handshake mechanism is illustrated with interframe spacing. Different inter frame spacing values for different types of frames enable prioritization among different frames. As in the classical CSMA/CA mechanism, before sending any frame, DIFS interval is used to prevent RTS collisions in four-way hand-

shake. Then the CTS is sent back to the STA-1 by AP-1 and STA-1 will start the transmission because the channel is in IDLE state. At the same time, STA-2 also receives both the RTS and CTS frames and it sets a NAV according to the duration information of transmission carried by these frames. Then STA-1 sends the DATA frame to the AP-1 and AP-1 verifies that the data has successfully received and sends this information by ACK frame.

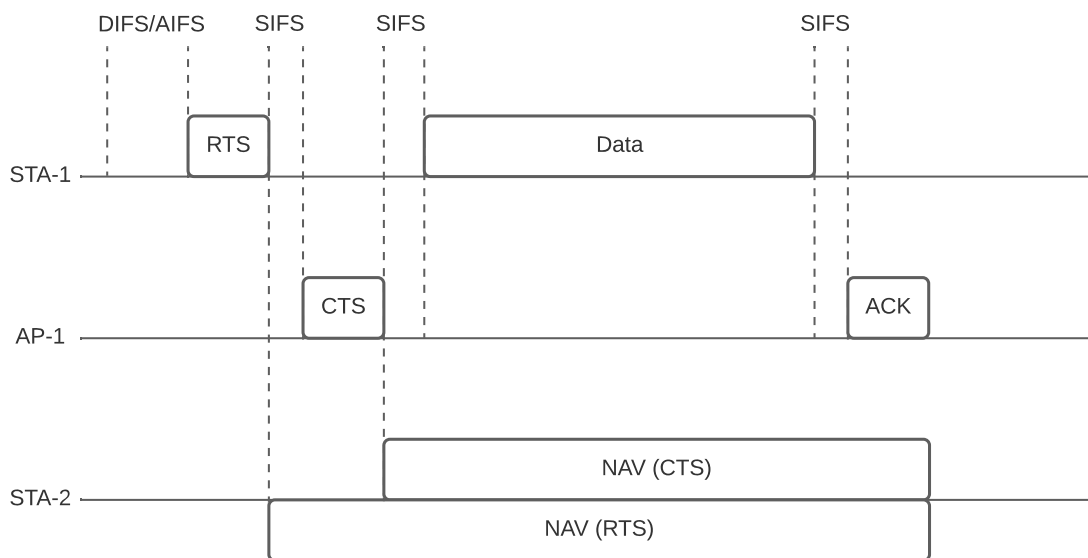


Figure 3.4. Four Way Handshake RTS/CTS mechanism.

Busy tone mechanisms are based on dividing the channel into portions and using them for transmission and protocol control operations. One of the earliest busy tone multiple access (BTMA) mechanism is introduced in receiver initiated busy tone multiple access (RI-BTMA) [28]. In Figure 3.5, RI-BTMA mechanism is illustrated. As in the MACA mechanism, the hidden node problem is solved by AP coordination. First, STA-1 sends a signal that contains the preamble portion and if AP-1 receives the preamble, it generates busy tone signal. The busy tone signal is carried via the tone channel and transmitted to STA-1 and STA-2 at the same time. Upon hearing this busy tone on the tone channel, STA-1 starts transmitting. At the same time, STA-2 decides to wait until the end of the busy tone signal. In short, the busy tone signal has two main objectives; the first objective is to use the busy tone signal as an acknowl-

edgement frame for the sender and the second objective is to warn the other hidden or non-hidden terminals about an ongoing transmission. In addition to RI-BTMA, dual busy tone multiple access (DBTMA), dual-channel MAC protocol for multihop ad hoc networks (DUCHA), jamming-based MAC protocol (JMAC), priority unavoidable multiple access (PUMA) and busy signal-based mechanism turned on (BusySiMO_n) mechanisms can be shown as examples of busy tone based mechanisms [23, 29–33].

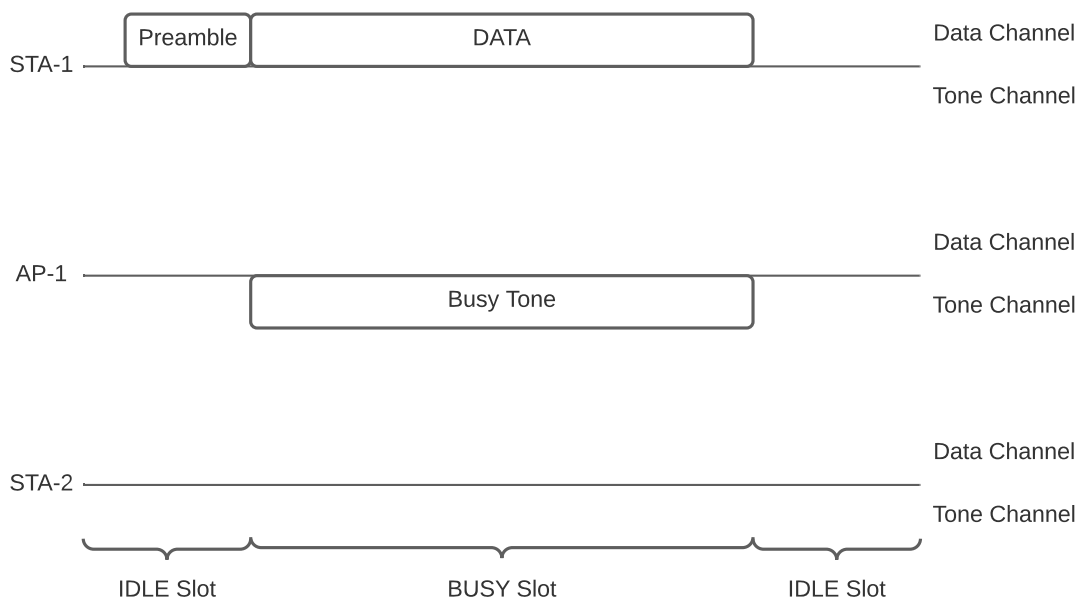


Figure 3.5. RI-BTMA mechanism.

The third class of protocol level solutions can be considered as power aware mechanisms. The power aware mechanisms are not specifically designed to alleviate the hidden node problems, instead aim to reduce the power consumption of the system. Nonetheless, they can also prevent the hidden node problem. One of the earliest power-aware mechanisms is the power-aware multiaccess protocol with signalling (PAMAS) based on the combination of both MACA and tone channel [34].

The working mechanism of PAMAS is illustrated in Figure 3.6. As seen in the figure, the standard RTS and CTS mechanism is being used, but the protocol control frames are transmitted in a separate channel. When STA-1 sends RTS and AP-1

confirms that the channel is IDLE by sending CTS frame, STA-1 initiates the data transmission. STA-2 also hears the CTS signal and to save power, it switches to the off state until the transmission is ended. Data is sent over the data channel, and control frames are sent over the tone channel. Using the separate channel for control frames makes a much more power efficient mechanism rather than the single channel mechanisms [34]. Since the AP coordinating mechanism is still here, in case of the hidden node problem, the STAs will hear the AP, and all STAs will be aware of the ongoing transmissions without collisions. Besides the PAMAS mechanism, single step power control (SSPC), Power controlled multiple access (PCMA) can be shown as examples of power aware mechanisms which can also eliminate the hidden node problem [23, 35].

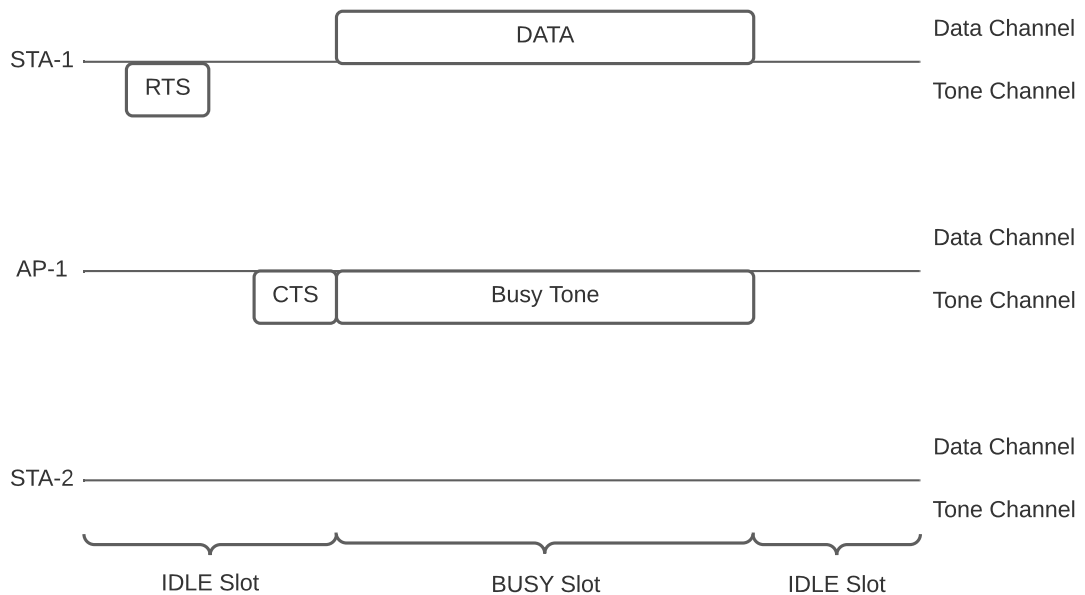


Figure 3.6. PAMAS Mechanism.

The fourth class of protocols, directional antenna-based mechanisms, are designed to remedy a variation of the base hidden node problem called the directional hidden node problem, which is very prevalent if a directional antenna is used in the wireless system. In such systems, since the beam form is directional and asymmetric, the existence of out-of-range STAs are more common. For these systems, RTS and CTS

frames that are sent via beamforming in a directional manner are called directional CTS (D-CTS) and directional RTS (D-RTS), respectively.

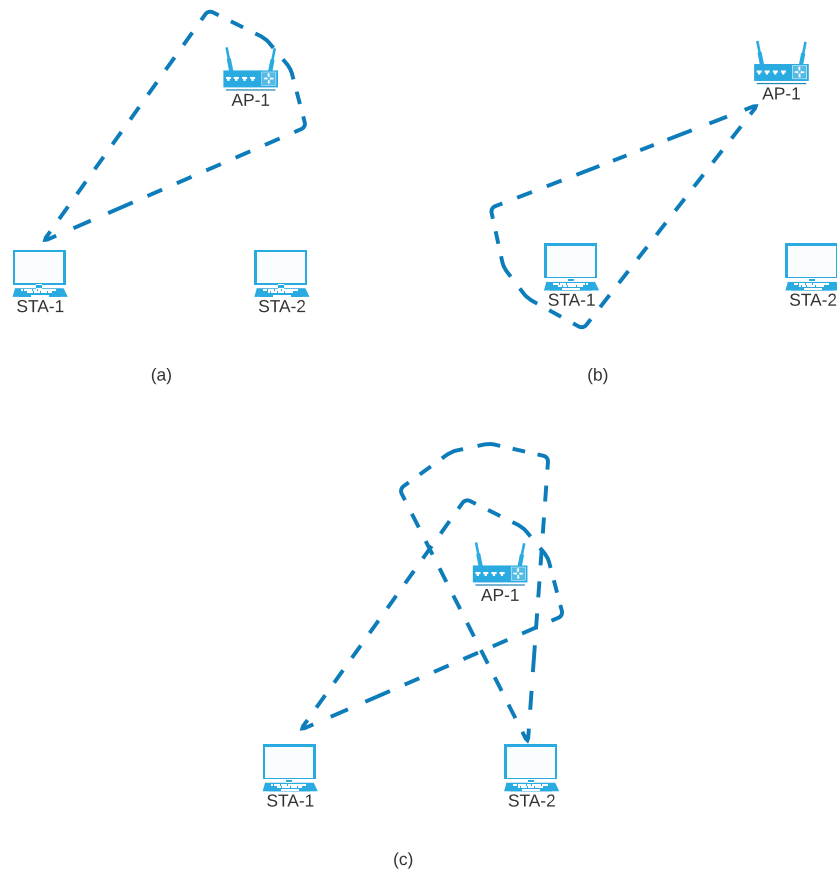


Figure 3.7. A scenario for directional hidden node problem.

In Figure 3.7, a directional hidden node problem is illustrated. In this scenario, even if the RTS/CTS mechanism is used the hidden node problem is persistent. In case (a), STA-1 wants to initiate transmission to AP-1 and sends a D-RTS frame. Since AP-1 is in the range of STA-1, in case (b) AP-1 sends back D-CTS to STA-1. Since the D-CTS is not received by STA-2, STA-2 is not aware of the channel state, which is BUSY. After receiving the D-CTS, STA-1 begins transmission and if STA-2 wants to transmit data as in case (c), since there is an ongoing transmission between STA-1 and AP-1, the D-RTS of STA-2 will create a collision. Directional MAC (DMAC) protocol works with a similar mechanism and uses four way handshake. Since the directional

beam cannot reach all the nodes, the directional hidden node problem occurs [23].

Therefore, the first directional antenna-based mechanisms for the hidden node problem is circular directional RTS MAC (CDR-MAC) that uses circular transmission and keeps the location of the STAs. By that way, the transmission is done according to the location of all STAs and this solves the hidden node problem [36]. Another protocol is DMAC with power control and directional receiving (DMAC-PCDR), which uses GPS to find the locations of other STAs and transmissions are done according to these locations [37]. To avoid the deafness due to the directional beams, RTS/CTS frames are used with omni-directional transmission in some protocols. Cooperative diversity MAC (CDMAC) and reservation-based directional MAC (RDMAC) use omni-directional transmission to do RTS/CTS transmission and for data transfer, directional transmission [38] [39]. By that way the negative effect of using directional antenna is re-mediated and hidden nodes can also hear the control frames of the ongoing transmissions.

The final type of protocols, the Multiple channel-based mechanisms, also use the advantage of different channels for the control frames and data transmission. The idea of the operation for minimizing the hidden node problem is the same with the busy tone based mechanisms, i.e., the control frames are used and operated by AP. There are three types of multi-channel based protocols; with common control channel, without common control channel, and hybrid protocols [23]. Multi channel based mechanisms with common control channel use a common channel for transmitting control frames (i.e., RTS/CTS). Multichannel variable radius multiple access (M-VRMA), self-adjustable multichannel MAC (SAM-MAC), cooperative CDMA-based multi-channel MAC (CCM-MAC) protocols are an example of multichannel-based protocols with common control channel that use sub channels; one for the control frame and the remaining ones are for data transmission [40] [41] [42]. Multi channel based mechanisms without common control channel use different channels for the control frames. As an example of these algorithms, JMAC that use two sub-channels for control frames; S and R. While channel S is used for RTS and DATA, channel R is used for CTS and ACK

frames [31]. In addition to JMAC, interleaved carrier sense multiple access (ICSMMA) and multichannel medium access control (MMAC) can be shown as examples of multiple channel based mechanisms without common control channel. The last multiple channel based mechanism type is hybrid protocols which can use a data channel for the control frames. MAC with a separate control channel (MAC-SCC) and “Hybrid Protocol” can be shown as an example of these type of protocols [23].

There are other mechanisms which use clusters to minimize the effect of hidden node problem [43]. These methods are based on dividing the STAs into clusters in the same BSS with a clustering on the aim of having no hidden nodes.

3.1.3.2. Solutions To the Exposed Terminal Problem. As discussed earlier, exposed node problem occurs in case of an Inter-BSS STA transmission, preventing the Intra-BSS transmission even if it is possible to transmit at the same time with this second traffic simultaneously. As in the hidden node problem case, RTS/CTS mechanism also helps to reduce exposed node problem in some certain conditions, such as synchronized nodes with the same packet size and data rate. In this situation, to solve the exposed node problem, the key frame is the CTS frame. After hearing the RTS frame from the sender node, if the exposed node is in range of the receiver, it can hear the CTS frame and it waits until the transmission ends. If it can not hear the CTS frame after the RTS frame, that means the receiver is out of range and transmission can be performed. If Figure 3.2 is recalled, STA-2 can hear STA-1 but not AP-1. Therefore, even if there is an ongoing transmission between STA-1 and AP-1, the CTS frame of AP-1 cannot reach STA-2. Similarly, when STA-2 sends an RTS frame, AP-1 will not be able to receive the RTS, transmission between STA-2 and AP-2 can be initiated without any problem.

There are multiple solutions which are proposed to mitigate this problem. One of the earliest such solutions, the medium access via collision avoidance with enhanced parallelism (MACA-P), was proposed based on MACA protocol [44]. In this protocol, there is a new mechanism named control gap time is introduced to solve the exposed

node problem. Control gap has brought in between RTS/CTS and DATA/ACK transmissions of the master node and it synchronizes the DATA/ACK period of all other nodes. In the RTS/CTS exchange phase, all the nodes perform this exchange and the beginning of DATA transmission is scheduled at the same time. This mechanism provides to STAs transmit simultaneously without collision.

In [45], another solution utilizing the RTS/CTS transmission has been proposed. According to this work, a STA detects RTS frames and corresponding source-destination addresses. In a normal situation, CTS must be heard after RTS frames, but if there is no CTS frame heard from the destination and DATA frame is transmitted from the source, that means it is an exposed node situation. In addition to this observation, the study argues that :

- (i) More than 50% of the internet traffic consists of small packets,
- (ii) Using RTS/CTS mechanism for the small packets is inefficient and degrades the overall network performance [45].

Considering these assumptions and the observation stated, this mechanism proposes exposed nodes not using RTS/CTS frames. Instead, they can transmit their frames without initiating RTS/CTS. One additional requirement of this mechanism is the need of synchronization between the exposed and transmitting nodes.

A third similar but more complex mechanism is proposed in [46]. In this work, the authors add a utility “interference range” on top of the similar approach of the previous mechanism [45]. In this mechanism primary sender and receiver that are the first pair of nodes begin transmission are defined. According to the interference range of the primary receiver, exposed node makes a decision on whether to send data or not.

In another solution that is introduced in [47], selective disregard NAV (SDN) is used to mitigate the exposed node problem. Although a very promising solution on its own, this mechanism requires some modifications on the base channel access

mechanism of WiFi and therefore will not be backwards compatible. Hence, its not applicable to a WiFi network.

In dense environments, by using the uplink connection information, each AP collects data related to the STAs and saves them into a database in [48]. This AP cooperation system analyzes the received frames from the STA and detects the hidden and exposed node problems. A similar approach is used in [49] and the exposed nodes are detected via offline training and then using the coordination of exposed links via newly introduced request-to-send-simultaneously (RTSS) and clear-to-send-simultaneously (CTSS) frames.

Another approach regarding the solution of exposed node problem is to control the transmission power and carrier sensing threshold. The main idea of this approach is to control the carrier sensing thresholds when an exposed terminal problem occurs. This approach does not fully solve the problem if the adjustable interval of the carrier sense threshold is so narrow [1]. In the next chapters this approach will be discussed in detail.

In [50], asymmetric RTS/CTS approach has been used. This mechanism is based on using a different rate for RTS and CTS frames depending on the power level which a transmission rate requires. Because of the nature of modulation, the higher rates have lower ranges. Since the frequency is increasing, the attenuation of the wave increases and the maximum distance that a data can reach also decreases. On the other hand, if the transmission rate is lower, the range increases. Asymmetric RTS/CTS methodology is based on this mechanism. Since the exposed node problem is originated from the RTS and DATA frames from the primary sender, primary sender can send RTS or DATA frames in higher rates and thus, the transmission range of this frame reduce. The CTS frame uses lower transmission rate and the transmission range of CTS frame will increase. By that way, primary sender reduces the transmission range with respect to a necessary interval, which it can preserve the connection with receiver. In [51] the asymmetric RTS/CTS idea has been used and extended for ad-hoc networks via

cross-layer design. To adjust the RTS frame rate of the terminals, the mechanism uses ad hoc on-demand distance vector (AODV) routing protocol and gets the information related to the terminals.

Besides all these methods, OBSS/PD mechanism which is introduced in 802.11ax amendment can be considered to mitigate the exposed node problem. By using the color mechanism and using the advantage of putting a threshold for Inter-BSS terminals, optimization on spatial reuse can be achieved and exposed node problem can be avoided in some cases. The mechanisms that use OBSS/PD threshold will be discussed further in the next chapters.

3.1.4. Proprietary Solutions

Aside from these aforementioned methods, WiFi chipset manufacturers (e.g., Broadcom, Quantenna, Qualcomm etc. . .) also utilize some proprietary solutions to address some of problems and increase the overall spatial reuse in WiFi networks. Unfortunately, being proprietary mechanisms, little to no publicly available information regarding such mechanisms are available. However, upon inspection of the workings of WiFi APs readily available in the market one can observe that such solutions at least include mechanisms that aim at reducing the impact of the exposed terminal problem by altering the carrier sense mechanism of the WiFi PHY layer. Although the details of such propriety carrier sense variations are very difficult to understand, they seem to be dynamically adapting the Rx-Sensitivity so that even the AP detects a WiFi signal with an RSSI value greater than -82 dBm, it tries to understand the impact of transmitting a signal concurrently; if transmitting will be clearly beneficial to the AP, the AP decides to send the signal in either a deterministic or probabilistic manner.

One can argue that such aggressive mechanisms will be harmful to other WiFi networks in the environment and if all WiFi networks utilize such greedy algorithms, the overall spatial reuse will not increase but instead decrease. There might be some additional parts to detect the impact of such aggressive behavior on other WiFi networks,

but without extensive testing it is impossible to understand how these mechanisms work.

3.1.5. Carrier Sensitivity Thresholds and OBSS/PD

Carrier sensitivity thresholds are used to distinguish whether the incoming signal is noise or not. As discussed in the earlier chapters, playing with the carrier sensitivity thresholds may increase the spectral efficiency and mitigate the problems which are originated from medium access. The main idea of using sensitivity thresholds to enhance the spectral performance is based on filtering the unwanted signals which cause interference and collisions.

In dense environments, since there are lots of nodes and some of them interfere with each other, tuning the carrier sensitivity threshold in an adaptive manner may help to improve overall network performance. In [52], a mechanism has been introduced to find an optimal sensitivity threshold in 802.11 homogeneous networks. Another physical carrier sensing algorithm is introduced, which is based on keeping operable SINR [53]. Moreover in [54], an algorithm named enhanced capacity 802.11 hotspots (ECHOS) also dynamically tunes the carrier sensing threshold based on SINR.

Some proposals are based on the location of the STAs. Since the locations of the STAs are known, the theoretical path loss and interference range can be optimized. Based on this information, carrier sensing threshold can be estimated. In [55], Access Points are linked and managed by a controller. The controller has a camera and can detect the locations of stations. By using the location information, the carrier sense threshold is adjusted.

In [56], a carrier sensing threshold algorithm is introduced based on BUSY/IDLE (BI) signals. The mechanism works like as follows: first, the AP sends BI signals to all STAs periodically. Then the STAs use the BI signal from AP and their own BI signal together to tune the carrier sensing threshold. This mechanism aims to mitigate both

the hidden node and exposed terminal problems by using the BI signal based threshold mechanism.

Another approach is used to tune the carrier sensing threshold is based on the RSSI of the neighbourhood terminals. In [57], TGax has proposed a RSSI based carrier sensing threshold algorithm named dynamic sensitivity control (DSC) and it is based on RSSI of beacon frame of AP. DSC algorithm is designed for uplink transmission of STAs.

In Figure 3.8, a pseudocode for the of DSC Algorithm has been given . Here, T_U is defined as the period for setting a new carrier sensing threshold; CCA_{Max}^{Thr} defines the maximum carrier sensing threshold; M defines a guard parameter for the incoming RSSI value for tuning against losses and inconsistencies in the medium; and weight defines the moving average of the recorded RSSIs. Since the last RSSI values are more significant in this algorithm, the weight of the last RSSI signal α should be higher than the historic ones. From the perspective of a STA, after setting the initial parameters of the algorithm, a timer starts and the STA starts waiting for the beacon frames. When the STA receives a beacon frame, it records the RSSI value of the beacon frame. If the RSSI value is bigger than the CCA_{Max}^{Thr} parameter, then the RSSI value is set by CCA_{Max}^{Thr} . The moving average of the received RSSI is calculated with the α parameter. Then, the STA checks whether the timer T is bigger than the T_U . If T is less than T_U , then the next beacon is waited and the whole process is repeated. If timer T is bigger than T_U , the CCA threshold is calculated by subtracting the M value from the average RSSI ($RSSI_{Avg}^{Beacon}$) and the algorithm resets by setting the timer again. Therefore, the main idea here is to adjust the carrier sensing threshold according to the RSSI values of the beacon frames.

In [58], a comprehensive study is done to evaluate the efficiency of DSC algorithm. According to the study, DSC algorithm increases the aggregated throughput and preserves the fairness among the nodes. In a complementary work, the same authors introduce a new mechanism based on DSC for APs [59].

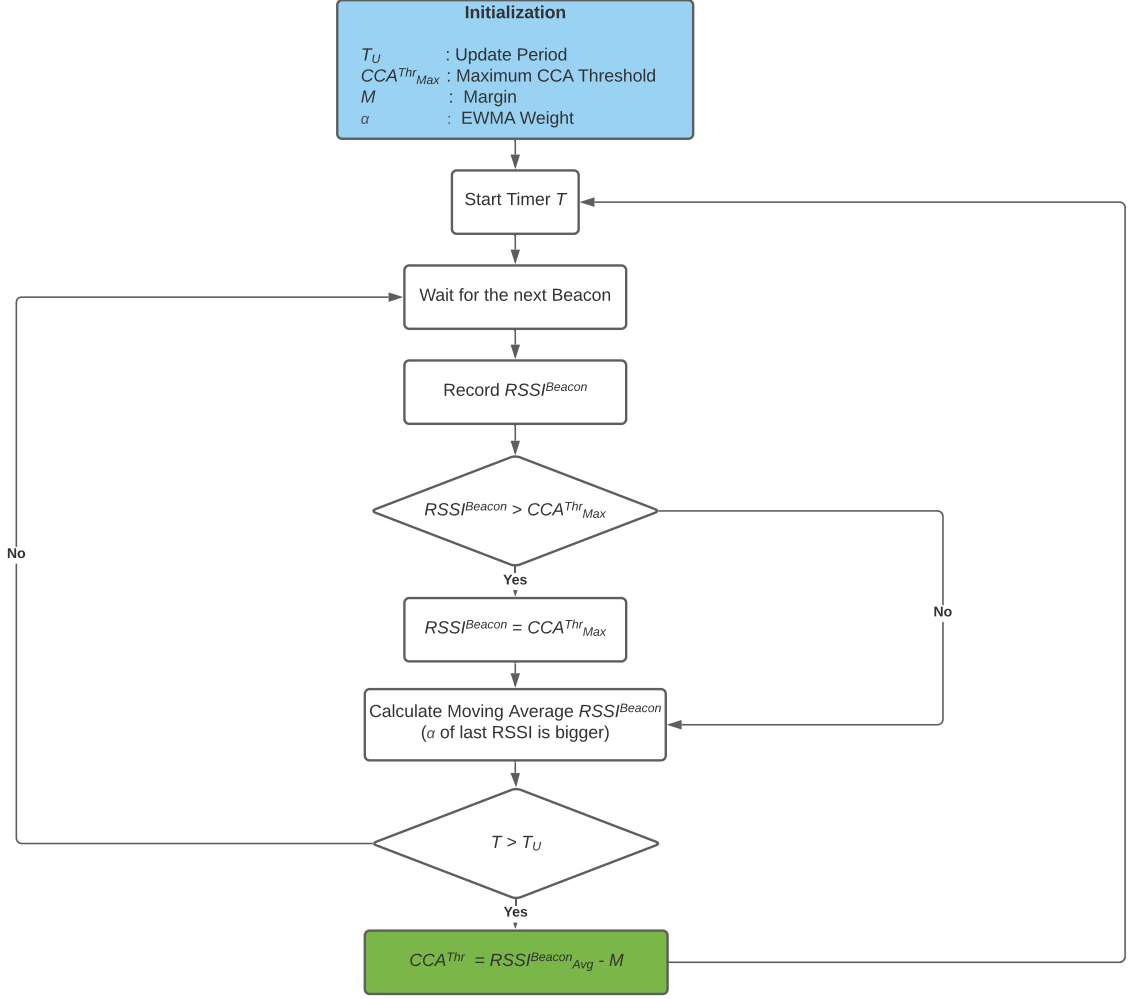


Figure 3.8. Dynamic sensitivity algorithm flowchart.

In this proposed mechanism, the AP collects the minimum RSSI of the associated STAs as $RSSI_{Min}^{INBSS-STA}$ and maximum RSSI of the other APs as $RSSI_{Max}^{OBSS-AP}$. In the mechanism, AP keeps the maximum RSSI values of the other APs. At the same time, in order not to lose the connection with the associated STAs, it records the minimum RSSI of the associated STAs. The threshold adjustment is done as

$$CCA^{Thr} = \min(\max(RSSI_{Min}^{INBSS-STA}, RSSI_{Max}^{OBSS-AP}) - M, RSSI_{Min}^{INBSS-STA}) \quad (3.1)$$

where CCA^{Thr} is the carrier sensitivity threshold, $RSSI_{Min}^{INBSS-STA}$ and $RSSI_{Max}^{OBSS-AP}$ minimum and maximum RSSI levels. $RSSI_{Min}^{INBSS-STA}$ is the beacon RSSI of the asso-

ciated AP. $RSSI_{Max}^{OBSS-AP}$ is the RSSI of the Inter-BSS STAs. M is the guard interval for the RSSI values same with the base DSC algorithm. According to the algorithm, the AP selects the maximum RSSI value from the $RSSI_{Min}^{INBSS-STA}$ and $RSSI_{Max}^{OBSS-AP}$ values and subtracts the M value from the selected RSSI. Then it compares the result with $RSSI_{Min}^{INBSS-STA}$ to ensure that AP does not lose its connectivity with its associated STAs. Then the resulting value is compared to CCA_{Max}^T and CCA_{Min}^{Thr} : if it is lower than CCA_{Min}^{Thr} , CCA_{Min}^{Thr} is assigned to CCA^{Thr} , if it is bigger than CCA_{Max}^{Thr} , then CCA_{Max}^{Thr} is assigned to CCA^{Thr} . By that way, CCA^{Thr} is kept in a boundary.

Several algorithms have been proposed based on this DSC algorithm. Among these, ax-Tech algorithm uses a similar approach to DSC, but additionally the transmit power is also adjusted linearly dependent on the carrier sensing threshold [60]. Another algorithm “Optimal Carrier Sense Threshold Adaptation” uses SINR to adjust the carrier sensing threshold and lastly, PRC algorithm adjusts the rate and transmit power while keeping the carrier sensing threshold fixed [52, 61]. In [62], a performance comparison among four different carrier sensing algorithm has been performed: DSC, ax-Tech, optimal carrier sense threshold adaptation and power rate control (PRC). According to this performance comparison, while in some cases, algorithms improve the performance, in some other cases performance degradation occurs. In a mixed population, BSS includes nodes that use both new generation and legacy WiFi protocols, it is observed that ax-Tech improves the performance of the nodes that use legacy protocols, but “optimal carrier sense threshold adaptation” algorithm degrades the performance of the nodes that use legacy protocols. For the nodes that are using the new generation protocol, the opposite effect is observed [62].

In [63], an algorithm is proposed which uses the expected transmission count (ETX) metric to adjust OBSS/PD. The algorithm is called ETX to power (ETP) and as the name indicates, it converts ETX to transmission power. ETX is a quality metric that is defined as the number of transmissions expected by STA to make successful transmission. Obtaining the transmission power from ETX is calculated by the Equation (3.2) where a and b are the variables to tune the algorithm. Then, the transmission

power is used to calculate OBSS/PD threshold by the Equation (3.3) since the minimum OBSS/PD and maximum transmission power values are predetermined. The simulations were performed with constant MCS and in uplink direction.

$$TxPower = a \times ETX + b, \quad (3.2)$$

$$OBSS/PD = OBSS/PD_{min} + (TxPower_{ref} - TxPower). \quad (3.3)$$

Here, ETX is the expected transmission count and $TxPower$ is the calculated transmission power. The $OBSS/PD_{min}$ is the minimum OBSS/PD threshold value and $TxPower_{ref}$ is the maximum transmission power.

One of the very first implementation of RSSI based OBSS/PD algorithm is the RSSI to OBSS threshold (RTOT) algorithm [64]. RTOT is also based on the aforementioned DSC algorithm where the only difference is RTOT adjusts OBSS/PD and transmission power at the same time. In Figure 3.9, the working mechanism of RTOT algorithm is shown. The parameter M is used as a guard interval for RSSI as the same in DSC algorithm. In each OFDM channel bandwidth, OBSS/PD, and transmission power operating intervals are defined. If the received beacon RSSI ($RSSI^{Beacon}$) is larger than the maximum OBSS/PD level ($OBSS/PD_{Max}$), the OBSS/PD threshold is assigned as a carrier sensing threshold and the minimum transmission power ($TxPower_{Min}$) is set because of the $OBSS/PD - TxPower$ relationship defined in 802.11ax amendment. If the received $RSSI^{Beacon}$ is less than the minimum OBSS/PD level ($OBSS/PD_{Min}$), then the minimum OBSS/PD level is assigned as a carrier sensing threshold and the maximum transmission power is set at the physical layer. If the received beacon RSSI is in the OBSS/PD operating interval, then by using the $TxPower - OBSS/PD$ relationship, the carrier sense threshold and $TxPower$ are adjusted. Since RTOT sets OBSS/PD with respect to $RSSI^{Beacon}$, the number of hidden nodes increases and the transmission power decreases to its possible lower value to preserve the connection between AP and its associated STAs. However, this decreases the number of available MCS indexes that is used by the adjusted transmission power.

```

1: Set  $M$ 
2: Collect  $RSSI^{Beacon}$ 
3:  $OBSS/PD = RSSI^{Beacon} - M$ 
4: if  $OBSS/PD > OBSS/PD_{Max}$  then
5:    $OBSS/PD = OBSS/PD_{Max}$ 
6:    $TxPower = TxPower_{Min}$ 
7: else if  $OBSS/PD < OBSS/PD_{Min}$  then
8:    $OBSS/PD = OBSS/PD_{Min}$ 
9:    $TxPower = TxPower_{Max}$ 
10: else
11:    $TxPower = TxPower_{Ref} + OBSS/PD_{Min} - OBSS/PD$ 
12: end if

```

Figure 3.9. RTOT algorithm.

Another DSC based algorithm is the control OBSS/PD sensitivity threshold (COST) that is operable for both AP and STA [65]. In addition to the logic of RTOT algorithm, COST algorithm uses the utilization of the color feature of 802.11ax protocol to recognize Inter-BSS signals. The margin (M) value is also adjusted via static and run-time parameters. In Figure 3.10 the workflow of the COST algorithm is shown.

COST uses a variable margin (M) value and uses three new parameters as $Diff$, $alpha$, and W . $Diff$ and $alpha$ values are the parameters to calculate M dynamically. Besides these parameters, W parameter is introduced for the window size of moving average window. After the initialization part a timer T is set and the incoming signals are analyzed. If the incoming WiFi frame is a WiFi6 frame, the color of the incoming signal is compared to the existing color of the node. If the color is the same the RSSI of the signal is recorded as $RSSI^{BSS}$ and the moving average of the RSSI is calculated as \overline{RSSI}^{BSS} .

If the color is different, then the opposite situation happens: the signal is recorded as $RSSI^{OBSS}$ and the moving average of the RSSI is calculated as \overline{RSSI}^{OBSS} .

```

1: Set  $M, OBSS/PD_{Min}, OBSS/PD_{Max}, T_U,$ 
    $W, alpha, Diff_{Min}, Diff_{Max}$ 
2: Set Timer  $T$ 
3: Wait for BSS and OBSS frames
4: if Color is Same then
5:   Record  $RSSI^{BSS}$ 
6:   Calculate  $\overline{RSSI}^{BSS}$ 
7: else
8:   Record  $RSSI^{OBSS}$ 
9:   Calculate  $\overline{RSSI}^{OBSS}$ 
10: end if
11: if  $T > T_U$  then
12:   Calculate  $Diff = max(Diff, Diff_{Min})$ 
13:   Calculate  $Margin_{New}$ 
14:   Calculate  $OBSS/PD_{Tmp}$ 
15:   Calculate  $OBSS/PD$  (Equation (3.4))
16:   GOTO Line 2
17: else
18:   GOTO Line 3
19: end if

```

Figure 3.10. COST algorithm.

If the timer T is less than $UpdatePeriod$, the subsequent packets are waited and the process is repeated.

If T is greater than T_U , $Diff$ is calculated as an absolute value of difference between \overline{RSSI}^{BSS} and \overline{RSSI}^{OBSS} . Then, the resulting $Diff$ value is used with $alpha$ parameter to calculate M_{New} . The temporary OBSS/PD parameter $OBSS/PD_{Tmp}$ is calculated by subtracting the M_{New} from the minimum of \overline{RSSI}^{BSS} and \overline{RSSI}^{OBSS}

values. Lastly, the OBSS/PD threshold is calculated via the Equation (3.4).

$$OBSS/PD = \min(\max(OBSS/PD_{Tmp}, OBSS/PD_{Min}), OBSS/PD_{Max}) \quad (3.4)$$

where $OBSS/PD_{min}$ and $OBSS/PD_{max}$ parameters are the minimum and maximum OBSS/PD values allowed to be set. $OBSS/PD_{tmp}$ is the temporary OBSS/PD threshold value that is used to in a comparison in the equation.

COST algorithm does not reduce its power fully to sustain transmission to the associated node. Instead, it reduces or increases the necessary amount of power to not hear the Inter-BSS interference while keeping the number of hidden nodes in a similar range. The simulations performed in [65] are done by constant MCS values; 0 and 5.

The same team has another algorithm in [66] named Damysus algorithm. Originally Damysus algorithm is a rate selection algorithm that uses the color and OBSS/PD feature of 802.11ax standard. Since there are new features of 802.11ax protocol, Damysus algorithm aims to use these to choose a rate more precisely and effective. As discussed earlier, OBSS/PD threshold is linearly dependent on the transmission power and changing the threshold affects the available MCS levels for rate selection algorithms. Each MCS level has its own minimum transmission power requirement, and if the transmission power is not enough to satisfy the MCS rate, it may affect the performance negatively.

In [67], an opportunity based OBSS/PD algorithm is introduced to increase the fairness among the nodes. The transmission opportunity (TXOP) of the previous time is used to adjust OBSS/PD and transmission power values. In Figure 3.11, TXOP based OBSS/PD algorithm is shown. The algorithm initializes an OBSS/PD value randomly and waits for the incoming signals. From the received signal information, if the received frame has the same color, then no change is made to OBSS/PD value. If the received frame has different color, then the TXOP of the previous time slot is looked. If there is a TXOP at the previous time slot, a new OBSS/PD level is selected

randomly in between the current OBSS/PD level ($OBSS/PD_{Curr}$) and the maximum OBSS/PD level ($OBSS/PD_{Max}$). If there is no TXOP at the previous time slot, a new OBSS/PD level is selected randomly in between $OBSS/PD_{Curr}$ level and the minimum OBSS/PD level ($OBSS/PD_{Min}$).

```

Set  $OBSS/PD_{Min}$  and  $OBSS/PD_{Max}$ 
Set  $OBSS/PD$  randomly
while True do
    Wait for the signals
    if Color is Same then
        Maintain OBSS/PD
    else
        if TXOP then
            Randomly select OBSS/PD in [ $OBSS/PD_{Curr}$ ,  $OBSS/PD_{Max}$ ]
        else
            Randomly select OBSS/PD in [ $OBSS/PD_{Min}$ ,  $OBSS/PD_{Curr}$ ]
        end if
    end if
end while

```

Figure 3.11. Opportunity based OBSS/PD algorithm.

In [68], an evaluation of OBSS/PD mechanism in 802.11ax protocol was performed with a constant MCS value. In simulations, no dynamic OBSS/PD algorithm is used, instead of this, the simulation is performed for several fixed OBSS/PD thresholds. Hence, an optimal OBSS/PD value range is obtained.

Besides the mechanisms above, a spatial reuse parameter (SRP) based carrier sensing threshold mechanism is proposed in [69]. In SRP, a Trigger Frame is sent to stations initially and stations receive the control information to access the channel and continue the backoff. This algorithm changes the frame format and adds new frame elements to the existing protocol. In the mechanism, the carrier sensing threshold is

named SRP_CCA is adjusted to increase spectral efficiency.

3.1.6. Spectral Efficiency in Other Wireless Protocols

In the previous section, 802.11 spatial reuse mechanisms were discussed. In this subsection, spatial reuse solutions for some of the other wireless protocols will be discussed.

In [70], an interference cancellation mechanism is proposed for ZigBee (IEEE 802.15.4) protocol. According to the paper, the main goal is reduce the exposed node problem in the medium, while keeping the hidden node problem at minimum. There is a trade-off between hidden and exposed node problems and this mechanism is testing the possibility of exploiting this trade-off. The main mechanism is based on applying successive interference cancellation to uncontrolled networks.

An opportunistic spatial reuse approach is introduced in IEEE 802.15.3c wireless personal area network (WPAN) standard in [71]. The mechanism is controlled by a 802.15.3c Piconet controller (PNC) and all nodes are collecting and measuring the channel status. PNC collects the information from the nodes to make adjustments. Then according to this information, PNC adjusts the available time slots are allocated for each node.

Another interesting spectral efficiency improvement is proposed for wireless body area network (WBAN) IEEE 802.15.6 protocol in [72]. In the proposed mechanism, a spatial reuse superframe is designed to increase aggregated throughput in cluster-based wireless sensor networks.

In [73], a scheduling and routing mechanism is proposed for IEEE 802.16 world-wide interoperability for microwave access (WiMAX) protocols. The mechanism is built on top of an interference model and on top of that scheduling and routing operations are performed. Another scheduling based spatial reuse algorithm for IEEE

802.16j WiMAX is introduced in [74]. The mechanism is called diversity scheduler SR-DIV, is based on scheduling users on OFDM subchannels in two-hop networks via two polynomial time scheduling algorithms [73].

3.2. Rate Selection Algorithms

In a wireless communication system, to transmit information between nodes, electromagnetic waves are used. In telecommunications, the periodic wave that is used to transmit data is called as “carrier signal”. Since the carrier signal is just a periodic signal and meaningless on its own, the data should be loaded into the carrier signal. The process of combining the data signal with the carrier signal is called “modulation”. Modulation can be performed by various kind of methodologies. The data can be carried by the variations on the amplitude, frequency, or phase of the carrier signal. The main types of modulations can be grouped in three main types: amplitude shift key (ASK), frequency shift key (FSK), and phase shift key (PSK). Since the modulated signal carries data, the carried data in a unit time is called data rate, is directly related to the network throughput. Each modulation technique has its own rate limitations and power requirements.

In IEEE 802.11ax wireless networks, the available data rates are represented via MCS, which is consisting of the modulation type and coding rate. Each combination of the modulation type and coding rate is represented by a unique MCS index. 802.11ax protocol has 11 different MCS indexes which contains the following modulation types: BPSK, QPSK, 16-QAM, 64-QAM, 256-QAM and 1024-QAM. Binary phase shift key (BPSK) is the basic form of PSK which uses 2 phases with 180 degree angle. Quadrature phase shift keying (QPSK) is a quadratic version of PSK and uses 4 phases with separated 90 degree angle. Quadrature amplitude modulation (QAM) is a form of ASK modulation which uses two digital bit streams and carries the data by modulating their amplitudes. In 802.11ax standard, two 1024-QAM MCSs are introduced and it increases the throughput up to gigabit level.

In IEEE 802.11 standard, as MCS index increases, the data rate that the modulation scheme can provide also increases as shown in the Table 2.2 and Table 2.3. During the transmission, selecting a correct rate is crucial. For example, according to the same tables, in 802.11ax OFDM MCS rate table at 160 MHz bandwidth and 3.2 μ s guard interval, while MCS1 provides 61.3 Mbit/s raw data rate, MCS11 provides 1020.8 Mbit/s raw data rate. Instead of MCS1, using MCS11 increases the raw throughput more than 16 times. To select a correct rate at run-time, transmission parameters and topology parameters may be used. In this section, rate selection algorithms will be discussed in detail.

Since the wireless medium is accessible by any node and open to noise sources, there are some losses while transmission occurs. The success of the modulation depends on SINR, which can be affected by fading, path loss and interference. If the SINR is low, the received signal cannot be decoded properly, which results in high bit error rate (BER) values. From this point, some of the rate selection algorithms are based on the estimation of the channel quality metrics like SINR, BER, etc.

In [75], automated rate fallback (ARF) rate selection algorithm is introduced. The rate mechanism tracks the ongoing transmission and in case of any disturbance in timing function or ACK frame, the rate alternates between 1 and 2 MBit/s. ARF initially sets the rate at 2MBit/s and keeps track of ACK frames. In case of any missing ACK frame, at first the algorithm does not do a rate fallback, but if the second ACK is not received properly, the algorithm lowers the rate to 1 MBit/s. The data rate can increase in two conditions; if the number of successful ACK frames are greater than 10 or the timer is reset, the data rate increases to 2 MBit/s.

Adaptive ARF (AARF) is the improved version of ARF algorithm and is proposed in [76]. Consider a scenario that ARF algorithm has found the ideal rate as the lower rate, if the channel condition is not changing in a short term period, the algorithm will try higher rate again. Since the higher rate is not an appropriate rate, there will be re-transmissions. After unsuccessful ACK frames, the rate will reduce to the lower

level again. Since the lower rate is the optimal rate condition, no packet loss will happen and after 10 successful ACK, ARF will try the higher rate again. As seen, it is not necessary to switch the higher rate and this makes inefficient to use ARF in long-term channel conditions. In order to avoid this problem, AARF algorithm has been introduced which can set an adaptive threshold for number of the successful ACK frames. Dynamically adjustment of the ACK threshold can prevent the rate reductions. Since AARF proposes an adaptive threshold, for the long-term channel conditions, the successive ACK threshold increases and unnecessary rate switching is prevented.

In [77], Onoe algorithm is deployed in MadWiFi project. This algorithm uses a credit-based rate selection with respect to the retransmission ratio. Initially, the credit score is set zero and each 1000ms time slot the credit is recalculated. If the retransmission ratio is below 10% this transmission is counted as a successful transmission and the credit score increases one point. If the credit score reaches 10 points, then the algorithm selects an higher rate and the credit is reset. In case of any unsuccessful transmission, a similar scenario is applied again except the rate does not reduce instantly. Instead of this rate, the reduction state is marked and after 10 seconds the data rate reduces.

Receiver-based auto rate protocol (RBAR) algorithm is another mechanism proposed in [78]. Even if the approach of the algorithm is useful, using the legacy standards may create some problems. RBAR algorithm uses RTS/CTS frames to measure the channel quality. The receiver takes the RTS frame and calculates the SINR. This SINR information is sent back to the sender node, and the sender node calculates the new data rate with respect to the SINR.

In [79], SampleRate algorithm is proposed that evaluates the new transmission rate based on the historical transmission performance. During the transmission, successive transmission, successive failures, and the transmission time are recorded with exponential weighted moving average (EWMA). The algorithm begins with the highest rate and If there are four successive failures at the transmission, the algorithm selects

the rate that has the lowest average transmission interval.

One of the most popular rate selection algorithm is the Minstrel algorithm that was developed for the Linux kernel drivers [80]. Instead of using the channel quality metrics, the minstrel algorithm looks at the successful and unsuccessful transmission, in other words the transmission statistics. To select a useful data rate, the algorithm builds a rate table and by experimenting the unexplored rates, it selects a new rate. For the decision table, Minstrel evaluates the probability of success and throughput for the MCS levels.

$$Throughput = \frac{PST \times MT}{T} \quad (3.5)$$

where PST is the probability of success for the transmissions and MT is the total transmitted data in Mbits. To operate the Minstrel algorithm, the number of successfully transmitted bits in a time interval is defined as $Throughput$ in Equation (3.5). T represents the time for one trial of a packet transmission. Then the $Throughput$ value of each rate is recorded in a statistics table historically via calculating EWMA of $Throughput$ for each rate. While 90% of transmissions are normal transmission, 10% of transmissions are “lookaround transmissions” to find whether if there is a rate with a better performance.

In Table 3.1, the retry chain of the Minstrel algorithm is shown. In the case of the normal transmission, Minstrel algorithm first tries the rate that has the best throughput. If the transmission attempt is not successful, then a second retry is done with the next best throughput, the third retry is done with the rate having the highest probability of success, last retry is done with the lowest baserate. This process continues until when a successful transmission is done for a rate or the end of the retry chain is reached if there is no successful transmission.

In the case of the lookaround transmission, the lookaround rate is compared to best rate and if it is greater than the best rate, first random rate is tried otherwise the

best rate is tried. If the transmission is not successful with the best rate, the algorithm tries the random rate at the next retransmission.

Table 3.1. Minstrel retry chain.

Minstrel Retry Chain			
Try	Lookaround Rate (10% of time)		Normal Rate (90% of time)
	Random < Best	Random > Best	
1	Best Throughput	Random Rate	Best Throughput
2	Random Rate	Best Throughput	Next Best Throughput
3	Highest Probability	Highest Probability	Highest Probability
4	Lowest Baserate	Lowest Baserate	Lowest Baserate

The newer version of Minstrel algorithm, Minstrel high throughput (Minstrel-HT), is also uses a similar mechanism, but additionally it uses 802.11ac high throughput (HT) rates [81]. The process begins with initializing the HT rate and after this the sampling table is initialized. Based on the sampling, the new rate is calculated.

An another efficient rate selection algorithm is called modified Thompson algorithm (MTS) is proposed in [82]. Thompson sampling is a solution of multi arm bandit problem. Bandit arm is basically a slot machine. In the problem statement, there are multiple slot machines and each of them are unique and has different expected gains. For a given limited time, the resources are allocated to the alternative choices to find the high gain machine. Similarly, selecting a data rate whose gain is higher than the other alternatives has common points with the multi arm bandit problem in terms of choosing the rate that can be considered as resource allocation. Since there are multiple data rates and the algorithm does not know which one has the better performance among them, using Thompson sampling algorithm may help to solve this problem.

The set of available rates has unknown success probabilities. At each trial Thompson algorithm chooses a rate and record whether it is a successful transmission or not.

The success probability of each rate is estimated by the beta distribution. These recorded statistics about transmission define the shape of the beta distribution.

$$f(\theta_i) = \frac{\theta_i^{S_i}(1 - \theta_i)^{F_i}}{B(S_i, F_i)} \quad \text{where } i = 0, 1, \dots, n, \quad (3.6)$$

$$B(S_i, F_i) = \frac{\Gamma(S_i)\Gamma(F_i)}{\Gamma(S_i + F_i)} \quad (3.7)$$

where S_i and F_i are the count of success and failed transmissions, $f(\theta_i)$ is the probability density function, θ_i is the success probability of the i 'th data rate, $B(S_i, F_i)$ is the beta function for successful and failed transmissions, and $\Gamma(\cdot)$ is the gamma function.

```

for Each Rate  $r_i$  where  $i = 0, 1, \dots, n$  do
     $S_i = 0$  and  $F_i = 0$ 
end for
for Each Step Time  $t = 1, 2, \dots$  do
    for Each Rate  $r_i$  do
         $\theta_i(t) \sim B(S_i + 1, F_i + 1)$ 
        Select  $r_i$ , where  $i_t = \underset{i}{\operatorname{argmax}} r_i \theta_i(t)$ 
        Obtain random transmission result  $X(t)$ 
        if  $X(t) = 1$  then
             $S_i = S_i + 1$ 
        else if  $X(t) = 0$  then
             $F_i = F_i + 1$ 
        end if
    end for
end for

```

Figure 3.12. Modified Thompson sampling (MTS) algorithm.

In Figure 3.12, the modified Thompson sampling (MTS) algorithm working principle is shown. First of all, for the all available rates, the count of success S_i , and

failure F_i transmissions are initialized with zero. For each time step, first of all, the success probability of each rate is estimated by the beta distribution based on success and failure counts as in Equation (3.6) and Equation (3.7). After getting the success probability for each rate, for the maximum success probability, a rate is selected. After selection of the rate, the transmission is performed and if the transmission is successful, the S_i parameter is increased by one otherwise F_i is increased by one. Then, for the next time step, the beta distribution function is updated and all steps are repeated.

4. RACEBOT ALGORITHM

In this section, our proposed algorithm RACEBOT will be explained. RACEBOT algorithm is basically an OBSS/PD threshold-based algorithm, which dynamically adjusts OBSS/PD threshold in the run-time. The main goal of RACEBOT algorithm is to find an effective OBSS/PD threshold and consequently transmit power to increase aggregated throughput while reducing Inter-BSS interference and reducing the possibility of hidden STAs.

Table 4.1. 802.11ax receiver minimum input level sensitivity [1].

MCS Index	Modulation	Rate	Minimum Sensitivity (dBm)			
			20 MHz	40 MHz	80 MHz	160 MHz
0	BPSK	1/2	-82	-79	-76	-73
1	QPSK	1/2	-79	-76	-73	-70
2	QPSK	3/4	-77	-74	-71	-68
3	16-QAM	1/2	-74	-71	-68	-65
4	16-QAM	3/4	-70	-67	-64	-61
5	64-QAM	2/3	-66	-63	-60	-57
6	64-QAM	3/4	-65	-62	-59	-56
7	64-QAM	5/6	-64	-61	-58	-55
8	256-QAM	3/4	-59	-56	-53	-50
9	256-QAM	5/6	-57	-54	-51	-48
10	1024-QAM	3/4	-54	-51	-48	-45
11	1024-QAM	5/6	-52	-49	-46	-43

According to the IEEE 802.11 standard, to demodulate a received signal, the SINR of the signal should be higher than a predefined threshold and the PER should be less than 10% [1]. Even if the modulation carries high amount of data, if it cannot be decoded properly, packet loss occurs. The Table 4.1 shows minimum required RSSI values for each IEEE 802.11ax MCS levels that receiver needs to demodulate a

corresponding signal with less than 10% PER [1].

Consider an example shown in Figure 4.1, there are two stations and one AP. STA-1 is associated with AP-1 and STA-2 is an Inter-BSS station.

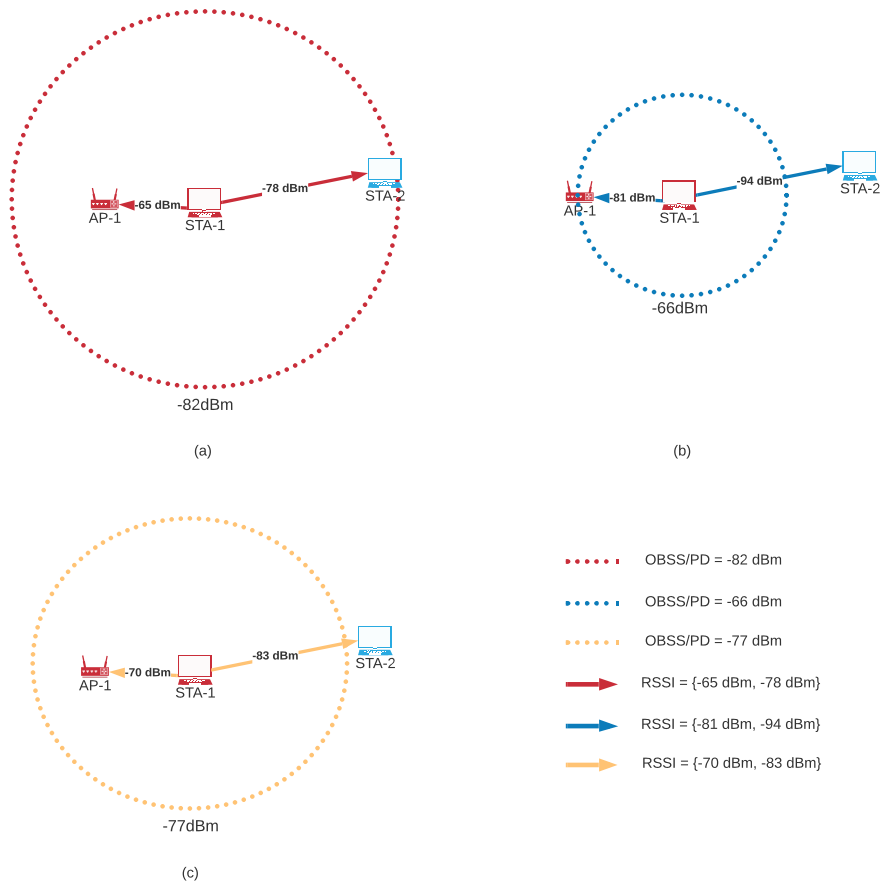


Figure 4.1. OBSS/PD threshold and TxPower adjustment scenario.

In Figure 4.1 and the case (a), both AP-1 and STA-2 are in the range of STA-1 which has -82 dBm OBSS/PD threshold. The RSSI levels of the signals originated from STA-1 are heard by STA-2 and AP-1 are -65 dBm and -78 dBm, respectively. if STA-1 increases its OBSS/PD level to -66 dBm like in case (b), then according to the Equation (4.1), the TxPower reduces by the same amount (16 dBm). Therefore, the RSSI levels of STA-1 signals that are heard by AP-1 and STA-2 will be -81 dBm and -94 dBm, respectively. This adjustment increases the OBSS/PD threshold to its maximum without losing the connection between STA-1 and AP-1, while STA-2 is not in the range of STA-1 anymore. However, even if there is no connection loss between

STA-1 and AP-1, since the received signal strength of STA-1 heard by AP-1 is -81 dBm, the transmission rate can be at most MCS-0 for this power level according to the Table 4.1. Therefore, the OBSS/PD adjustment of case (b) prevents the usage of higher MCS levels. However, if the OBSS/PD threshold is adjusted like in case (c) which uses high tolerance OBSS/PD threshold, the rate can be selected up to MCS-4 for -70dBm according to the Table 4.1. At the same time, the interference between STA-1 and STA-2 is also prevented. Our proposed RACEBOT algorithm uses this logic to create a chance for the rate algorithm to use higher MCS levels.

$$TxPower = (OBSS/PD_{min} - OBSS/PD) + TxPower_{ref} \quad (4.1)$$

where $TxPower_{ref}$ is the maximum transmission power and $OBSS/PD_{min}$ is the minimum OBSS/PD threshold value that is allowed to be set.

Adjusting the OBSS/PD threshold with respect to RSSI can be implemented in various ways. As discussed earlier, some of these algorithms are based on beacon RSSI and some of the other algorithms are using both beacon RSSI and RSSI of OBSS STAs. RACEBOT algorithm also uses the both RSSI types for two reasons: using beacon RSSI to keep connection with the associated AP and using OBSS RSSI to avoid OBSS interference. RACEBOT algorithm records each RSSI with their counts named OBSS frame count (OFC) in a specific time period. These *OFC* values are used to adjust OBSS/PD thresholds in the next stages of the algorithm. In Figure 4.2, an example histogram of *OFC*s for a scenario is given.

RSSI based carrier sensitivity threshold algorithms generally use the average of RSSI values. In the example, since the *OFC* values of RSSI for -68 dBm and -70 dBm are 2 and 1 respectively, adjusting OBSS/PD threshold regarding these RSSIs may not be useful. The significant change in *OFC* occurs in -77 dBm and using this RSSI as a reference may give a better performance. By using this logic, RACEBOT algorithm adjusts the OBSS/PD threshold based on -77 dBm RSSI for this specific scenario.

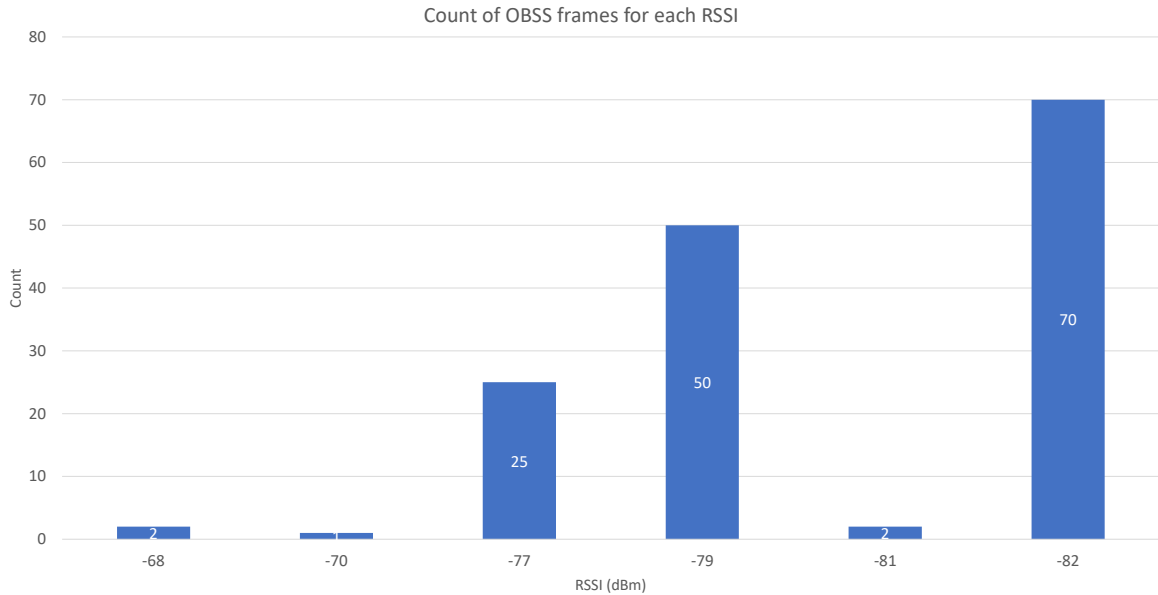


Figure 4.2. A histogram for OBSS frame counts for each RSSI.

In Figure 4.3, another example for *OFC* histogram of RSSIs that shows a different pattern is given. In this scenario, since the higher RSSI levels have bigger *OFC* values, using the average RSSI to adjust OBSS/PD threshold may not give a decent performance.

To select the appropriate OBSS/PD threshold, RACEBOT algorithm sets an *OFC* threshold named OFC_{Thr} and selects the maximum RSSI, whose count is greater than the OFC_{Thr} value. For example, in Figure 4.2, if the value of OFC_{Thr} is set to 6, then -68 dBm, -70 dBm and -81 dBm RSSI values are ignored, because their *OFC* values are less than OFC_{Thr} . Then among the remaining ones, the maximum RSSI value is selected. For the scenario in Figure 4.2, the selected RSSI value is -77 dBm.

In the scenario that is shown in Figure 4.3, since the *OFC* values of -77 dBm, -79 dBm, 81 dB, and -82 dBm RSSI levels are less than the OFC_{Thr} , the maximum RSSI value is selected among the remaining RSSI levels. In this case this RSSI level is -68 dBm. By adjusting OFC_{Thr} , different results may be obtained.

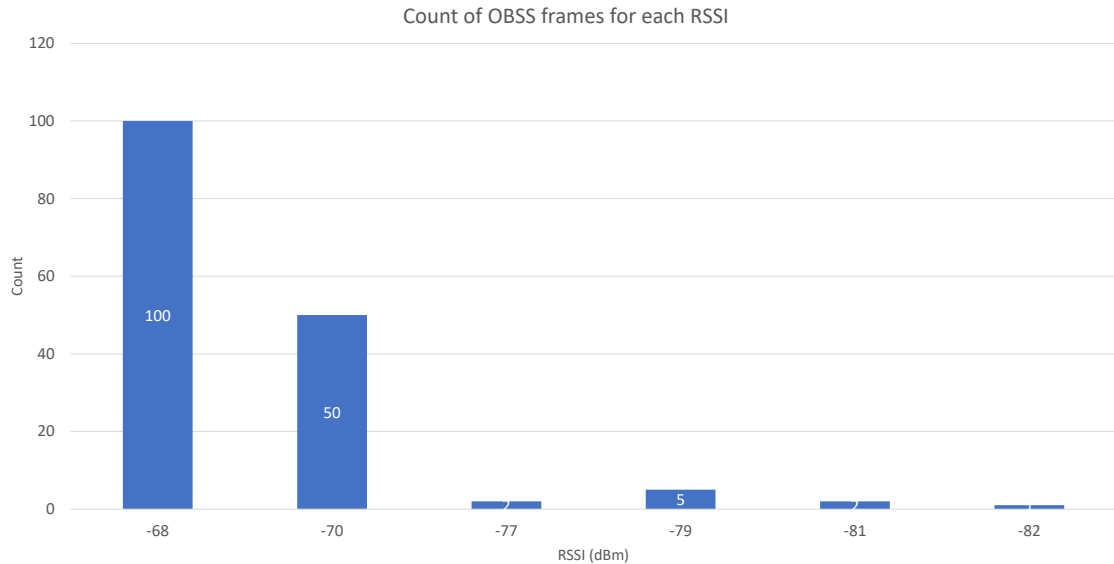


Figure 4.3. Another histogram for OBSS frame counts for each RSSI.

RACEBOT algorithm consists of two parts: finding a goal OBSS/PD threshold and adjusting the threshold by increasing the OBSS/PD value step by step with considering the effects of the change in transmission power. In Figure 4.4, working mechanism of RACEBOT algorithm is shown. First of all, M , γ , a , T_U , OFC_{Thr} , $RSSI^{OBSS}$, \overline{RSSI}^{BSS} , $OBSS/PD^G$, \overline{MCS} and \overline{OFC} parameters are initialized. T_U is a periodic time interval for the algorithm to update some of the run-time parameters. If the timer T is greater than T_U , T is reset and goal OBSS/PD ($OBSS/PD^G$) value of each node is initialized with -101 dBm. The $OBSS/PD^G$ parameter is the aimed OBSS/PD threshold that the RACEBOT algorithm tries to reach in run-time. For each RSSI, EWMA of OFC values are defined by \overline{OFC} parameter as in the Equation (4.2).

$$\overline{OFC}(T) = \alpha \times OFC(T) + (1 - \alpha) \times \overline{OFC}(T - 1). \quad (4.2)$$

To calculate the $OBSS/PD^G$ parameter, first the OFC values for each RSSI are compared to OFC_{Thr} parameter, which is a predefined positive real number from \mathbb{R}^+ . OFC_{Thr} value helps to prune the received RSSI values with considering the rareness

by OFC values. \overline{RSSI}^{BSS} is the EWMA of the beacon RSSI of the associated AP.

```

1: Initialize  $M, \gamma, \alpha, T_U, OFC_{Thr}, RSSI^{OBSS}, \overline{RSSI}^{BSS}, OBSS/PD^G, \overline{MCS}, \overline{OFC}$ 
2: while RUN do
3:   if  $T > T_U$  then
4:     Set  $T = 0, OBSS/PD_i^G = -101dBm$  where  $i = 1, 2, \dots, n$ 
5:     for Each  $Node_i$  do
6:       for Each  $RSSI_{i,j}^{OBSS}, j = 1, 2, \dots, m$  do
7:         if  $\overline{OFC}_{i,j}(T) > OFC_{Thr}$  and  $RSSI_{i,j}^{OBSS} > OBSS/PD_i^G$  then
8:            $OBSS/PD_i^G = \min(RSSI_{i,j}^{OBSS} + M, \overline{RSSI}_i^{BSS} - M)$ 
9:         end if
10:       end for
11:     end for
12:     Reset  $RSSI^{OBSS}, \overline{OFC}$ 
13:   end if
14:
15:   Collect  $\overline{RSSI}^{BSS}$  and  $RSSI^{OBSS}$ 
16:   if  $\overline{MCS}(T-1) \times \gamma > \overline{MCS}(T)$  then
17:      $OBSS/PD = \max(\frac{(OBSS/PD + \overline{RSSI}^{BSS} - M)}{2}, OBSS/PD_{min})$ 
18:      $OBSS/PD^G = \frac{(OBSS/PD + OBSS/PD^G)}{2}$ 
19:   else if  $\overline{MCS}(T-1) \times \gamma \leq \overline{MCS}(T)$  then
20:      $OBSS/PD = \min(\frac{(OBSS/PD + OBSS/PD^G)}{2}, OBSS/PD_{max})$ 
21:   end if
22: end while

```

Figure 4.4. RACEBOT algorithm.

RACEBOT also uses M value, which is a positive real number from \mathbb{R}^+ to be used as a margin. For a single node, the algorithm looks whether OFC value of corresponding RSSI is greater than OFC_{Thr} and $RSSI^{OBSS}$ is bigger than $OBSS/PD^G$ or not. If so, the M value is added to $RSSI^{OBSS}$ and subtracted from \overline{RSSI}^{BSS} then

minimum of them is assigned to the $OBSS/PD^G$ parameter. It is repeated for all the nodes in the system. Then $RSSI^{OBSS}$ and \overline{OFC} are reset to collect new ones. RACEBOT algorithm follows the changes of MCS level.

As discussed earlier, each MCS level requires a minimum RSSI and maximum PER at the receiver side. Therefore, increasing OBSS/PD threshold, reduces the transmission power and it may prevent using higher MCS levels. In order to overcome this issue, RACEBOT algorithm collects EWMA of MCS levels and compares the current average MCS level ($\overline{MCS}(T)$) with average MCS level of the previous step time ($\overline{MCS}(T - 1)$). In this step there is also a constant γ , which is a real number between 0 and 1. The γ parameter is multiplied by the $\overline{MCS}(T - 1)$ to compare how much change happened to \overline{MCS} . For example if γ is 0.7, it is checked that whether the \overline{MCS} value decreases or not by more than 30%.

In Figure 4.4, adjusting mechanism of an OBSS/PD threshold is shown. If \overline{MCS} value decreases for a given criteria, OBSS/PD threshold is reduced. In order to reduce OBSS/PD level, an average of current OBSS/PD threshold or \overline{RSSI}^{BSS} are assigned as a new OBSS/PD threshold. If this value is above the $OBSS/PD_{min}$ level, then $OBSS/PD^G$ is reduced to the average of the new OBSS/PD threshold and $OBSS/PD^G$. If \overline{MCS} does not decrease for a given criteria, OBSS/PD threshold is increased and the average of the OBSS/PD threshold. $OBSS/PD^G$ value is assigned as OBSS/PD threshold, if it is less than $OBSS/PD_{max}$. In Figure 4.4, the $OBSS/PD_{min}$ and $OBSS/PD_{max}$ boundary values are used in the comparisons at lines 18 and 20 to prevent any inconsistencies in the signal power in case of the existence of a signal that is out of the OBSS/PD boundary.

In Figure 4.5, a high-level illustration of RACEBOT algorithm is shown. As seen in the figure, the algorithm changes OBSS/PD threshold by keeping track of the changes in MCS level. At the same time, it tries to keep the transmission power in higher levels to create a chance for the higher MCS levels that rate algorithms can use. The main contributions of RACEBOT algorithm can be summarized as follows:

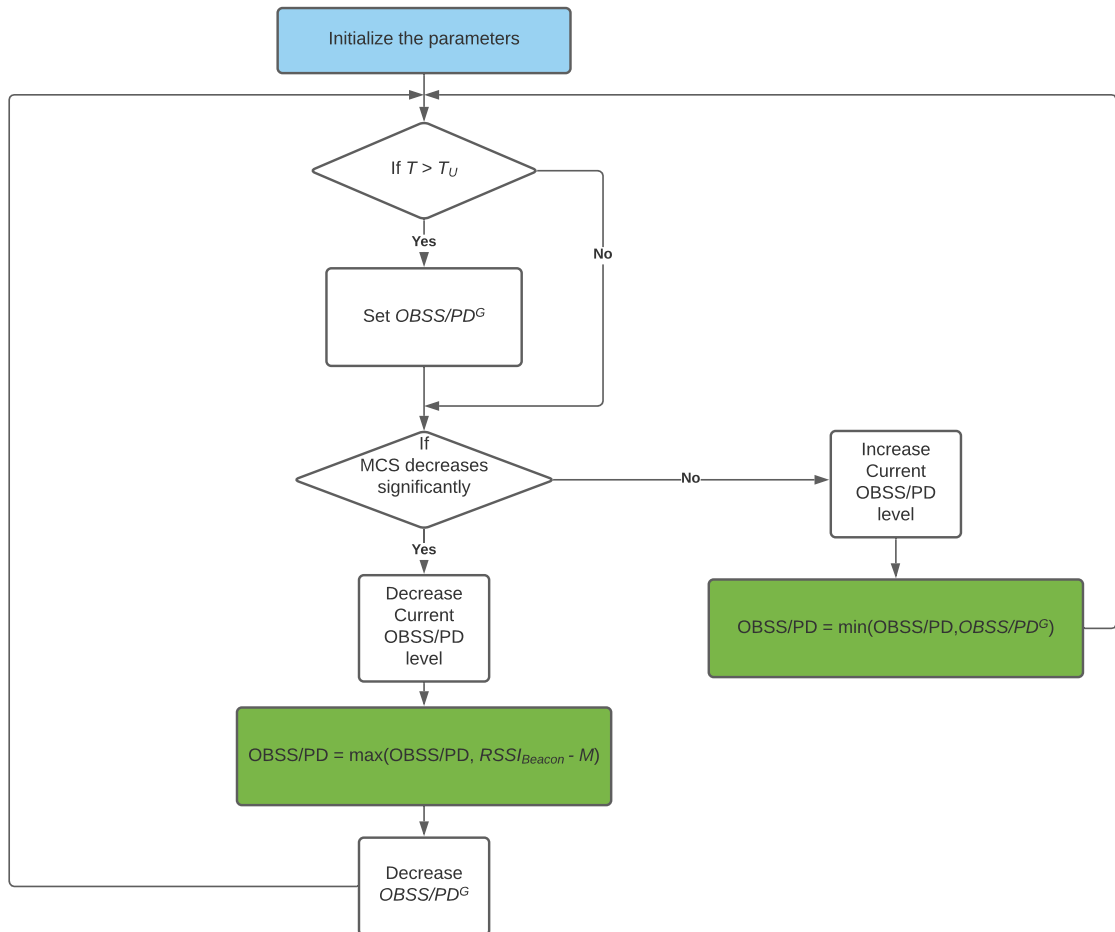


Figure 4.5. RACEBOT flowchart.

- (i) RACEBOT algorithm is adaptive to selected data rates by rate selection algorithms and it creates a chance for the upper MCS levels that rate algorithms can use. Therefore transmission can be performed via higher throughput.
- (ii) The algorithm decreases the number of exposed nodes by adjusting an effective OBSS/PD threshold.
- (iii) RACEBOT algorithm does not decrease the transmission power sharply. Therefore, while decreasing the number of exposed nodes, it keeps the number of the hidden nodes in acceptable levels.
- (iv) The algorithm can work with other rate selection algorithms.
- (v) The Algorithm works at both sparse and high density networks without having problem.

5. EXPERIMENTAL SETUP AND SIMULATION RESULTS

In this section, setup parameters, simulation topology and the experimental results of RACEBOT algorithm are discussed. The simulations are performed by using NS-3 framework and several modules have been developed for RACEBOT algorithm. In the simulation, NS-3-dev version is used and a dynamic OBSS/PD threshold module is developed on top of this.

5.1. NS-3 Simulation Framework

NS-3 is an open source discrete network simulation framework which has very extensive capabilities and flexibility to work on scientific researches [83]. Since the tool is open source and modular, for the research purposes, new utilities can be added or existing ones can be easily modified. The framework is written in C++ primarily for Linux and macOS while considering backwards compatibility with the previous version NS-2 [84]. NS-3 is available at its gitlab repository and once downloaded from there, via *waf* tool, the build process can be performed [85] [86].

In NS-3 each network device is called as *Node* like in graph theory. During simulation, programmed activities between nodes are called as *Application* and users may create various of specific types of *Application* by using the object-oriented structure of NS-3. Using the same OOP structure, communication channel mechanisms are operated by *Channel* object and various channel types can be derived from the existing class or a totally new one can be created.

In the simulator, the nodes can connect to the network channel via *NetDevice* which is a simulation of both hardware and software components of a network interface card (NIC). As the previous objects, *NetDevice* has also OOP logic and can be used to derive various of new NICs. The last abstract component of the main components

are “Topology Helpers” which are used for a number of tasks like connecting devices, assigning IP addresses, connecting a *NetDevice* to a channel etc.

Since NS-3 has a modular structure, a new model can be created and integrated with the existing structure easily. Besides this modularity, the main components of NS-3 have APIs and the new models can use these API to perform their tasks.

5.2. System Parameters and Performance Metrics

In the simulations, the parameters used in the RACEBOT algorithm are as given in Table 5.1. As discussed earlier, OBSS/PD mechanism is proposed in IEEE 802.11ax amendment. Since RACEBOT algorithm is based on OBSS/PD mechanism, 802.11ax protocol has been used in the simulations. Among the three operational frequencies in 802.11ax, 2.4 GHz, 5 GHz, and 6 GHz, we choose the 5 GHz frequency band. As the modulation schema, OFDM is used with 20 MHz channel bandwidth. As a guard interval (GI), 0.8 μ s short GI is used. As for spatial streams, all devices are set to have a single spatial stream (i.e., a 1x1 MIMO scheme).

The direction of the traffic is set to be the UL direction. As the traffic generator, a constant bit rate (CBR) traffic combined with a Poisson traffic model is used. Since delay is not a concern of this study, to saturate the traffic buffer, 300 Mbps constant data rate and 1024 bytes payload size are used. Since RACEBOT algorithm is designed to be used with rate selection algorithms, in the scenario, a modified version of Minstrel-HT for 802.11ax HE-rates and Thompson Rate Algorithm that are inside ns3-dev are used as rate selection algorithms.

In the next chapter, one of the TGax outdoor scenarios is used. Also, based on this scenario, additional random custom scenarios are generated and used. As OBSS/PD threshold boundaries, In 20 MHz bandwidth, default $OBSS/PD_{min}$ and $OBSS/PD_{max}$ values -82 dBm and -62 dBm are used.

Table 5.1. System parameters.

Parameter	Value
Protocol Standard	802.11ax
Frequency	5 GHz
Modulation Schema	OFDM
Bandwidth	20 MHz
Guard Interval	Short (0.8 μ s)
Traffic Type	UDP CBR Poisson
Traffic Direction	Uplink
Rate	300 Mbps
Payload Size	1024 Bytes
MCS selection	(Minstrel, Thompson)
Scenario	Original Box5 and Custom Box5
Number of Antennas	1
$OBSS/PD_{min}, OBSS/PD_{max}$	-82 dBm, -62 dBm
Preamble Detection Threshold	-82 dBm
RxSensitivity	-82 dBm
RTS/CTS	Disabled
CCA/ED	-62 dBm
TxPower AP/STA	21 dBm / 21 dBm
Simulation Time	50 s
Loss Model	Friis Loss Model
OFC	10
γ	0.7

The default preamble detection and $RxSensitivity$ thresholds that NS-3 uses are both adjusted to -82 dBm and the energy detection threshold CCA/ED is adjusted to -62 dBm. The initial $TxPower$ of both AP and STA's are set to 21 dBm, but at the run-time each $TxPower$ of nodes may change according to variations in the OBSS/PD thresholds due to our algorithm. As the loss model, Friis free space propagation model is used. This model works for the far field region. Because of this, the scenarios are

designed to operate according to this condition. Finally, all the simulations run for 50 seconds simulation time.

In the simulations, our performance metric is aggregated throughput, which is defined as the overall throughput of the system. Throughput of a single node in Mbits is calculated as

$$Throughput_i = \frac{rBytes_i \times 8}{1000 \times 1000 \times T_{Step}} \quad \text{where } i = 0, 1, 2, \dots \quad (5.1)$$

where $rBytes_i$ is the total received data in bytes for each T_{Step} and T_{Step} is the step time. Then, the aggregated throughput of all nodes in the system for the given time step is evaluated as

$$Throughput_s^{Agg} = \sum_{i=1}^n Throughput_i \quad (5.2)$$

where n is the number of nodes in the system. Finally, the aggregated total data that is transferred in the total simulation time is calculated as

$$TM_{Tot} = T_{Step} \times \sum_{s=0}^{N_{Step}} Throughput_s^{Agg} \quad (5.3)$$

where N_{Step} is defined as the total number of steps in the whole simulation.

5.3. Simulation Topology

In this section, the topology that is used in the simulations will be discussed. In [87], there are multiple scenarios developed by the collaboration of different product vendors inside TGax to evaluate and calibrate the performance of the systems.

In Figure 5.1, you can see one of the sophisticated outdoor scenarios in the TGax test suite named ‘‘Box5’’ is shown [87]. This topology consists of three BSSs (i.e., 3 APs) and 30 STA.

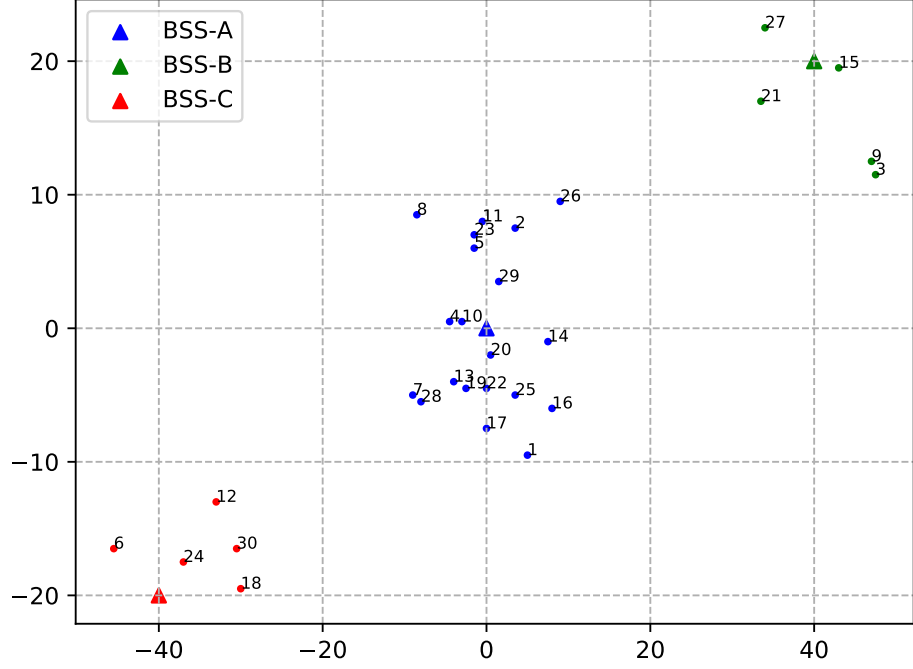


Figure 5.1. TGax Box5 outdoor topology.

While BSS-A has 20 associated STAs, BSS-B and BSS-C have 5 STAs each. In this study, the simulations are performed based on this topology. Besides, the “Box5” topology is modified and a set of simulations are performed by the customized “Box5” topology. We will call such modified topologies as “Custom Box5” topologies in this study. The generation algorithm of “Custom Box5” topology is shown in Figure 5.2.

“Custom Box5” topology generator generates various topologies which are similar to “Box5” topology based on five parameters: $Seed$, $nSTA_{AP}$, R^{Min} , R^{Max} and $AP_{(x,y)}$. $Seed$ parameter defines the seed value given to the random number generator that builds the topology. In a “Custom Box5” topology, each BSS has an equal number of nodes described by the $nSTA_{AP}$ parameter. Variation in this parameter directly affects the node density in the area. R^{Min} is defined to prevent the algorithm to put a station in the near field. This is required to satisfy the requirement of Friis path loss model. R^{Max} is the maximum range that a STA can be put away from the corresponding AP.

```

1: Input:  $Seed, nSTA_{AP}, R^{Min}, R^{Max}, AP_{(x,y)}: (0,0), (40,20), (-40,-20)$ 
2: Create 3 BSS
3: Assign a color to each BSS
4: for Each  $AP_{(x,y)}$  do
5:   Create an AP
6: end for
7: for i in  $[0, nSTA_{AP})$  do
8:   for Each  $AP_j, j=0,1,2$  do
9:     while TRUE do
10:      Generate Random coordinate  $(x, y)$  with  $Seed$ 
11:      if  $(x, y)$  is not in  $(x, y)_{AP}$  and  $(x, y)_{STA}$  then
12:        if  $(x, y)$  in  $[R_{AP_j}^{Min}, R_{AP_j}^{Max}]$  then
13:          Create a STA
14:          Assign the color of  $AP_j$  to STA
15:          BREAK
16:        end if
17:      end if
18:    end while
19:   end for
20: end for

```

Figure 5.2. Custom Box5 topology generator algorithm.

Since the “Custom box5” scenario is based on the original “box5” scenario, the number of APs and the locations of APs are fixed and given as input to the algorithm given with the $AP_{(x,y)}$ parameter set.

The algorithm first creates 3 different BSSs and assigns them a color. Then by using $AP_{(x,y)}$, it creates the APs same with “box5” topology. Then, for each AP $nSTA_{AP}$ number of STAs are generated with random coordinates according to the $Seed$ parameter and the range restrictions by R^{Min} and R^{Max} parameters. Finally, each STA is given a color same as the associated AP. The number of STAs for each

AP can be modified by $nSTA_{AP}$ parameter and if different *Seed* is set at each time, different topologies with the same number of STAs can be obtained.

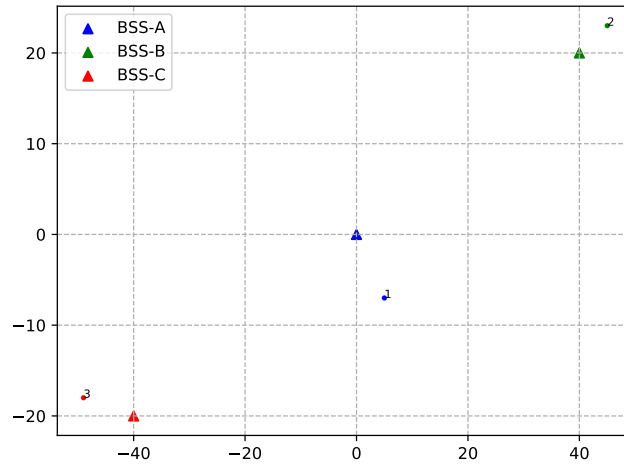


Figure 5.3. Custom Box topology with 3 STA and *Seed*=1.

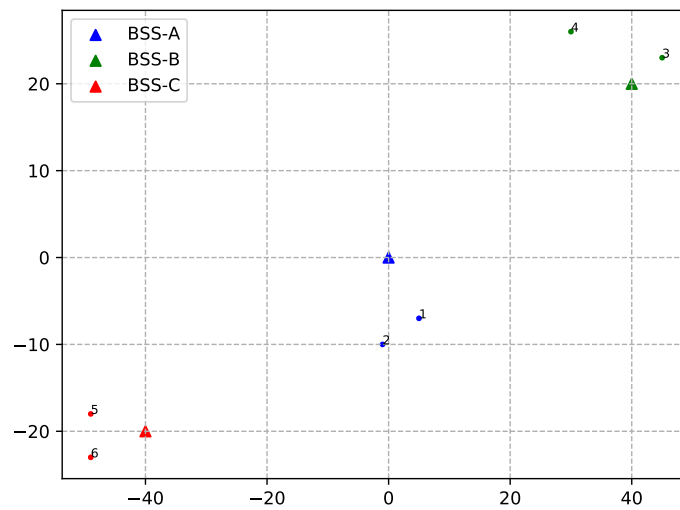


Figure 5.4. Custom Box topology with 6 STA and *Seed*=1.

In Figure 5.3 a topology with 3 STAs and *Seed*=1 is illustrated. In the simulations, if the performance of the algorithm while changing the topology is to be compared with another topology's performance where there are one more STA per AP, increasing the $nSTA_{AP}$ by 1 and keeping the *Seed* value would be enough. For exam-

ple, in Figure 5.4 number of stations are increased by 1 and the first three STA's are the same with the topology in Figure 5.3.

In Figure 5.4, a different *Seed* is used and the locations of the STA's are totally different than the topology in the Figure 5.5. Lastly, in Figure 5.6, a dense topology which has 45 STA is illustrated. By changing the number of STA's and their locations by *Seed* numbers, lots of different topologies can be obtained and by that way the performance comparison can be made more reliable.

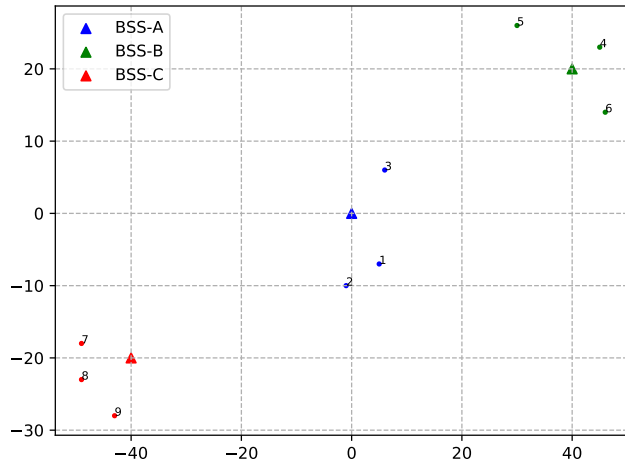


Figure 5.5. Custom Box topology with 6 STA and *Seed*=2.

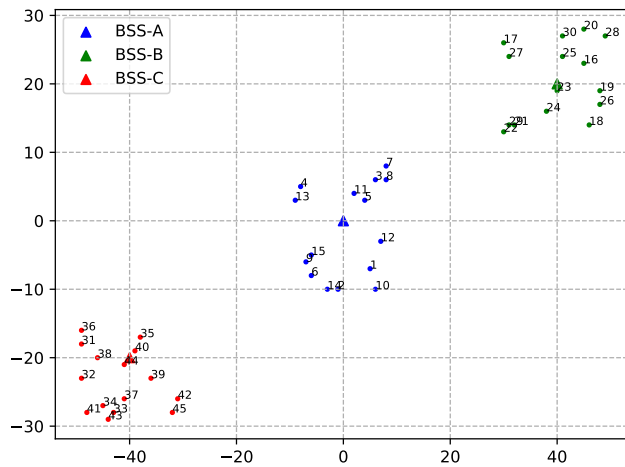


Figure 5.6. Custom Box topology with 45 STA and *Seed*=2.

In the simulations, various topologies have been generated and performance measurements have been done. For the “Custom Box5” topology, since the performance results for a single topology may not show the real accuracy, the given scenarios are repeated three times with different *Seed* values. Then the average of the results has been taken. In that way, if any outlier exists, the effect of the outlier will be reduced and the results will be much more accurate.

For the “TGax Box5” scenario, a single topology inside the TGax documentation is used [87]. Since this topology is used for performance comparisons and calibration, the corresponding result of the simulations may give some inferences.

5.4. Simulation Results

To evaluate the performance of RACEBOT algorithm, different scenarios are generated. Real life applications in wireless networks take advantage of rate selection algorithms to get maximum performance from the system. In the scenarios of the thesis study, modified version of Minstrel-HT algorithm for HE-rates and Thompson rate selection algorithm with $decay = 0.1$ are used as reference algorithms [81] [82]. Since each rate algorithm has different performance, the simulations are evaluated for each rate selection algorithm separately.

To compare RACEBOT algorithm with the other carrier sensing threshold algorithms, DSC algorithm, RTOT algorithm, and a scenario (named NO-OBSSPD) which does not use any carrier sensing threshold mechanism are used as reference algorithms in the scenarios [57] [64].

5.4.1. Box5 Scenario

‘Box5 Scenario’ is an outdoor scenario of TGax that is mentioned at the beginning of the Section 5.3 composed of three BSSs as: BSS-A contains 1 AP and 15 STAs, each of BSS-B and BSS-C contains 1 AP and 5 STAs (Figure 5.1).

In the Figure 5.7, simulation results of RACEBOT, RTOT, DSC, and NO-OBSSPD with Minstrel rate selection algorithm have been illustrated. Here, DSC algorithm gives a reduced total throughput compared to the other algorithms. As for our RACEBOT algorithm, it starts with slightly worse performance than RTOT and NO-OBSSPD algorithms, but after 42 s, the slope of the curve increases and its results converge to that of RTOT and NO-OBSSPD.

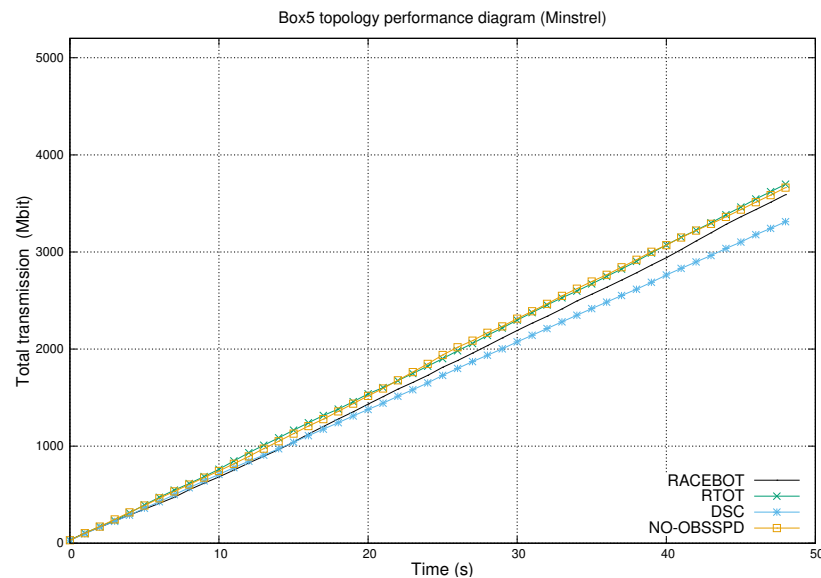


Figure 5.7. Scenario Box5 - Minstrel.

When we switch to the Thompson rate selection algorithm in the same scenario, the results change considerably as seen in the Figure 5.8. Again, DSC algorithm has shown worse performance than the other algorithms, and again, RTOT and NO-OBSSPD algorithms have similar performance. However, our proposed algorithm RACEBOT has shown a slightly better result than the other three algorithms and the discrepancy keeps increasing as time passes. It shows that DSC algorithm has some limitations in both rate selection algorithms. It even shows worse performance than the case that does not use any carrier sensing threshold algorithm.

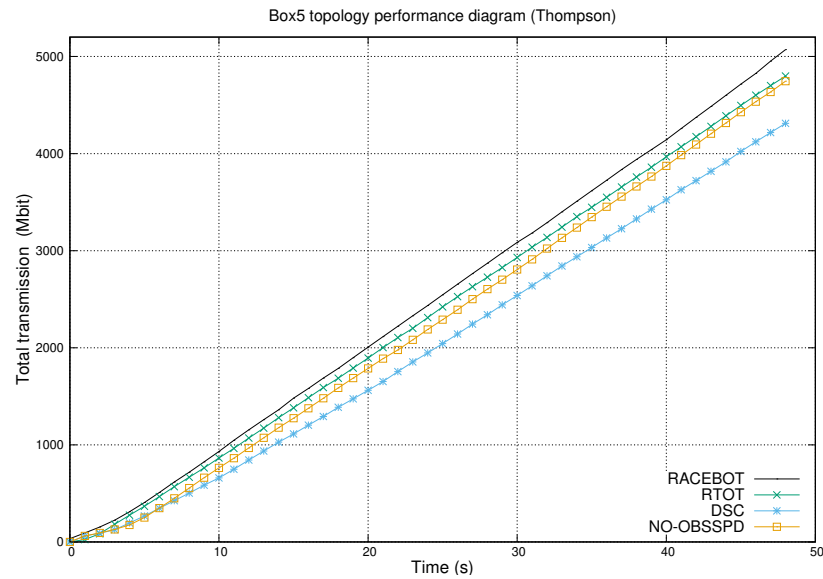


Figure 5.8. Scenario Box5 - Thompson.

5.4.2. Minstrel Scenarios

In the simulations, one of the most significant observations is that using an OBSS/PD mechanism with the Minstrel rate selection algorithm does not create any improvement. As seen in the Figure 5.9, no algorithm shows superiority to other algorithms. Therefore, we can conclude that, using OBSS/PD mechanism with the Minstrel rate selection algorithm does not provide any performance enhancement.

5.4.3. Thompson custom Box5 Scenario 1

In this scenario, three topologies are generated. Each topologies are consisting of 3 BSSs and each BSS contains one AP and one STA. Each topology is generated by different *Seed* values. At the end of the simulation, the average of the throughput of the three topologies are taken for each time step. In Figure 5.10, a topology with *Seed* = 1 is shown. The other two topologies are similar to this, but their STAs are generated by *Seed* = 2 and *Seed* = 3 values. To evaluate the overall performance, the average of the throughput values of all three seeds was taken.

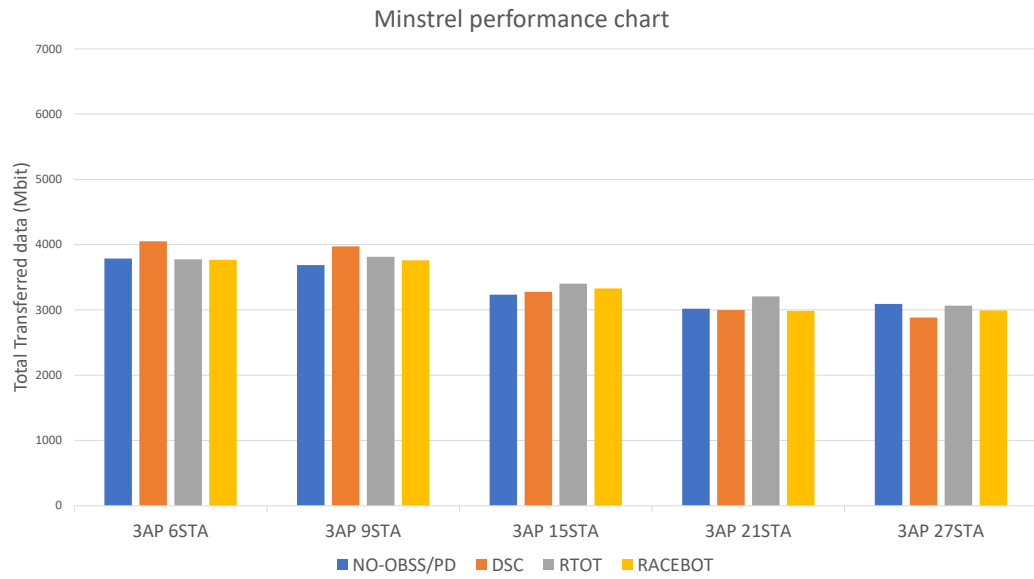


Figure 5.9. Minstrel performance diagram.

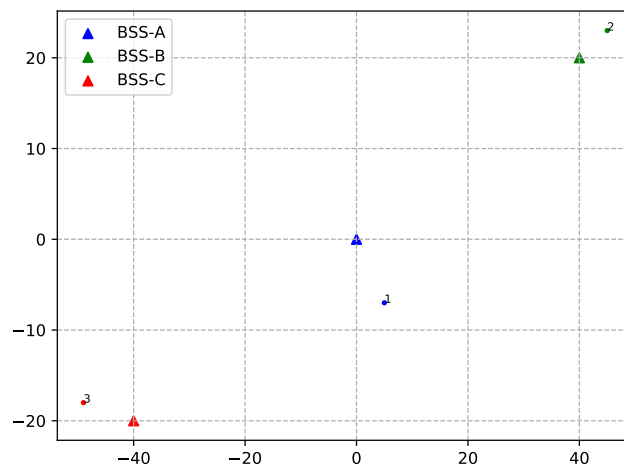


Figure 5.10. Scenario 1 - Topology for $Seed = 1$.

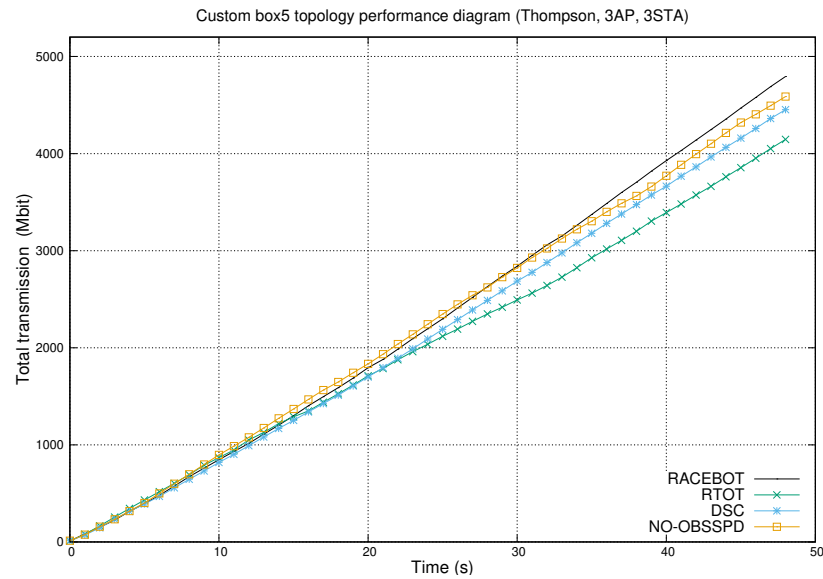


Figure 5.11. Scenario 1: 3 STA 3 AP Custom Box5 Thompson rate algorithm.

In Figure 5.11, the simulation result of scenario 1 is shown for the Thomson rate selection algorithm. In this case, RACEBOT algorithm has shown slightly better performance than the other algorithms, but again, using OBSS/PD threshold did not create a significant improvement on the performance in this sparse scenario. As in the scenario that uses Minstrel algorithm, RTOT algorithm has given slightly worse performance than the others in this setup.

5.4.4. Thompson custom Box5 Scenario 2

Scenario 2 is the extension of scenario 1 that three more STAs are added to the system. In scenario 2, there are three BSSs and each BSS has two STAs. To get reliable results, three topologies are generated by using 1, 2, and 3 as *Seed* values, then the average of the total transmission at each time step is taken. In Figure 5.12, one of the topologies that is generated by using *Seed* = 1 is shown.

In Figure 5.13, RACEBOT algorithm has shown better performance than the other carrier sensing threshold algorithms.

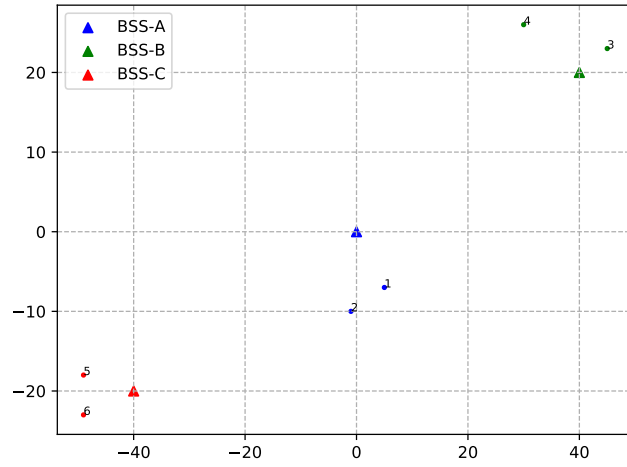


Figure 5.12. Scenario 2 - Topology for $Seed = 1$.

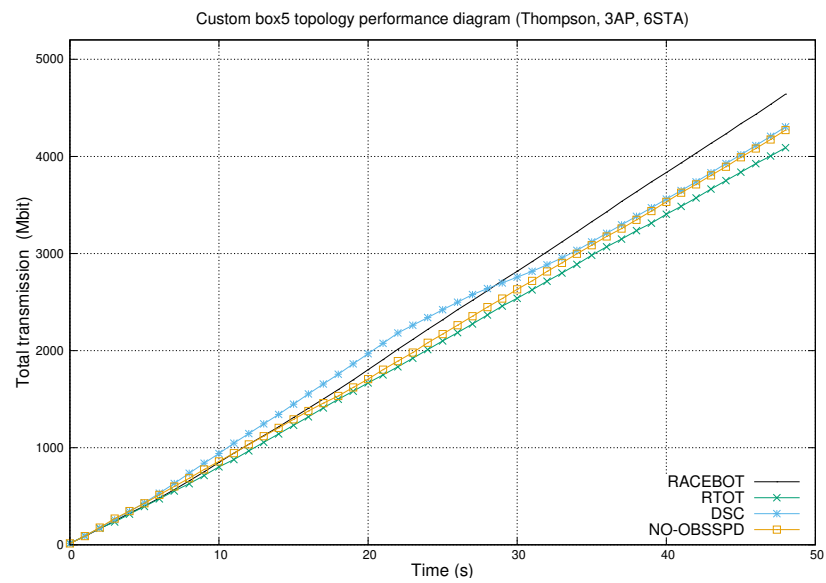


Figure 5.13. Scenario 2: 6 STA 3 AP Custom Box5 Thompson rate algorithm.

In the first 25 seconds, although DSC algorithm has shown a better performance than the others, after that time, the performance of DSC algorithm has gradually decreased. RTOT algorithm has shown worse performance than the other carrier sensing threshold algorithms. That shows DSC and RTOT did not show an enhancement on the performance rather than the case that uses no OBSS/PD mechanism. RACEBOT algorithm has shown stable and better performance than the other algorithms. Even if in the first 25 seconds, the performance of RACEBOT algorithm is under DSC algorithm, but then RACEBOT has preserved its stability and gave better performance.

5.4.5. Thompson custom Box5 Scenario 3

In scenario 3, one more STA is added to each BSS of scenario 2 (see Figure 5.14) and again, Thompson rate selection algorithm is used in the simulations. In the

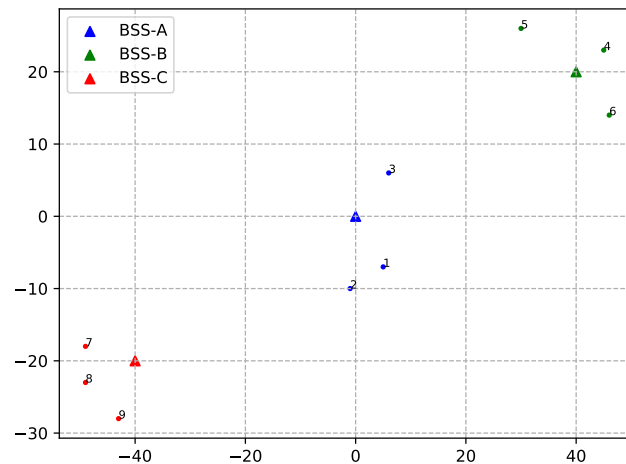


Figure 5.14. Scenario 3 - Topology for $Seed = 1$.

Figure 5.15, RACEBOT and DSC algorithm did not increase the performance of the system, but they also did not cause any performance degradation and have shown similar performance to the case which has no OBSS/PD mechanism. However, using RTOT algorithm affected the system negatively. The total transmission of the system has been decreased compared to the scenario which does not use any OBSS/PD mechanism.

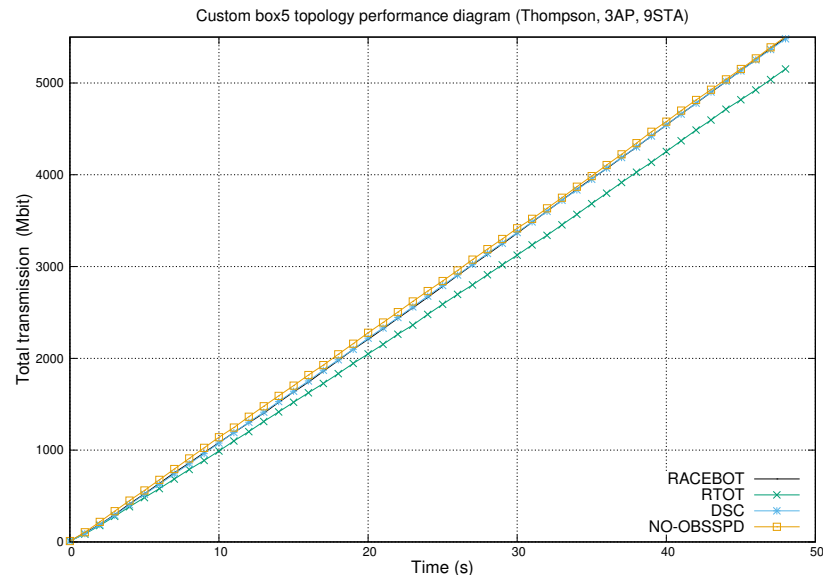


Figure 5.15. Scenario 3: 9 STA 3 AP Custom Box5 Thompson rate algorithm.

From the results, it can be inferred that, even if RACEBOT algorithm did not help to increase the system performance, it preserved the system performance and stability.

5.4.6. Thompson custom Box5 Scenario 4

The scenario 4 is consisting of three BSSs. Each BSS has one AP and each AP has five STAs as shown in Figure 5.16. Again, for Thompson rate selection algorithm, each carrier sensing threshold algorithms are evaluated.

In the Figure 5.17 and the Figure 5.18, it is clearly seen that RACEBOT algorithm has shown better performance than the other carrier sensing threshold algorithms.

The worst performance belongs to the case that does not use any carrier sensing threshold algorithm. DSC and RTOT algorithms have shown slightly better performance than no OBSS/PD cases.

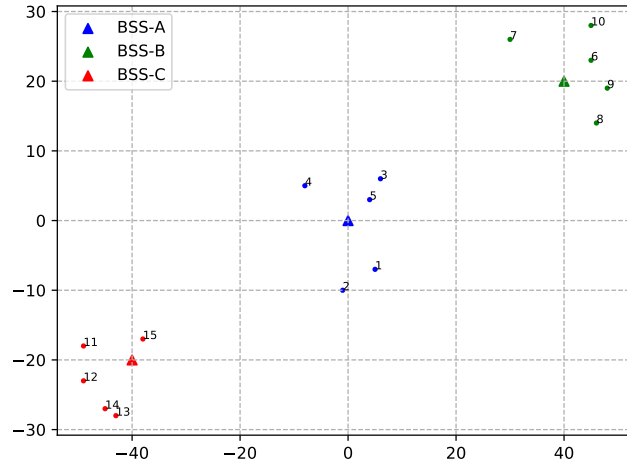


Figure 5.16. Scenario 4 - Topology for $Seed = 1$.

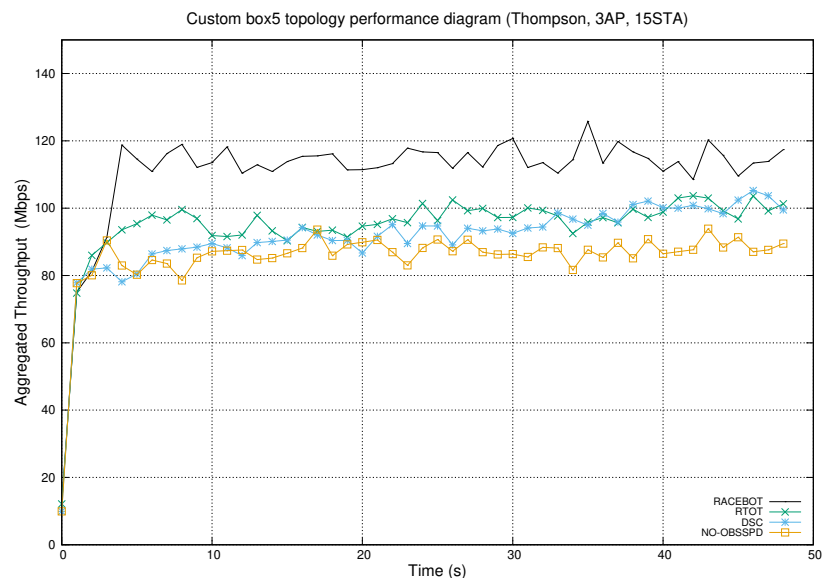


Figure 5.17. Scenario 4: 15 STA 3 AP Custom Box5 Thompson rate algorithm aggregated throughput.

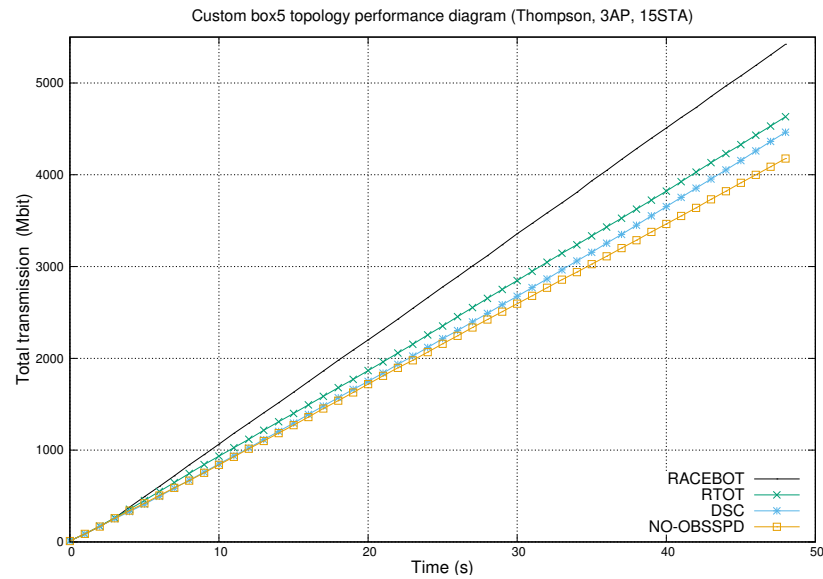


Figure 5.18. Scenario 4: 15 STA 3 AP Custom Box5 Thompson rate algorithm.

5.4.7. Thompson custom Box5 Scenario 5

In scenario 5, similar topology is generated that is consisting of 3 BSSs and each BSS has 1 AP. There are 7 STA in each AP (see Figure 5.19) and the simulations are done for Thompson rate selection algorithm. The simulation result is consisting of the average of three different seed values.

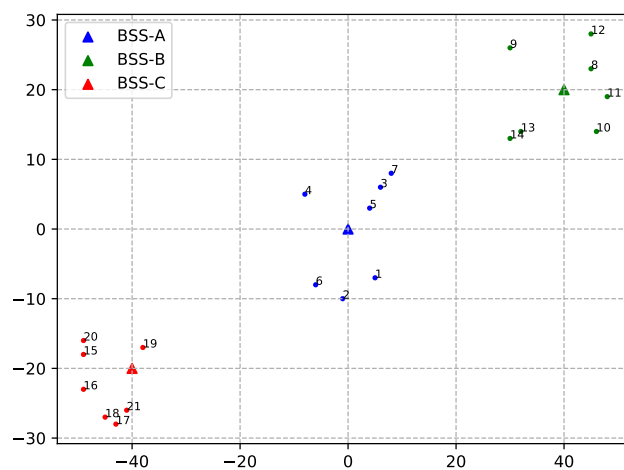


Figure 5.19. Scenario 5 - Topology for $Seed = 1$.

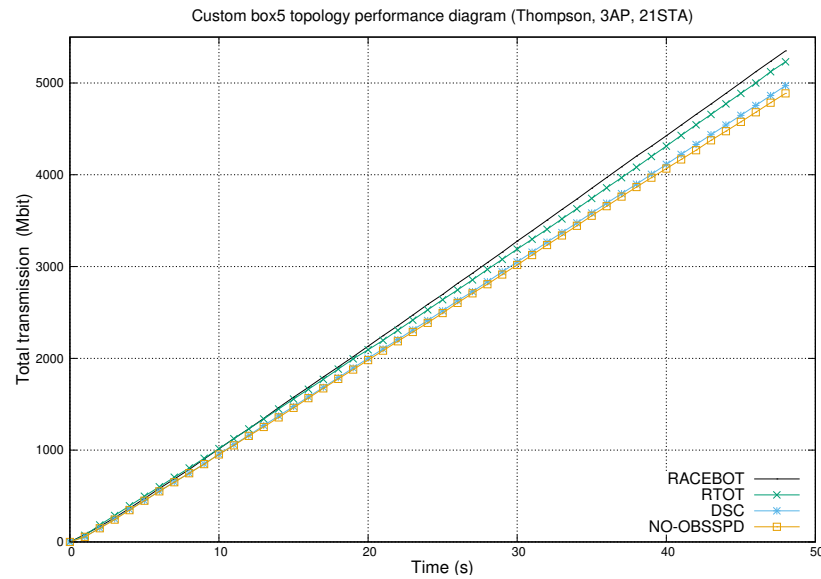


Figure 5.20. Scenario 5: 21 STA 3 AP Custom Box5 Thompson rate algorithm.

In the Figure 5.20 , a scenario with Thomson rate selection algorithm is shown. In the graphs, DSC algorithm shows similar performance to the scenario that the carrier sensing threshold algorithm was not used. However, RACEBOT algorithm and RTOT algorithm have better performance than the others. The performance of RACEBOT algorithm is slightly better than RTOT algorithm in this situation.

5.4.8. Thompson custom Box5 Scenario 6

The final custom scenario is shown in the Figure 5.21. The same number BSS and AP are also used in this scenario. Additionally, there are 9 STAs for each AP and again the simulations are done for both Minstrel and Thompson rate selection algorithms.

In the Figure 5.22 and Figure 5.23, again RACEBOT algorithm has shown better performance among the other carrier sensing threshold algorithms in the system that uses Thompson rate selection algorithm. DSC and RTOT algorithms have shown similar performance and did not increase the performance of the system.

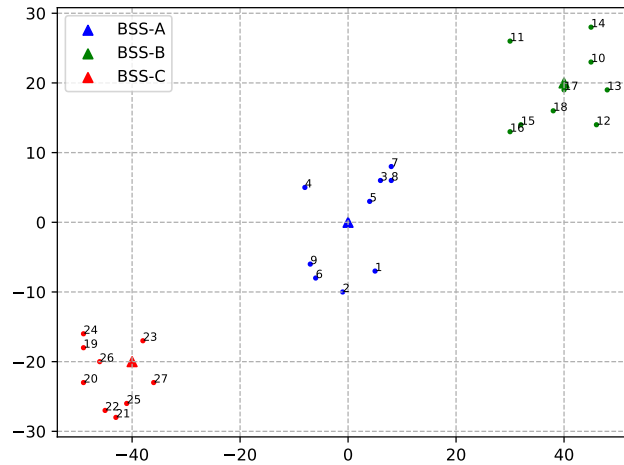


Figure 5.21. Scenario 6: 27 STA 3 AP Custom Box5 Thompson rate algorithm.

5.4.9. Overall Comparison of Scenarios

In this section, the overall comparison of the algorithms have been performed. We divided the scenarios in three groups: sparse, medium, and high density scenarios.

In the Figure 5.24, sparse density scenarios have been compared. It is seen that RTOT algorithm has worse performance than the other three algorithms. RTOT algorithm shows even worse performance than the NO-OBSSPD scenario. It can be inferred that, in sparse scenarios, RTOT algorithm may deteriorate the performance of the system that does not use any carrier sensing threshold algorithm. and RACEBOT has shown better performance than the other algorithms.

In the Figure 5.25, the result of medium node density scenarios have been illustrated. RACEBOT algorithm has shown quite stable and better performance than the other algorithms.

As seen, while in 9-STA case, RTOT and DSC algorithms have quite similar performance, in 15-STA case they show worse and unstable performance. As a result of these findings, it can be inferred that, as the node density increases, the stability of the legacy algorithms decrease.

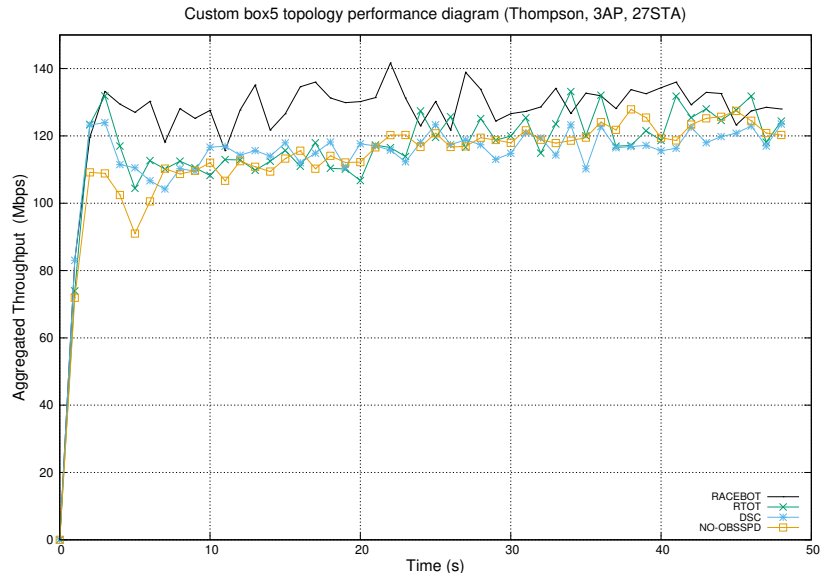


Figure 5.22. Scenario 6: 27 STA 3 AP Custom Box5 Thompson rate algorithm aggregated throughput.

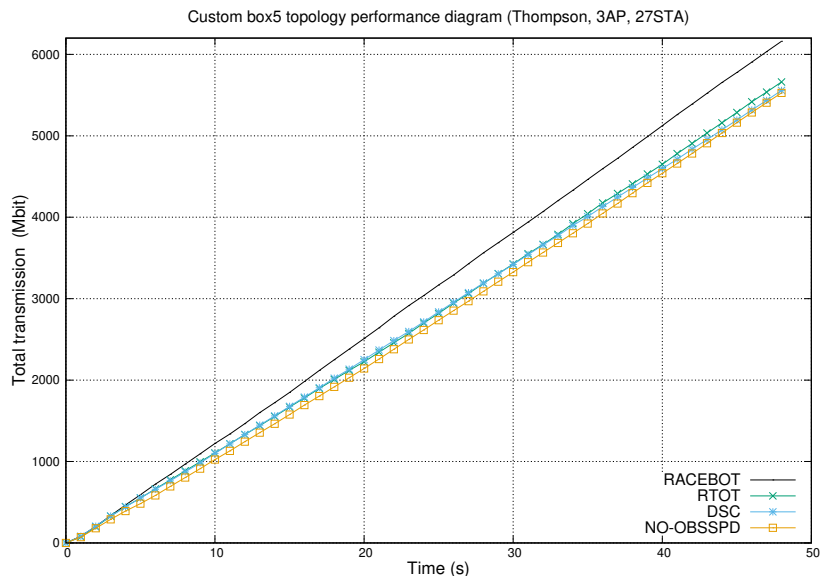


Figure 5.23. Scenario 6: 27 STA 3 AP Custom Box5 Thompson rate algorithm.

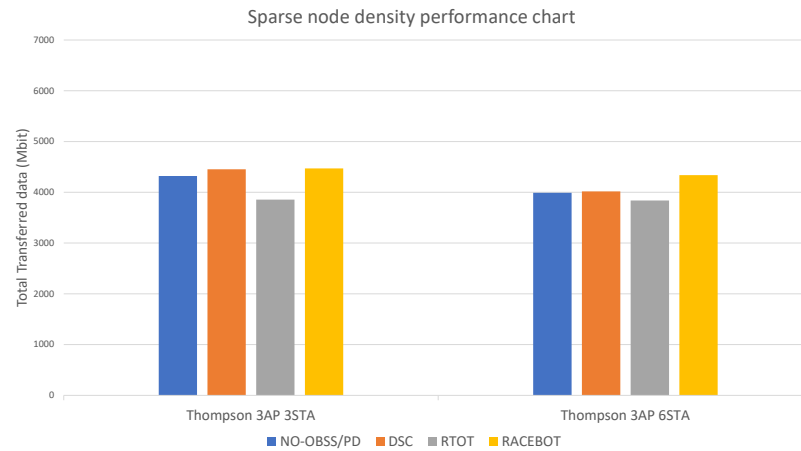


Figure 5.24. Sparse node density performance comparison.

Lastly, in the Figure 5.26, the high node density scenarios have been shown. Results for high density scenarios are similar to the medium node density scenarios. For the Thompson rate selection algorithm, the enhancement of RACEBOT algorithm can be clearly seen.

RACEBOT algorithm shows better and stable performance than the other legacy algorithms. Therefore, it can be inferred that using OBSS/PD threshold algorithm with Thompson rate selection algorithm may enhance the network performance. Moreover, the proposed RACEBOT algorithm is in coherence with the Thompson rate selection algorithm and RACEBOT is more stable compared to RTOT and DSC while varying the node density.

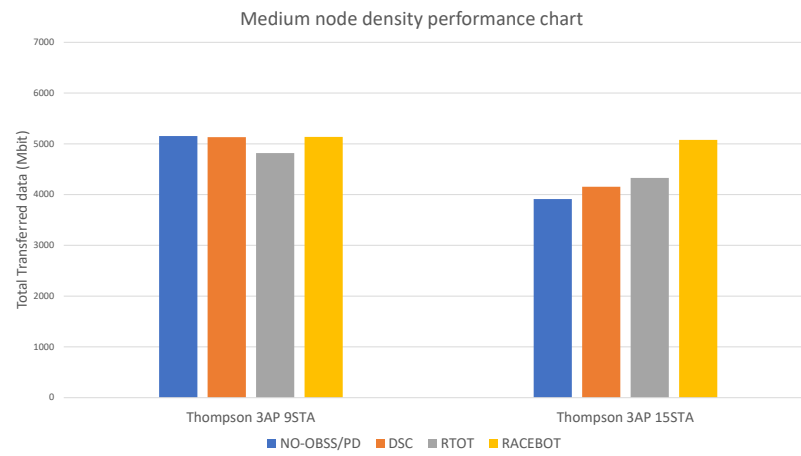


Figure 5.25. Medium node density performance comparison.

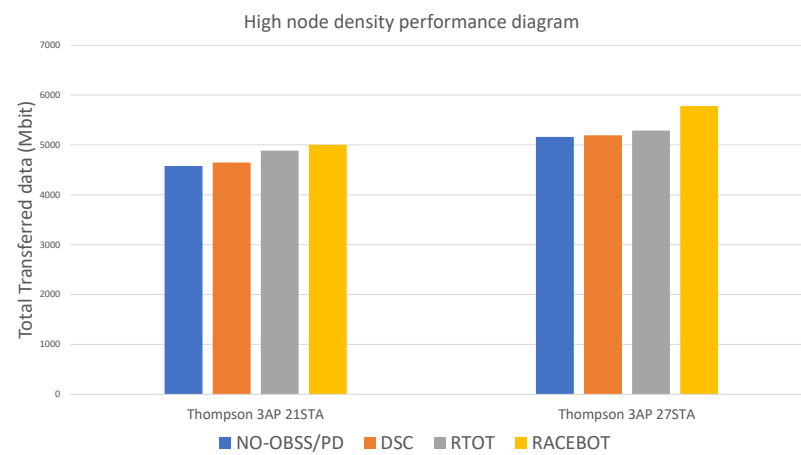


Figure 5.26. High node density performance comparison.

6. CONTRIBUTIONS AND FUTURE DIRECTIONS

6.1. Contributions of RACEBOT Algorithm

In this section, the contributions of RACEBOT algorithm and the future potential directions that can be improved based on these results are discussed.

RACEBOT algorithm uses the advantage of controlling transmission power and having information of conflicts to increase the overall performance. Since the transmission power is directly related to the data rate, RACEBOT algorithm does not decrease the transmission power sharply and it creates a chance for the rate selection algorithm to use higher rates.

RACEBOT algorithm uses OFC and OFC_{Thr} parameters for pruning exceptional RSSI values. These parameters are used to neglect RSSIs, which are rare and have potential to degrade the performance. By that way, RACEBOT algorithm can use higher transmission powers and higher data rates.

Sharp changes in transmission power may degrade the performance of rate selection algorithms. Therefore, RACEBOT algorithm does not increase the OBSS/PD level sharply, it increases OBSS/PD level step by step with considering the changes of MCS levels. RACEBOT algorithm keeps track of MCS deterioration while changing the OBSS/PD level.

In the simulations, using OBSS/PD threshold with minstrel rate selection algorithm did not show any improvements for all the legacy algorithms and our proposed algorithm. However, with the Thompson rate selection algorithm, our proposed algorithm has shown better result than the other algorithms. It can be inferred that using RACEBOT algorithm with modern rate selection algorithms can give better results.

Our algorithm decreases the number of exposed nodes via lowering the OBSS/PD threshold. Since the RACEBOT algorithm varies the OBSS/PD level step by step, it has the potential to keep the hidden nodes lower than the algorithms varying the OBSS/PD level sharply. The algorithm can work in both sparse and dense environments. And it can be used along with any rate selection algorithm.

6.2. Future Directions

In a coordinated infrastructure, as a future direction, this mechanism can be modified and to be coordinated by a central location. Power, location, and collision information of each node can be used to determine an optimal OBSS/PD threshold. We plan to establish a system that can be coordinated centrally to operate OBSS/PD mechanism

Besides this, we plan to develop a new rate selection algorithm that can use this OBSS/PD mechanism internally. By that way, nodes will be able to use the OBSS/PD mechanism with another rate selection algorithm or inside the new rate selection algorithm by choice.

We plan to optimize the parameters of the RACEBOT algorithm for different situations and we will try to design an auto-adjustment algorithm for self-adaptation. Moreover, we will design a new algorithm with adaptive step size for varying the OBSS/PD level while moving towards the goal OBSS/PD.

REFERENCES

1. IEEE 802.11ax Task Group, “IEEE Standard for Information Technology–Telecommunications and Information Exchange between Systems Local and Metropolitan Area Networks–Specific Requirements Part 11: Wireless LAN Medium Access Control (MAC) and Physical Layer (PHY) Specifications Amendment 1: Enhancements for High-Efficiency WLAN”, *IEEE Std 802.11ax-2021 (Amendment to IEEE Std 802.11-2020)*, pp. 1–767, 2021.
2. Bell, A., “The Photophone”, *Science*, Vol. os-1, pp. 130–134, 2007.
3. Sarkar, T. K., R. Mailloux, A. A. Oliner, M. Salazar-Palma and D. L. Sengupta, *Historical German Contributions to Physics and Applications of Electromagnetic Oscillations and Waves*, pp. 327–348, John Wiley & Sons, 2006.
4. Wifi Alliance, “Who We Are - History”, <https://www.wi-fi.org/who-we-are/history>, accessed in July 2021.
5. Crow, B., I. Widjaja, J. Kim and P. Sakai, “IEEE 802.11 Wireless Local Area Networks”, *IEEE Communications Magazine*, Vol. 35, No. 9, pp. 116–126, 1997.
6. IEEE 802.11 Task Group, “IEEE Standard for Information Technology- Telecommunications and Information Exchange Between Systems- Local and Metropolitan Area Networks- Specific Requirements- Part 11: Wireless LAN Medium Access Control (MAC) and Physical Layer (PHY) Specifications”, *ANSI/IEEE Std 802.11, 1999 Edition (R2003)*, pp. i–513, 2003.
7. Task Group-ax, “High Efficiency (HE) Wireless LAN Task Group”, https://www.ieee802.org/11/Reports/tgax_update.htm, 2014, accessed in July 2021.
8. IEEE 802.11ac Task Group, “IEEE Standard for Information Technology–Telecommunications and Information Exchange Between Systems Local and

- Metropolitan Area Networks— Specific Requirements—Part 11: Wireless LAN Medium Access Control (MAC) and Physical Layer (PHY) Specifications— Amendment 4: Enhancements for Very High Throughput for Operation in Bands below 6 GHz.”, *IEEE Std 802.11ac-2013 (Amendment to IEEE Std 802.11-2012, as Amended by IEEE Std 802.11ae-2012, IEEE Std 802.11aa-2012, and IEEE Std 802.11ad-2012)*, pp. 1–425, 2013.
9. Kaiying, L., “IEEE 802.11 Task Group-ax, MAC Ad hoc 2019 Meeting Minutes - IEEE 802.11-19/1163r0”, <https://mentor.ieee.org/802.11/dcn/19/11-19-1163-01-00ax-comment-resolution-for-qtp.docx>, 2019, accessed in July 2021.
 10. Chen, Q. and Y.-H. Zhu, “Scheduling Channel Access Based on Target Wake Time Mechanism in 802.11ax WLANs”, *IEEE Transactions on Wireless Communications*, Vol. 20, No. 3, pp. 1529–1543, 2021.
 11. Khorov, E., A. Kiryanov, A. Lyakhov and G. Bianchi, “A Tutorial on IEEE 802.11ax High Efficiency WLANs”, *IEEE Communications Surveys Tutorials*, Vol. 21, No. 1, pp. 197–216, 2019.
 12. Yin, H. and S. Alamouti, “OFDMA: A Broadband Wireless Access Technology”, *Proceedings of the IEEE Sarnoff Symposium*, pp. 1–4, 2006.
 13. Fuemmeler, J. A., N. H. Vaidya and V. V. Veeravalli, “Selecting Transmit Powers and Carrier Sense Thresholds in CSMA Protocols for Wireless Ad Hoc Networks”, *Proceedings of the International Workshop on Wireless Internet (WICON)*, p. 15–es, Association for Computing Machinery, New York, NY, USA, 2006.
 14. Hedayat, R., M. Cheong, Y. H. Kwon, Y. Noh and L. Cariou, “Spatial Reuse Group Challenges: IEEE 802.11-17/383r0”, <https://mentor.ieee.org/802.11/dcn/17/11-17-0383-00-00ax-spatial-reuse-group-challenges.pptx>, 2017, accessed in July 2021.

15. Wilhelmi, F., S. B. Muñoz, C. Cano, I. Selinis and B. Bellalta, “Spatial Reuse in IEEE 802.11ax WLANs”, <https://arxiv.org/abs/1907.04141>, 2021, accessed in July 2021.
16. Qu, Q., B. Li, M. Yang, Z. Yan, A. Yang, D.-J. Deng and K.-C. Chen, “Survey and Performance Evaluation of the Upcoming Next Generation WLAN Standard - IEEE 802.11ax”, *Mobile Networks and Applications*, Vol. 14, p. 1461–1474, 2018.
17. Ergen, S. C. and P. Varaiya, “TDMA Scheduling Algorithms for Wireless Sensor Networks”, *Wireless Networks*, Vol. 16, p. 985–997, 2010.
18. San-qiLi and J.C.Majithia, “Performance Analysis of a DTDMA Local Area Network for Voice and Data”, *Computer Networks*, Vol. 8, pp. 81–91, 1984.
19. Lans, H., “Position Indicating System: US Patent US5506587A”, <https://patents.google.com/patent/US5506587A/en>, 1996, accessed in July 2021.
20. Salehi, J., “Code Division Multiple-Access Techniques in Optical Fiber Networks. I. Fundamental Principles”, *IEEE Transactions on Communications*, Vol. 37, No. 8, pp. 824–833, 1989.
21. Ottersten., B., “Spatial Division Multiple Access (SDMA) in Wireless Communications”, *Proceedings of the Nordic Radio Symposium*, pp. 1–7, 1995.
22. Kapadia, V. V., S. N. Patel and R. H. Jhaveri, “Comparative Study of Hidden Node Problem and Solution Using Different Techniques and Protocols”, *Journal of Computing*, Vol. 2, pp. 65–67, 2010.
23. Kosek-Szott, K., “A Survey of MAC Layer Solutions to the Hidden Node Problem in Ad-Hoc Networks”, *Ad Hoc Networks*, Vol. 10, pp. 635–660, 2012.
24. Karn, P., “MACA - A New Channel Access Method for Packet Radio”, *Proceedings of the Computer Networking Conference*, pp. 1–7, 1990.

25. Bharghavan, V., A. Demers, S. Shenker and L. Zhang, "MACAW: A Media Access Protocol for Wireless LAN's", *SIGCOMM Computer Communication Review*, Vol. 24, No. 4, p. 212–225, Oct. 1994.
26. Talucci, F., M. Gerla and L. Fratta, "MACA-BI (MACA By Invitation)-A Receiver Oriented Access Protocol for Wireless Multihop Networks", *Proceedings of the IEEE International Symposium on Personal, Indoor and Mobile Radio Communications (PIMRC)*, Vol. 2, pp. 435–439, 1997.
27. Fullmer, C. L. and J. J. Garcia-Luna-Aceves, "Floor Acquisition Multiple Access (FAMA) for Packet-Radio Networks", *SIGCOMM Computer Communication Review*, Vol. 25, No. 4, p. 262–273, Oct. 1995.
28. Wu, C. and V. Li, "Receiver-Initiated Busy-Tone Multiple Access in Packet Radio Networks", *SIGCOMM: Proceedings of the ACM Workshop on Frontiers in Computer Communications Technology*, p. 336–342, 1987.
29. Haas, Z. and J. Deng, "Dual Busy Tone Multiple Access (DBTMA)-A Multiple Access Control Scheme for Ad Hoc Networks", *IEEE Transactions on Communications*, Vol. 50, No. 6, pp. 975–985, 2002.
30. Zhai, H., J. Wang and Y. Fang, "DUCHA: A New Dual-Channel MAC Protocol for Multihop Ad Hoc Networks", *IEEE Transactions on Wireless Communications*, Vol. 5, No. 11, pp. 3224–3233, 2006.
31. Ye, S., Y. Wang and Y. Tseng, "A Jamming-Based MAC Protocol to Improve the Performance of Wireless Multihop Ad-Hoc Networks", *Wireless Communications and Mobile Computing*, Vol. 4, pp. 75–84, 2004.
32. Natkaniec, M. and A. Pach, "PUMA - A New Channel Access Protocol for Wireless LANs", *Proceedings of the International Symposium on Wireless Personal Multimedia Communications*, Vol. 3, pp. 1351–1355, 2002.

33. Kosek-Szott, K., M. Natkaniec and A. R. Pach, “BusySiMOn - A New Protocol for IEEE 802.11 EDCA-Based Ad-Hoc Networks with Hidden Nodes”, *Proceedings of the IEEE Global Telecommunications Conference (GLOBECOM)*, pp. 1–6, 2010.
34. Singh, S. and C. S. Raghavendra, “PAMAS-Power Aware Multi-Access Protocol with Signalling for Ad Hoc Networks”, *SIGCOMM Computer Communication Review*, Vol. 28, No. 3, p. 5–26, Jul. 1998.
35. Bambos, N. and S. Kandukuri, “Power controlled multiple access (PCMA) in wireless communication networks”, *Proceedings of the IEEE International Conference on Computer Communications (INFOCOM)*, Vol. 2, pp. 386–395, 2000.
36. Korakis, T., G. Jakllari and L. Tassiulas, “CDR-MAC: A Protocol for Full Exploitation of Directional Antennas in Ad Hoc Wireless Networks”, *IEEE Transactions on Mobile Computing (TMC)*, Vol. 7, No. 2, pp. 145–155, 2008.
37. Takatsuka, Y., M. Takata, M. Bandai and T. Watanabe, “A MAC Protocol for Directional Hidden Terminal and Minor Lobe Problems”, *Proceedings of the Wireless Telecommunications Symposium (WTS)*, pp. 210–219, 2008.
38. Wang, J., H. Zhai, P. Li, Y. Fang and D. Wu, “Directional Medium Access Control for Ad Hoc Networks”, *Wireless Networks*, pp. 1059–1073, 2009.
39. Chang, J.-J., W. Liao and T.-C. Hou, “Reservation-Based Directional Medium Access Control (RDMAC) Protocol for Multi-Hop Wireless Networks with Directional Antennas”, *Proceedings of the IEEE International Conference on Communications, (ICC)*, pp. 1–5, 2009.
40. Yeh, C.-H., H. Zhou, P.-H. Ho and H. Mouftah, “A Variable-Radius Multichannel MAC Protocol for High-Throughput Low-Power Heterogeneous Wireless Ad Hoc Networks”, *Proceedings of the IEEE Global Telecommunications Conference (GLOBECOM)*, Vol. 3, pp. 1284–1289, 2003.

41. Huang, R., H. Zhai, C. Zhang and Y. Fang, “SAM-MAC: An Efficient Channel Assignment Scheme for Multi-Channel Ad Hoc Networks”, *Computer Networks*, Vol. 52, No. 8, pp. 1634–1646, 2008.
42. Moon, Y. and V. R. Syrotiuk, “A Cooperative CDMA-Based Multi-Channel MAC Protocol for Mobile Ad Hoc Networks”, *Computer Communications*, Vol. 32, No. 17, pp. 1810–1819, 2009.
43. Choi, W.-Y., “Clustering Algorithm for Hidden Node Problem In Infrastructure Mode IEEE 802.11 Wireless LANs”, *Proceedings of the International Conference on Advanced Communication Technology (ICACT)*, Vol. 2, pp. 1335–1338, 2008.
44. Acharya, A., A. Misra and S. Bansal, “MACA-P: A MAC for Concurrent Transmissions in Multi-Hop Wireless Networks”, *Proceedings of the IEEE International Conference on Pervasive Computing and Communications (PERCOM)*, pp. 505–508, 2003.
45. Shukla, D., L. Chandran-Wadia and S. Iyer, “Mitigating the Exposed Node Problem in IEEE 802.11 Ad Hoc Networks”, *Proceedings of the IEEE International Conference on Computer Communications and Networks (ICCCN)*, pp. 157–162, 2003.
46. Kim, D. and E.-s. Shim, “P-MAC: Parallel Transmissions in IEEE 802.11 Based Ad Hoc Networks with Interference Ranges”, C. Kim (Editor), *Proceedings of the Information Networking Convergence in Broadband and Mobile Networking*, pp. 735–744, Springer Berlin Heidelberg, Berlin, Heidelberg, 2005.
47. Jiang, L. B. and S. C. Liew, “Improving Throughput and Fairness by Reducing Exposed and Hidden Nodes in 802.11 Networks”, *IEEE Transactions on Mobile Computing (TMC)*, Vol. 7, No. 1, pp. 34–49, 2008.
48. Nishide, K., H. Kubo, R. Shinkuma and T. Takahashi, “Detecting Hidden and Ex-

- posed Terminal Problems in Densely Deployed Wireless Networks”, *IEEE Transactions on Wireless Communications*, Vol. 11, No. 11, pp. 3841–3849, 2012.
49. Mittal, K. and E. M. Belding, “RTSS/CTSS: Mitigation of Exposed Terminals in Static 802.11-Based Mesh Networks”, *Proceedings of the IEEE Workshop on Wireless Mesh Networks*, pp. 3–12, 2006.
 50. Matoba, A., M. Hanada, H. Kanemitsu and M. W. Kim, “Asymmetric RTS/CTS for Exposed Node Reduction in IEEE 802.11 Ad Hoc Networks”, *Journal of Computing Science and Engineering*, Vol. 8, No. 2, pp. 107–118, 2014.
 51. Weyulu, E., M. Hanada, H. Kanemitsu, E.-C. Park and M. W. Kim, “Cross-Layer Design for Exposed Node Reduction in Ad Hoc WLANs”, *IEICE Transactions on Communications*, Vol. E101.B, No. 7, pp. 1575–1588, 2018.
 52. Zhu, J., X. Guo, L. Yang and W. Conner, “Leveraging Spatial Reuse in 802.11 Mesh Networks with Enhanced Physical Carrier Sensing”, *Proceedings of the IEEE International Conference on Communications (ICC)*, Vol. 7, pp. 4004–4011, 2004.
 53. Zhu, J., S. Roy, X. Guo and W. Steven Conner, *Maximizing Aggregate Throughput in 802.11 Mesh Networks with Physical Carrier Sensing and Two-Radio Multi-Channel Clustering*, pp. 137–166, Springer US, Boston, MA, 2005.
 54. Vasan, A., R. Ramjee and T. Woo, “ECHOS - Enhanced Capacity 802.11 Hotspots”, *Proceedings of the Conference of the IEEE Computer and Communications Societies.*, Vol. 3, pp. 1562–1572, 2005.
 55. Murakami, K., T. Ito and S. Ishihara, “Improving the Spatial Reuse of IEEE 802.11 WLAN by Adaptive Carrier Sense Threshold of Access Points Based on Node Positions”, *Proceedings of the International Conference on Mobile Computing and Ubiquitous Networking (ICMU)*, pp. 132–137, 2015.
 56. Haghani, E., M. N. Krishnan and A. Zakhor, “Adaptive Carrier-Sensing for

- Throughput Improvement in IEEE 802.11 Networks”, *Proceedings of the IEEE Global Telecommunications Conference (GLOBECOM)*, pp. 1–6, 2010.
57. Smith, G., “Dynamic Sensitivity Control-v2”, <https://mentor.ieee.org/802.11/dcn/13/11-13-1012-04-0wng-dynamic-sensitivity-control.pptx>, 2013, accessed in July 2021.
58. Afaqui, M. S., E. Garcia-Villegas, E. Lopez-Aguilera, G. Smith and D. Camps, “Evaluation of Dynamic Sensitivity Control Algorithm for IEEE 802.11ax”, *Proceedings of the IEEE Wireless Communications and Networking Conference (WCNC)*, pp. 1060–1065, 2015.
59. Afaqui, M. S., E. Garcia-Villegas, E. Lopez-Aguilera and D. Camps-Mur, “Dynamic Sensitivity Control of Access Points for IEEE 802.11ax”, *Proceedings of the IEEE International Conference on Communications (ICC)*, pp. 1–7, 2016.
60. Cariou, L., “IEEE P802.11 Wireless LANs - CR for OBSS PD-Based Spatial Reuse – 25.9.2: IEEE 802.11-16/1223r6”, <https://mentor.ieee.org/802.11/dcn/16/11-16-1223-06-00ax-cr-for-section-25-9-2-obss-pd-spatial-reuse.docx>, Accessed in 2021.
61. Kim, T.-S., H. Lim and J. C. Hou, “Improving Spatial Reuse through Tuning Transmit Power, Carrier Sense Threshold, and Data Rate in Multihop Wireless Networks”, *Proceedings of the International Conference on Mobile Computing and Networking (MOBICOM)*, p. 366–377, Association for Computing Machinery, New York, NY, USA, 2006.
62. Voicu, A. M., F. Giorgi, L. Simić and M. Petrova, “Wi-Fi Evolution for Future Dense Networks: Does Sensing Threshold Adaptation Help?”, *Proceedings of the IEEE Wireless Communications and Networking Conference (WCNC)*, pp. 1–6, 2018.

63. Ropitault, T. and N. Golmie, “ETP Algorithm: Increasing Spatial Reuse in Wireless LANs Dense Environment Using ETX”, *Proceedings of the IEEE International Symposium on Personal, Indoor, and Mobile Radio Communications (PIMRC)*, pp. 1–7, 2017.
64. Ropitault, T., “Evaluation of RTOT Algorithm: A First Implementation of OBSS PD-Based SR Method for IEEE 802.11ax”, *Proceedings of the IEEE Annual Consumer Communications Networking Conference (CCNC)*, pp. 1–7, 2018.
65. Selinis, I., K. Katsaros, S. Vahid and R. Tafazolli, “Control OBSS/PD Sensitivity Threshold for IEEE 802.11ax BSS Color”, *Proceedings of the IEEE International Symposium on Personal, Indoor and Mobile Radio Communications (PIMRC)*, pp. 1–7, 2018.
66. Selinis, I., K. Katsaros, S. Vahid and R. Tafazolli, “Damysus: A Practical IEEE 802.11ax BSS Color Aware Rate Control Algorithm”, *International Journal of Wireless Information Networks*, Vol. 26, pp. 285–307, 2019.
67. Kim, Y., G. Kim, T. Kim and W. Choi, “Transmission Opportunity-Based Distributed OBSS/PD Determination Method in IEEE 802.11ax Networks”, *Proceedings of the International Conference on Artificial Intelligence in Information and Communication (ICAIIIC)*, pp. 469–471, 2020.
68. Šepić, N., E. Kočan and M. Pejanović-Djurišić, “Evaluating Spatial Reuse in 802.11ax Networks with Interference Threshold Adjustment”, *Proceedings of the International Conference on Information Technology & Systems (ICITS)*, pp. 1–4, 2020.
69. Yan, Y., B. Li, M. Yang and Z. Yan, “ESR: Enhanced Spatial Reuse Mechanism for the Next Generation WLAN - IEEE 802.11ax”, *Proceedings of the International Conference on Internet of Things as a Service*, pp. 265–274, Springer International Publishing, 2019.

70. Halperin, D., T. Anderson and D. Wetherall, “Taking the Sting out of Carrier Sense: Interference Cancellation for Wireless LANs”, *Proceedings of the ACM International Conference on Mobile Computing and Networking (MOBICOM)*, p. 339–350, Association for Computing Machinery, New York, NY, USA, 2008.
71. Jin, S., M. Choi, K. Kim and S. Choi, “Opportunistic Spatial Reuse in IEEE 802.15.3c Wireless Personal Area Networks”, *IEEE Transactions on Vehicular Technology*, Vol. 62, No. 2, pp. 824–834, 2013.
72. Hiep, P. T., “Spatial Reuse Superframe for High Throughput Cluster-Based WBAN with CSMA/CA”, *Adhoc & Sensor Wireless Networks*, Vol. 31, No. 1-4, pp. 69–87, 2016.
73. Fu, L., Z. Cao and P. Fan, “Spatial reuse in IEEE 802.16 Based Wireless Mesh Networks”, *Proceedings of the IEEE International Symposium on Communications and Information Technology (ISCIT)*, Vol. 2, pp. 1358–1361, 2005.
74. Sundaresan, K. and S. Rangarajan, “On Exploiting Diversity and Spatial Reuse in Relay-Enabled Wireless Networks”, *Proceedings of the ACM International Symposium on Mobile Ad Hoc Networking and Computing (MOBIHOC)*, p. 13–22, Association for Computing Machinery, New York, NY, USA, 2008.
75. Kamerman, A. and L. Monteban, “WaveLAN®-II: A High-Performance Wireless Lan for the Unlicensed Band”, *Bell Labs Technical Journal*, Vol. 2, pp. 118–133, 2007.
76. Lacage, M., M. H. Manshaei and T. Turetletti, “IEEE 802.11 Rate Adaptation: A Practical Approach”, *Proceedings of the ACM International Symposium on Modeling, Analysis and Simulation of Wireless and Mobile Systems (MSWiM)*, p. 126–134, Association for Computing Machinery, New York, NY, USA, 2004.
77. Madwifi Project, “Onoe Rate Selection Algorithm”, <http://madwifi.>

sourceforge.net/, accessed in July 2021.

78. Holland, G., N. Vaidya and P. Bahl, “A Rate-Adaptive MAC Protocol for Multi-Hop Wireless Networks”, *Proceedings of the International Conference on Mobile Computing and Networking (MOBICOM)*, p. 236–251, Association for Computing Machinery, New York, NY, USA, 2001.
79. Bicket, J. C., *Bit-Rate Selection in Wireless Networks*, Master’s Thesis, Massachusetts Institute of Technology, 2005.
80. Berg, J., “Minstrel Rate Algorithm”, <https://wireless.wiki.kernel.org/en/developers/documentation/mac80211/ratecontrol/minstrel>, accessed in July 2021.
81. Fietkau, F., “Minstrel-HT Rate Algorithm”, <https://lwn.net/Articles/376765/>, accessed in July 2021.
82. Gupta, H., A. Eryilmaz and R. Srikant, “Low-Complexity, Low-Regret Link Rate Selection in Rapidly-Varying Wireless Channels”, *Proceedings of the IEEE International Conference on Computer Communications (INFOCOM)*, pp. 540–548, 2018.
83. Henderson, T., G. Riley, S. Floyd and S. Roy, “NS-3 Simulator”, <https://www.nsnam.org/>, accessed in July 2021.
84. McCanne, S., S.Floyd and K. Fall, “NS-2 Simulator”, http://nsnam.sourceforge.net/wiki/index.php/User_Information, accessed in July 2021.
85. Henderson, T., G. Riley, S. Floyd and S. Roy, “NS-3 codebase”, <https://gitlab.com/nsnam>, accessed in July 2021.
86. Nagy, T., “Waf Codebase”, <https://gitlab.com/ita1024/waf/>, accessed in July 2021.

87. Merlin, S., "TGax Simulation Scenarios", <https://mentor.ieee.org/802.11/dcn/14/11-14-0980-16-00ax-simulation-scenarios.docx>, 2015, accessed in July 2021.